การควบคุมแบบป้อนกลับสัญญาณขาออกของเฮลิคอปเตอร์สี่ใบพัด ด้วยวิธีเชิงเส้นแปรผันตามพารามิเตอร์ที่มีเงื่อนไขบังคับอิ่มตัว

นายอภิชาต เสรีโรจนกุล

วิทยานิพนธ์นี้เป็นส่วนหนึ่งของการศึกษาตามหลักสูตรปริญญาวิศวกรรมศาสตรมหาบัณฑิต
สาขาวิชาวิศวกรรมไฟฟ้า ภาควิชาวิศวกรรมไฟฟ้า
คณะวิศวกรรมศาสตร์ จุฬาลงกรณ์มหาวิทยาลัย
ปีการศึกษา 2555

OUTPUT FEEDBACK CONTROL OF QUAD-ROTOR HELICOPTER USING LINEAR PARAMETER-VARYING METHOD WITH SATURATION CONSTRAINTS

Mr. Apichart Serirojanakul

A Thesis Submitted in Partial Fulfillment of the Requirements
for the Degree of Master of Engineering Program in Electrical Engineering
Department of Electrical Engineering
Faculty of Engineering
Chulalongkorn University
Academic Year 2012

Thesis Title	OUTPUT FEEDBACK CONTROL OF QUAD-ROTOR HELICOPTER USING LINEAR PARAMETER-VARYING METHOD WITH SATURATION CONSTRAINTS
By	Mr. Apichart Serirojanakul
Field of Study	Electrical Engineering
Thesis Advisor	Assistant Professor Manop Wongsaisuwan, Ph.D.

Accepted by the Faculty of Engineering, Chulalongkorn University in Partial Fulfillment of the Requirements for the Master's Degree

. . . . . Dean of the Faculty of Engineering
(Associate Professor Boonsom Lerdhirunwong, Dr. Ing.)

THESIS COMMITTEE

. . . . . Chairman
(Professor David Banjerdpongchai, Ph.D.)

. . . . . Thesis Advisor
(Assistant Professor Manop Wongsaisuwan, Ph.D.)

. . . . . External Examiner
(Itthisek Nilkhamhang, Ph.D.)

อภิชาต เสรีโรจนกุล : การควบคุมแบบป้อนกลับสัญญาณขาออกของเฮลิคอปเตอร์สี่ใบพัดด้วยวิธีเชิงเส้นแปรผันตามพารามิเตอร์ที่มีเงื่อนไขบังคับอิ่มตัว. (OUTPUT FEEDBACK CONTROL OF QUAD-ROTOR HELICOPTER USING LINEAR PARAMETER-VARYING METHOD WITH SATURATION CONSTRAINTS) อ.ที่ปรึกษาวิทยานิพนธ์หลัก : ผศ. ดร. มานพ วงศ์สายสุวรรณ, 79 หน้า.

วิทยานิพนธ์นี้นำเสนอการควบคุมแบบป้อนกลับสัญญาณขาออกของเฮลิคอปเตอร์สี่ใบพัดที่มีเงื่อนไขบังคับอิ่มตัวสัญญาณขาเข้า แนวคิดหลักในการออกแบบตัวควบคุมคือการแปลงแบบจำลองของเฮลิคอปเตอร์สี่ใบพัดจากแบบจำลองไม่เชิงเส้นไปเป็นแบบจำลองเชิงเส้นแปรผันตามพารามิเตอร์ จากนั้นจึงประยุกต์ใช้วิธีการควบคุมแบบเชิงเส้นแปรผันตามพารามิเตอร์ ในการออกแบบตัวควบคุม เราเริ่มพิจารณาจากการควบคุมแบบเชิงเส้นคุมค่าแบบเหมาะที่สุดตามฟังก์ชันกำลังสองของระบบเชิงเส้นแปรผันตามพารามิเตอร์ที่ไม่มีเงื่อนไขบังคับอิ่มตัว เราพบว่า ตัวควบคุมไม่สามารถรับประกันเสถียรภาพของระบบที่มีความอิ่มตัวได้ ดังนั้น เราจึงนำเสนอเพิ่มเติมการควบคุมแบบเชิงเส้นคุมค่าแบบเหมาะที่สุดตามฟังก์ชันกำลังสองของระบบเชิงเส้นแปรผันตามพารามิเตอร์ที่มีเงื่อนไขบังคับอิ่มตัว โดยพิจารณาตัวควบคุมที่มีเงื่อนไขบังคับอิ่มตัวทั้งแบบอัตราขยายต่ำและแบบอัตราขยายสูงสุดท้าย เพื่อจะควบคุมแบบป้อนกลับสัญญาณขาออก เราพิจารณาการใช้ส่วนขยายของตัวกรองคาลมานเพื่อประมาณสถานะระบบ ผลการจำลองแบบสามมิติได้ให้ไว้เพื่อยืนยันประสิทธิผลของตัวควบคุมทั้งหมด

ภาควิชา……วิศวกรรมไฟฟ้า……..ลายมือชื่อนิสิต……..……..

สาขาวิชา……วิศวกรรมไฟฟ้า……ลายมือชื่อ อ.ที่ปรึกษาวิทยานิพนธ์หลัก…….

ปีการศึกษา….2555……

5270712221 : MAJOR ELECTRICAL ENGINEERING

KEYWORDS : LINEAR MATRIX INEQUALITIES / LINEAR PARAMETER-VARYING / LINEAR QUADRATIC REGULATOR / KALMAN FILTER / SATURATION CONSTRAINT

APICHART SERIROJANAKUL : OUTPUT FEEDBACK CONTROL OF QUAD-ROTOR HELICOPTER USING LINEAR PARAMETER-VARYING METHOD WITH SATURATION CONSTRAINTS. THESIS ADVISOR : ASST. PROF. MANOP WONGSAISUWAN, Ph.D., 79 pp.

This thesis presents the output feedback control of the quad-rotor helicopter (quadrotor) with input saturation constraints. The main idea underlying controller design is the transformation of the nonlinear model to an linear parameter-varying (LPV) model of the quadrotor. Then, the LPV control technique is applied. To design the LPV controller, we first consider the linear quadratic regulator control of LPV systems. This results in the linear parameter-varying quadratic regulator (LPVQR) control. Next, when the input saturation is taken into account, the LPVQR is inadequate to guarantee stability of the systems. Therefore, we propose the LPVQR control of the saturated LPV systems. Two approaches for saturated controller, the low-gain and the high-gain, are considered. As a result, the saturated LPVQR (SLPVQR) and the high-gain SLPVQR are obtained, respectively. Finally, to deal with the output feedback control problem, we consider the use of the extended Kalman filter for state estimation. The 3D visualization for the quadrotor simulation is given at the end to demonstrate the effectiveness of the controllers.

Department : Electrical Engineering
Field of Study : Electrical Engineering
Academic Year : 2012

Student's Signature .....
Advisor's Signature .....

Acknowledgements

I am sincerely grateful to my advisor, Assistant Professor Manop Wongsaisuwan, for the helpful advice and continuous support he gave me during the development of this research. I am sure that this thesis would not have been possible without his help. I would like to offer my special thanks to the thesis committees, Professor David Banjerdpongchai and Dr. Itthisek Nilkhamhang, for their useful and constructive recommendations on this thesis. Finally, I wish to thank my parents for their support and encouragement throughout my study.

Contents

CHAPTER Page

CHAPTER Page

List of Tables

Table Page

List of Figures

Figure Page

CHAPTER I

INTRODUCTION

1.1 Research motivation

In the last couple of years, the quad-rotor helicopter, shortly called the quadrotor, has recieved increasingly significant attention as an Unmanned Aerial Vehicle (UAV) platform. The quadrotor concept was established in an attempt to simplify many troublesome issues. Comparing to the conventional helicopter, it is essentially simpler to build and control. Today, there are many useful applications such as surveillance, rescue, scout, etc. Therefore, it is essential to autonomously control its motion with accuracy.

Throughout the last 20 years, the Linear Parameter-Varying (LPV) control framework has become a promising theoretical approach used to control mildly nonlinear systems. It gives the better performance than what the classical Linear Time-Invariant (LTI) control can provide, while the simplicity of the powerful LTI analytical tools are preserved. In this thesis, the LPV control method is used to control the quadrotor, because it can be applied to the optimal and robust control problems giving quite attractive results.

In practice, the limit of the force produced by each propeller may make the quadrotor unstable, if the controller is designed regardless of the input saturation. Thus, in this thesis, the control theory for saturated linear systems is considered to be applied to the LPV control.

The controller obtained in this thesis is based on the full state feedback control. However, in the real system, only partial information of the states can be observed from the noisy measurements. Therefore, the state estimation problem is also considered in order that our controller can be applied to the real system of the quadrotor.

1.2 Literature review

This section presents some important works on the control of the quadrotor and the development of the LPV control framework.

1.2.1 Quadrotor dynamic modeling and control

The quadrotor has become a popular UAV platform in the last decade due to its simplicity in building and control with many useful applications [1, 2]. Many researchers are interested in studying the model of the quadrotor [3–6] as well as the development of the control algorithm [7–10].

Mistler et al. [9] presented the basic nonlinear dynamic model of the quadrotor and the full state feedback control by means of the exact linearization. In their work, to simplify the nonlinear model, the inputs and the outputs were decoupled into independent single input single output channels. This made the linearized model uncontrollable via the static state feedback control law. Thus, a dynamic state feedback control law was given to solve this problem.

In many publications, e.g., [7, 8], to simplify the controller design, the control loop is decoupled into translational control and orientational control. However, this is the wasteful cancellation of the mutual dynamics.

There exist few researchs on the control of the quadrotor whose the actuators are saturated. In Alexis et al. [11], the quadrotor dynamics was modeled as a piecewise linear system. Then, the constrained finite time optimal control was used to stabilize the input-constrained quadrotor around the nominal angles of operation. In this work, however, the control inputs were transformed into total force in the z–direction and total torques in the roll angle, the pitch angle, and the yaw angle. This representation somehow cannot reflect the real saturation of the control inputs.

Rangajeeva and Whidborne [10] applied the LPV control method. In his work, to control the quadrotor in only the xy plane, the linear velocities in x and y directions, the roll angle, the pitch angle, and the total thrust were considered as the time-varying parameters. The simulation results were given to show that the LPV control outperforms the $\mathcal{H}_\infty$ control.

Since the LPV control has been appeared to be a powerful tool in the control analysis of uncertain nonlinear systems, in this thesis, we are interested in using it to optimally control the quadrotor. Next, a review on the LPV control is given.

1.2.2 Linear Parameter-Varying Control

The LPV control framework, introduced by Shamma and Athans [12], was originated from gain scheduling control [13, 14]. In brief, the gain scheduling is the controller design based on philosophy of divide and conquer. A feedback control law of nonlinear and/or time-varying systems is constructed from a collection of local LTI controllers that are designed for each local aspect. These controllers are integrated in real-time via switching or interpolation according to the scheduling variable for achieving the global control solution to the entire operating regime. Though the gain scheduling control had been successfully applied to many engineering applications [13, 15–17], it is theoretically unable to guarantee stability of the systems. Therefore it was continuously developed and eventually the concept of the LPV control was arisen.

In Shamma and Athans [12,18], the context of LPV systems was given along with the stability condition guaranteeing performance robustness in such a slowly varying system. In addition, the control of rate constrained LPV systems was also introduced in Shamma and Xiong [19].

In Packard [20], the state space $\mathcal{H}_\infty$ control theory was taken into consideration of the LPV

controller synthesis. The controller design was then treated as a finite-dimensional convex optimization problem. The solvability condition through the linear matrix inequality (LMI) constraints was also studied and given in Apkarian et al. [21, 22]. Kajiwara et al. [23] applied the LPV control method to the arm-driven inverted pendulum for obtaining a wide-range stabilization. Their work illustrated that the LPV control outperforms the classical robust LTI control for both the $\mathcal{H}_\infty$ synthesis and the μ synthesis in terms of performance robustness.

The stability analysis of LPV systems has been studied intensively [24, 25]. It is quite similar to the stability analysis of linear systems with uncertain parameters [26–31]. Thus, both are coexistingly devoloped. In Montagner et al. [32], the LMI conditions for the existence of a quadratic stabilizing state feedback gain for LPV systems was given. By using the common quadratic Lyapunov function, these conditions are adequate to guarantee stability of the LPV systems with unknown or unbounded variation rate of the parameters. However, using this kind of the Lyapunov function for guaranteeing all the admissible trajectories of the parameters makes the close-loop performance suffered from the conservatism. In Geromel and Colaneri [33], the close-loop performance was improved by replacing the common quadratic Lyapunov function with the parameter-dependent quadratic Lyapunov function. Though the use of this kind of the Lyapunov function can significantly improve the close-loop performance, it requires the knownledge about the bound on the variation rate of the parameters, which is rarely possible in practice. Thus, in this thesis, this problem will be considered.

Having been appeared in publications, the LPV control can be applied to many fields of control with many successful applications [34–38]. In this thesis, we will focus only on the optimal control of LPV systems, which will be used to control the quadrotor.

1.3 Thesis objective

The aim of this thesis is to control the quadrotor by using the LPV control method with input saturation constraints. The nonlinear dynamic model of the quadrotor is first considered. Then, it is transformed to an approximated LPV model in order that the LPV control can be applied. To optimally control the quadrotor, the LQR control is considered to be applied to the LPV model of the quadrotor. In practice, the quadrotor may be unstable, if the controller is designed regardless of the saturation. Thus, the saturation constraints are also considered. In addition, only the partial state of the quadrotor can be measured. In this thesis, a well-known nonlinear state estimator called the EKF will be used to construct the output feedback controller.

1.4 Scope of thesis

1. To derive the nonlinear model and the LPV model of the quadrotor.

2. To build a 3D simulation tool of the quadrotor.
3. To design the LPV controller that can optimally control the saturated LPV systems.
4. To autonomously control the quadrotor, whose the control inputs are bounded, by using the output feedback LPV control method with saturation constraints.

1.5 Methodology

1. Literature review on the quadrotor dynamic modeling.
2. Literature review on the LPV modeling and control.
3. Literature review on the control of saturated linear systems.
4. Build a 3D visualization of the quadrotor simulation for testing the control algorithm.
5. Design the state feedback LPV controller with and without the saturation constraints and test the controller.
6. Combine the EKF for constructing an output feedback controller.

1.6 Contributions

1. An LPV model of the quadrotor.
2. An LPV controller that can optimally control LPV systems with input saturation constraints.
3. An LPV controller that can autonomously control the quadrotor.
4. A 3D simulation tool used to verify the control of the quadrotor.

1.7 Thesis outline

The organization of this thesis is as the following. In the next chapter, an overview of the related theories used in this thesis is given. Then, the dynamic modeling including the nonlinear model and the LPV model of the quadrotor are presented in Chapter 3. In Chapter 4, the linear parameter-varying quadratic regulator control problem is considered. Additionally, in Chapter 5, the input saturation is taken into account. All the controllers derived from Chapter 4 and Chapter 5 are applied to the LPV model of the quadrotor and the simulation results are illustrated in Chapter 6. Finally, conclusions of this thesis are given in Chapter 7.

CHAPTER II

RELATED THEORIES

In this chapter, an overview of the related theories used in this thesis will be discussed. Since the thesis is concerned with the control of LPV systems, the definition of the LPV systems is firstly considered in Section 2.1. To extract any nonlinear models to an equivalent polytopic LPV representation, in Section 2.2, the tensor product model transformation is considered. Next, in Section 2.3, to design the controller that can guarantee stability of the LPV systems, the Lyapunov stability conditions, accompanying with various types of the Lyapunov function, are given. The aim of this thesis is to design the controller by means of solving the LMI optimization problem. Therefore, in Section 2.4, the preliminary LMI conditions are also given. As stated in the introduction, the control design policy is to obtain the controller that can guarantee and minimize the worst case performance of a given cost function. In Section 2.5, the linear quadratic regulator (LQR) control problem is then considered. Of course, the problem is also treated to an LMI optimization problem. To do the linear quadratic regulator, the system states are assumed to be known. This is rarely possible in practice. Therefore, in Section 2.6, the problem of the optimal state estimation is considered.

2.1 Linear parameter-varying systems

The LPV systems can be viewed as a bridge between the linear systems and the nonlinear systems. There are several representations of the LPV systems [39]. However, in this thesis, we focus only on the LPV systems whose the parameters vary in a certain convex polytope, i.e.,

Definition 2.1 (polytopic LPV systems)**.** *An LPV system is called 'polytopic' if it can be represented by the state space matrices, $A(\rho), B(\rho), C(\rho)$, and $D(\rho)$, which are the affine functions depending on the parameter ρ. Moreover, the parameter ρ ranges over a fixed polytope. Clearly,*

$$\rho \in \operatorname{co}\{\rho_1, \ldots, \rho_N\} \tag{2.1}$$

and the state-space matrices range over a matrix polytope

$$\begin{pmatrix} A(\rho) & B(\rho) \\ C(\rho) & D(\rho) \end{pmatrix} \in \operatorname{co}\left\{ \begin{pmatrix} A(\rho_i) & B(\rho_i) \\ C(\rho_i) & D(\rho_i) \end{pmatrix}, \ \forall i \in I[1, N] \right\}, \tag{2.2}$$

where $I[1, N]$ denotes the set of intergers from 1 to N.

By treating the nonlinear system of the form

$$\dot{x} = f(x, u), \tag{2.3}$$

$$y = h(x, u), \tag{2.4}$$

to the linear system subject to the variable parameter ρ, i.e.,

$$\dot{x} = A(\rho)x + B(\rho)u, \tag{2.5}$$

$$y = C(\rho)x + D(\rho)u, \tag{2.6}$$

the control of this nonlinear system then falls to the scope of the Linear Time-Varying (LTV) control. Though the LPV systems are similar to the LTV systems, the parameter trajectories of the LPV systems are unknown in advance. This distinguishes the LPV systems from the LTV systems. The control of the LPV systems involves the behavior of the systems along the admissible trajectories. In contrast, the behavior of the LTI systems is valid only some particular value of the parameters.

2.2 Tensor product model transformation

The Tensor Product (TP) model transformation is a numerical reconstruction of the Higher-Order Singular Value Decomposition (HOSVD) [40] of continuous functions. It was first used in the controller design by *Peter Baranyi* [41] through the capable of transforming a given nonlinear function into a finite basis TP structure. For any nonlinear functions, possibly matrix or even tensor, the TP model is given by

$$\begin{aligned} F(x) &= \mathcal{F} \otimes_{n=1}^{N} w_n(x_n) \\ &= \sum_{i_1=1}^{I_1} \sum_{i_2=1}^{I_2} \cdots \sum_{i_N=1}^{I_N} \prod_{n=1}^{N} \omega_{n,i_n}(x_n) F_{i_1,i_2,\ldots,i_N}, \end{aligned} \tag{2.7}$$

for any parameter x, as the parameter-varying combination of a finite number of the bases $F_{i_1,i_2,\ldots,i_N}$. More details about the tensor operations can be found in [40]. The TP model has various forms. Here, we consider only the TP model that is the convex function, i.e., $\omega_{n,i_n}(x_n) \geq 0$, for all $n,\ i_n,\ x_n$ and $\sum_{i_n=1}^{I_n} \omega_{n,i_n}(x_n) = 1$, for all $n,\ x_n$. Further details on the TP model are provided in [42–45]. In order to obtain the TP model of any nonlinear functions, we use the MATLAB toolbox called the TP tool, which is free downloadable at [46].

2.3 Lyapunov stability analysis

The Lyapunov stability analysis play a fundamental role in the stability analysis of dynamical systems. For a dynamical system defined by

$$\dot{x} = f(x), \tag{2.8}$$

such that $x \in \mathbb{R}^n$ and $f : \mathbb{R}^n \to \mathbb{R}^n$, the point x^* at which $f(x^*) = 0$ is called the equilibrium point or rest point of the system. It is stable in sense of the Lyapunov stability if for any given bounded neighbourhood U of x^*, there exists $V \subseteq U$ such that any solution $x(\cdot)$ starting in V never leaves U. The Lyapunov stability is named to celebrate *Aleksandr Mikhailovich Lyapunov*,

a Russian mathematician, who proposed the methods for demonstrating the stability of dynamical systems. In his original work [47], the two methods for proving the stability were presented. The first method proved the stability by considering the convergence within the limits of the solution to the dynamical systems. The second method concerned with seeking the Lyapunov function $V(x) : \mathbb{X}^n \subseteq \mathbb{R}^n \to \mathbb{R}$, defined around x^*, such that

a) $V(x^*) = 0,\ V(x) > 0\ \forall x \in \mathbb{X}^n \backslash \{x^*\}$, and

b) $\dot{V}(x) := \langle \nabla V(x), f(x) \rangle \leq 0\ \forall x \in \mathbb{X}^n$.

Clearly, the Lyapunov function is a non-negative function having a strict minimum on $\mathbb{X}^n$ at x^*. In this thesis, we are interested only the use of the second method. Next, we will consider various kinds of the Lyapunov function used in this thesis.

2.3.1 Common quadratic Lyapunov function

Consider the following LPV system

$$\dot{x} = A(\rho)x. \tag{2.9}$$

One typical Lyapunov function is a positive definite quadratic function of the form

$$V(x) = x^T P x, \tag{2.10}$$

where P is a positive defintie matrix. Its time derivative is computed as follows

$$\dot{V}(x) = x^T \left(PA(\rho) + A(\rho)^T P \right) x. \tag{2.11}$$

Thus, to verify the stability of the LPV system (2.9), one might seek for a positive definite matrix P such that

$$PA(\rho) + A(\rho)^T P \leq 0, \tag{2.12}$$

for all possible $A(\rho)$.

2.3.2 Parameter-dependent quadratic Lyapunov function

Since we are dealing with the LPV systems, it is too restrictive to use the common P for all possible $A(\rho)$. An alternative choice of the quadratic Lyapunov function is the use of the parameter-dependent positive definite matrix $P(\rho)$. This leads to the following quadratic Lyapunov function

$$V(x) = x^T P(\rho) x. \tag{2.13}$$

With this Lyapunov function, we have the following time derivative

$$\dot{V}(x) = x^T \left(\dot{P}(\rho) + P(\rho)A(\rho) + A(\rho)^T P(\rho) \right) x. \tag{2.14}$$

Therefore, to verify the stability of the LPV system (2.9), one might seek for a positive definite matrix-valued function $P(\rho)$ such that

$$\dot{P}(\rho) + P(\rho)A(\rho) + A(\rho)^T P(\rho) \leq 0, \tag{2.15}$$

for all possible trajectory of the parameter.

2.3.3 Composite quadratic Lyapunov function

The difficulty of using the parameter-dependent quadratic Lyapunov function arises when the matrix derivative term appears. This will be discussed later in Chapter 4. To avoid this problem, we consider the use of the composite quadratic Lyapunov function [48, 49]. With a set of positive-definite matrices $\{P_1, \ldots, P_N\}$, let $Q_i = P_i^{-1}$ for all $i \in I[1, N]$. For a vector $\rho \in \Lambda_N$ such that

$$\Lambda_N = \left\{ \rho \in \mathbb{R}^N : \sum_{i=1}^{N} \rho_i = 1,\ \rho_i \geq 0 \quad \forall i \in I[1, N] \right\}, \tag{2.16}$$

the two positive definite matrix-valued functions are defined as follows

$$Q(\rho) := \sum_{i=1}^{N} \rho_i Q_i, \tag{2.17}$$

$$P(\rho) := Q(\rho)^{-1}. \tag{2.18}$$

With these definitions, we obtain the composite quadratic Lyapunov function, which is defined by

$$V_c(x) := \min_{\rho \in \Lambda_N} x^T P(\rho) x. \tag{2.19}$$

Clearly, $Q(\rho)$, $P(\rho) > 0$ for all $\rho \in \Lambda_N$ and $V_c(\cdot)$ is a non-negative function that is continuously differentiable. A very nice property of the composite quadratic Lyapunov function is stated as the following lemma.

Lemma 2.1 (Composite quadratic Lyapunov function)**.** *Let $\rho^*(x)$ be the optimal ρ such that*

$$x^T P(\rho^*(x)) x = \min_{\rho \in \Lambda_N} x^T P(\rho) x, \tag{2.20}$$

then the derivative of $V_c(x)$ with respect to x is computed as follows

$$\frac{\partial V_c}{\partial x} = 2P(\rho^*(x))x. \tag{2.21}$$

Proof. See Appendix A.1 in [48]. □

Using this lemma, the term $\dot{P}(\rho)$ in the time derivative of the Lyapunov function (2.14) is vanished.

2.4 Linear matrix inequality

In this thesis, the LMI is the main tools used to design the controller, especially in the Lyapunov stability analysis. Generally, the LMI is used to formulate the convex optimization problem, then it is solved by the LMI tools provided by MATLAB. In this section, the preliminary LMI conditions used in this thesis are given.

2.4.1 Schur complement

In the matrix theory, the Schur complement of the matrix block D in X, such that

$$X = \begin{bmatrix} A & B \\ C & D \end{bmatrix}, \tag{2.22}$$

is defined by

$$S = A - BD^{-1}C. \tag{2.23}$$

It is named to celebrate *Issai Schur*, who used the above definition to prove the Schur's lemma [50]. The Schur complement is provably useful in the LMI optimization problems [51]. Let X be a symmetric matrix given by

$$X = \begin{bmatrix} A & B \\ B^T & C \end{bmatrix}, \tag{2.24}$$

and S be the Schur complement of the matrix block C in X, i.e.,

$$S = A - BC^{-1}B^T. \tag{2.25}$$

If $C > 0$, then $X \geq 0$ if and only if $S \geq 0$. Clearly, the condition $S \geq 0$ is nonlinear in B and C. However, if the condition $C > 0$ is satisfied, then the linear condition $X \geq 0$ can be used instead.

2.4.2 Containment of an ellipsoid inside a polyhedron

Consider a polyhedral set defined by

$$\mathcal{L}(K, \sigma) := \left\{ x \in \mathbb{R}^n : K \in \mathbb{R}^{m \times n},\ |k_i x| \leq \sigma,\ k_i :\ i^{\text{th}} \text{ row of } K \right\}. \tag{2.26}$$

Since the Lyapunov function, defined by $V(x) = x^T P x$, is related to an ellipsoidal set of the form

$$\mathcal{E}(P, \gamma) := \left\{ x \in \mathbb{R}^n : x^T P x \leq \gamma,\ P = P^T > 0 \right\}, \tag{2.27}$$

it is easier to verify the stability of an ellipsoidal set than the polyhedral set. Therefore, we will restrict our analysis domain in an inner approximated ellipsoidal set of the polyhedral set. As stated in [52], we have the following LMI condition, which is used to verify the containment of an ellipsoid inside the polyhedron.

Lemma 2.2 (Containment of an ellipsoid inside the polyhedron)**.** *For a matrix $P = P^T > 0 \in \mathbb{R}^{n \times n}$, a matrix $K \in \mathbb{R}^{m \times n}$, and two positive scalars σ and γ, let k_i be the i^{th} row of K. The ellipsoid $\mathcal{E}(P, \gamma)$ is inside the polyhedron $\mathcal{L}(K, \sigma)$ if and only if*

$$\gamma k_i P^{-1} k_i^T \leq \sigma^2 \Leftrightarrow \begin{bmatrix} \sigma^2 & k_i \left(P/\gamma\right)^{-1} \\ \left(P/\gamma\right)^{-1} k_i^T & \left(P/\gamma\right)^{-1} \end{bmatrix} \geq 0,\ \forall i \in I[1, m].$$

This lemma will be useful in the analysis of saturated systems, which will be seen later in Chapter 5.

2.5 Linear quadratic regulator

To obtain the controller that can guarantee and minimize the worst case performance of a given quadratic cost function, in this section, the LQR control is studied. For a given LTI system

$$\dot{x}(t) = Ax(t) + Bu(t), \tag{2.28}$$

the LQR control seeks for a state feedback control law

$$u(t) = -Kx(t), \tag{2.29}$$

that is not only asymptotically stabilizable (2.28), but also the best choice among all such the feedback control law, regarding to the performance criterion of the form

$$J(x(0), u(\cdot)) = \int_0^\infty \left(u(t)^T R u(t) + x(t)^T Q x(t)\right) dt. \tag{2.30}$$

The solution of this problem is related to finding a positive definite matrix P satisfying the following Algebraic Riccati Equation (ARE) [53]

$$A^T P + PA - PBR^{-1}BP + Q = 0, \tag{2.31}$$

and the optimal state feedback gain, corresponding to the ARE, is computed as follows

$$K = R^{-1}B^T P. \tag{2.32}$$

A systematic way for solving this problem is stated in the following theorem

Theorem 2.1 (Linear quadratic regulator via linear matrix inequality optimization)**.** *Assume the existence of a positive definite matrix Y and an arbitrary real matrix L satisfying*

$$\begin{aligned} &\max_{Y,\,L} \ \operatorname{tr}(Y) \\ &\text{s.t.} \ \begin{bmatrix} -(AY - BL) - (AY - BL)^T & Y & L^T \\ Y & Q^{-1} & 0 \\ L & 0 & R^{-1} \end{bmatrix} > 0, \end{aligned} \tag{2.33}$$

then the LTI system (2.28) under the control law (2.29) satisfies

$$J(x(0), u(\cdot)) < \min_{Y,\,L} x(0)^T P x(0),$$

where $K = LP$ and $P = Y^{-1}$.

Proof. See Appendix A.1.1 □

2.6 Optimal state estimation

In practical consideration, the process noise causes the actual state of the system to diverge from the desired state. While the full state of the system cannot be observed, we have only the partial information of the system from the noisy measurement data. So as to do the full state feedback control, in this section, the optimal state estimation will be considered.

The Kalman filter, established in 1960s by *Rudolf E. Kalman* [54], is known as a fundamental tool for solving the estimation problem. In general, the Kalman filter applications are implemented in the discrete-time domain. However, in this thesis, to study the behavior of the dynamical system, the Kalman filter is considered to be implemented in the continous-time domain. The continuous-time Kalman filter is the collaborated work of *Rudolph Kalman* and *Richard Bucy*. Thus, it is sometimes called the Kalman-Bucy filter [55]. For any linear systems, the Kalman filter performs recursively the estimation on streams of noisy data to produce a minimum mean square estimation error. Nevertheless, to deal with the nonlinear model of the quadrotor, the Kalman filter cannot give the satisfactory result. Therefore, we need to explore the nonlinear extension of the Kalman filter. The Extended Kalman Filter (EKF) [56], which was proposed by *Stanley Schmidt*, is selected. The basic idea underlying the EKF is that the nonlinear system is linearized around the estimated state, then the conventional Kalman filter is applied.

Before we move on to the state estimation problem, the relationship between the continuous-time and the discrete-time white noise is first considered. Then, the continous-time EKF algorithm will be given. Finally, to ensure that the optimal state estimation is well defined for the optimal control problem, the principle of the separation between the optimal control and the optimal state estimation will be discussed.

2.6.1 Continuous-time white noise

In practice, both the process noises and the measurement noises are acquired and expressed in the discrete-time covariance matrices. However, to study the behavioral dynamics of the quadrotor, the continuous-time filter is considered. In particular, for simulating purpose, the relationship between the discrete-time and the continuous-time white noise is given as the following:

Process noise

The continuous-time process noise is defined by

$$E\left[w(t)w(\tau)^T\right] = Q_c\delta(t-\tau), \tag{2.34}$$

where $\delta(\cdot)$ is the impulse function. From this definition, we have the following relationship between the discrete-time and the continuous-time process noise

$$Q_c = Q_d/T. \tag{2.35}$$

To be cleared, the continuous-time dynamical system having the identity state transition matrix will be considered

$$\begin{aligned} \dot{x}(t) &= w(t), && (2.36) \\ w(t) &\sim (0, Q_c). && (2.37) \end{aligned}$$

The discrete-time model with a sample time of T, approximated to the above system, is computed as follows

$$\begin{aligned} x_k &= x_{k-1} + w_{k-1}, && (2.38) \\ w_k &\sim (0, Q_d). && (2.39) \end{aligned}$$

It is assumed that the initial condition is zero. The state covariance, derived from the continuous-time model, is computed as follows

$$\begin{aligned} E\left[x(t)x(t)^T\right] &= \int_0^t \int_0^t E\left[w(\alpha)w(\beta)^T\right] d\alpha d\beta \\ &= Q_c t, && (2.40) \end{aligned}$$

and also the state covariance, derived from the discrete-time model, is computed as follows

$$\begin{aligned} E\left[x(t)x(t)^T\right] &= E\left[x_k x_k^T\right] \\ &= E\left[(w_0 + \ldots + w_{k-1})(w_0 + \ldots + w_{k-1})^T\right] \\ &= kQ_d. && (2.41) \end{aligned}$$

Since $t = kT$, this implies that

$$Q_d = Q_c T. \quad (2.42)$$

Here, we see that the state covariance of the continuous-time model and the discrete-time model increases with time in exactly the same way. Although it is counter-intuitive because $w(t)$ is zero correlated with $w(\tau)$ when $t \neq \tau$, but it is infinitely correlated with $w(\tau)$ when $t = \tau$. However, it is mathematically well defined, which can describe the real processes approximately.

Measurement noise

The continuous-time measurement noise is defined likewise the continuous-time process noise. That is

$$E\left[v(t)v(\tau)^T\right] = R_c \delta(t - \tau), \quad (2.43)$$

where $\delta(\cdot)$ is the impulse function. Nevertheless, the relationship between the discrete-time and the continuous-time measurement noise is given by

$$R_c = R_d T. \quad (2.44)$$

This relationship is obtained by considering the following discrete-time measurement model, derived approximately from the continuous-time measurement model.

$$\begin{aligned} y_k &= \frac{1}{T}\int_{t_{k-1}}^{t_k} y(t)dt \\ &= \frac{1}{T}\int_{t_{k-1}}^{t_k} \left(Cx(t)+v(t)\right)dt \\ &\approx Cx_k + \frac{1}{T}\int_{t_{k-1}}^{t_k} v(t)dt. \end{aligned} \tag{2.45}$$

This implies that

$$v_k = \frac{1}{T}\int_{t_{k-1}}^{t_k} v(t)dt. \tag{2.46}$$

Consequently, we have

$$\begin{aligned} R_d &= E\left[v_k v_k^T\right] \\ &= \frac{1}{T^2}\int_{t_{k-1}}^{t_k}\int_{t_{k-1}}^{t_k} E\left[v(\alpha)v^T(\beta)\right]d\alpha d\beta \\ &= R_c/T. \end{aligned} \tag{2.47}$$

Now, we have the conversion between the discrete-time white noise and the continous-time white noise. Next, we will consider the problem of the optimal state estimation of the continuous-time nonlinear systems.

2.6.2 Continuous-time extended Kalman filter

As mentioned before, the Kalman filter is known as a linear quadratic estimator giving least mean square estimation error. However, if the systems we are interested are nonlinear systems, the conventional Kalman filter is inadequate for estimating the system state. Thus, the continuous-time EKF is given here. Its algorithm can be summarized as follows.

Algorithm 2.1 (Continuous-time extended Kalman filter)**.**

1. *Suppose that the nonlinear dynamic system is given by the following equations:*

$$\dot{x} = f(x,u,w), \tag{2.48}$$
$$y = h(x,v), \tag{2.49}$$
$$w \sim (0,Q_c), \tag{2.50}$$
$$v \sim (0,R_c), \tag{2.51}$$

where w and v are assumed to be continuous-time zero mean white gaussian noises.

2. *Compute the following Jacobian matrices, then evaluate them at the current estimated state:*

$$A = \left.\frac{\partial f}{\partial x}\right|_{\hat{x}}, \tag{2.52}$$

$$L = \left.\frac{\partial f}{\partial w}\right|_{\hat{x}}, \tag{2.53}$$

$$C = \left.\frac{\partial h}{\partial x}\right|_{\hat{x}}, \tag{2.54}$$

$$M = \left.\frac{\partial h}{\partial v}\right|_{\hat{x}}. \tag{2.55}$$

3. *Compute the following matrices:*

$$\tilde{Q} = LQ_cL^T, \tag{2.56}$$

$$\tilde{R} = MR_cM^T. \tag{2.57}$$

4. *Initialize the following mean and covariance:*

$$\hat{x}(0) = E\left[x(0)\right], \tag{2.58}$$

$$P(0) = E\left[(x(0)-\hat{x}(0))(x(0)-\hat{x}(0))^T\right]. \tag{2.59}$$

5. *As the system is processing, execute the following Kalman filter equation:*

$$\dot{P} = AP + PA^T + \tilde{Q}^T - PC^T\tilde{R}^{-1}CP, \tag{2.60}$$

$$K = PC^T\tilde{R}^{-1}, \tag{2.61}$$

$$\hat{x} = f(\hat{x},u,0) + K(y - h(\hat{x},0)). \tag{2.62}$$

Obviously, the continuous-time EKF is straightforward combination of the continous-time Kalman filter and the conventional discrete-time EKF. The full derivation of the algorithm stated above can be found in [57], Chapter 13.

2.6.3 The separation principle

Taking into account the process noise and the measurement noise of the optimal state feedback control, this leads to the so-called optimal stochastic control. The problem of designing an optimal state feedback control for a stochastic system is involved. To facilitate the design, the separation principle, formally known as a principle of separation of estimation and control, will be discussed.

The separation principle states that if the state feedback control loop and the state estimation loop are both stable, then the overall system is stable. To proof the separation principle, the following linear, possibly time-varying, system will be considered

$$\dot{x}(t) = Ax(t) + Bu(t), \tag{2.63}$$

$$y(t) = Cx(t). \tag{2.64}$$

Here, the optimal state feedback control law is given by

$$u = -K_c\hat{x}, \tag{2.65}$$

and the optimal state estimator is computed as follows

$$\dot{\hat{x}} = (A - K_eC)\hat{x} + Bu + K_ey. \tag{2.66}$$

By defining the estimated error as $e = x - \hat{x}$, the closed-loop dynamics can be written as the following

$$\begin{bmatrix} \dot{x} \\ \dot{e} \end{bmatrix} = \begin{bmatrix} A - BK_c & BK_c \\ 0 & A - K_eC \end{bmatrix} \begin{bmatrix} x \\ e \end{bmatrix}. \tag{2.67}$$

Since the system matrix is a triangular matrix, the stability of the state feedback control and the state esimation are obviously independent. Figure 2.1 illustrates the block diagram of the state feedback control of stochastic systems. This shows that the state feedback control and the state estimation can be separated explicitly.

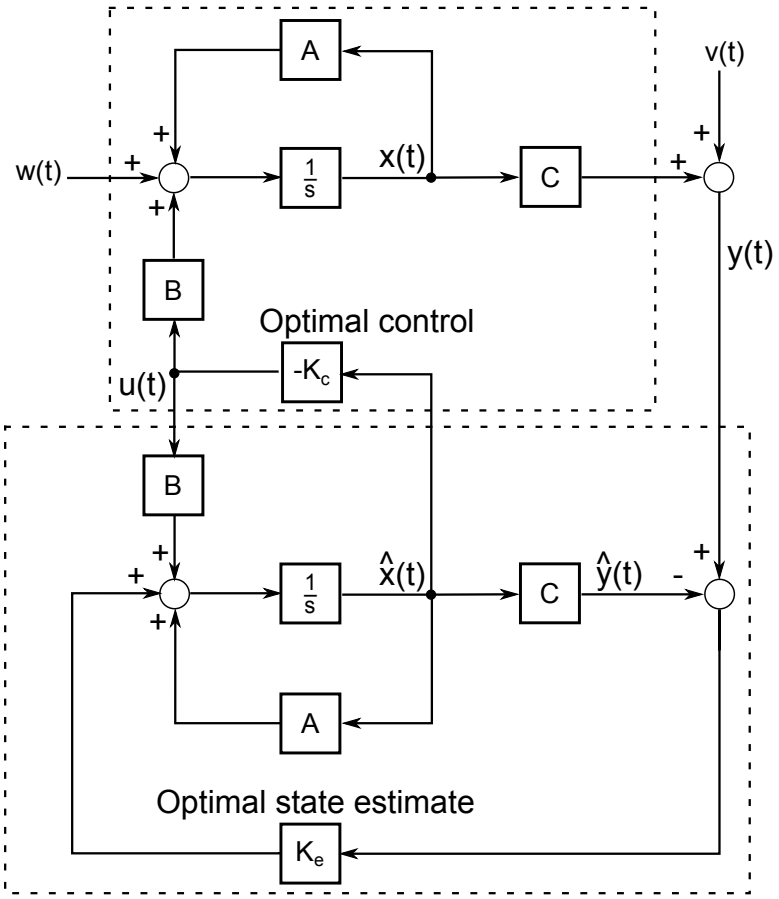

Figure 2.1: Optimal stochastic linear quadratic regulator control.

CHAPTER III

QUAD-ROTOR HELICOPTER DYNAMIC MODELING

In order to control any dynamical systems, the dynamic model is firstly required. Therefore, this chapter is dedicated to the dynamic modeling of the quadrotor. In Section 3.1, the representation of rigid motions in the three dimensional space is considered. The goal of this section is to provide the mathematical tools that will be used to represent the kinematics of the quadrotor. In Section 3.2, the nonlinear dynamic model of the quadrotor, including its kinematics and dynamics, is derived. To apply the LPV control, in Section 3.3, the nonlinear dynamic model is then transformed to an approximated LPV dynamic model.

3.1 Rigid motions in the three dimensional space

This section is related to establishing the representation of the kinematics of moving objects on the Earth-fixed coordinate frame, which is an inertial space. Of course, both the Earth-fixed coordinate frame and the Body-fixed coordinate frame, which is attached to the objects, are the cartesian coordinate. And also, the attitude of the objects comprises the positions and the orientations. To represent the positions, we project all forces into the Earth-fixed coordinate frame, then apply the Newton's law, $\Sigma F = ma$. Because the objects are rotateable, the angles used to compute the projection of the forces are also variable. Therefore, in this section, the rotation matrix, the coordinate rotation, the Euler angles, and the Euler angle rates used to describe the relationship between the moving objects and the fixed coordinate frame will be considered.

3.1.1 Rotation matrix and the coordinate rotation

The rotation matrix is a matrix that can rotate the vector with the same length. There are two possible conventions for defining the rotation matrix: the rotation of an object relative to the fixed reference frame and the rotation of the reference frame. However, in the attitude representation, only the rotation of the reference frame is used. For example, in Figure 3.1, the point v is represented by the two coordinate frames specified by v^0 and v^1. The rotation matrix describing the relationship between these two coordinate frames is given by

$$R_\theta = \begin{bmatrix} c_\theta & s_\theta \\ -s_\theta & c_\theta \end{bmatrix}, \tag{3.1}$$

and the relationship between v^0 and v^1 is obtained as follows

$$v^1 = R_\theta v^0. \tag{3.2}$$

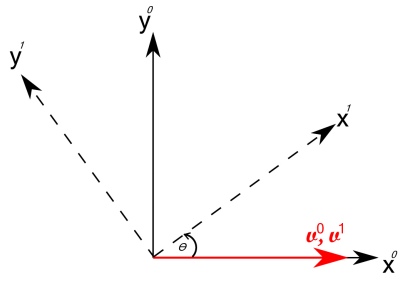

Figure 3.1: Rotation of the reference frame.

In the three-dimensional coordinate systems, the basic rotation matrices representing the rotation about the x-axis, y-axis, and z-axis are given by

$$R_{x,\theta} = \begin{bmatrix} 1 & 0 & 0 \\ 0 & c_\theta & s_\theta \\ 0 & -s_\theta & c_\theta \end{bmatrix}, \quad R_{y,\theta} = \begin{bmatrix} c_\theta & 0 & -s_\theta \\ 0 & 1 & 0 \\ s_\theta & 0 & c_\theta \end{bmatrix}, \quad R_{z,\theta} = \begin{bmatrix} c_\theta & s_\theta & 0 \\ -s_\theta & c_\theta & 0 \\ 0 & 0 & 1 \end{bmatrix},$$

respectively. It is easy to verify that these basic rotation matrices have the following property

$$(R_{i,\theta})^{-1} = (R_{i,\theta})^T, \tag{3.3}$$

where i represents x, y, or z. The multiplication of two rotation matrices yields another rotation matrix. Thus, we can form a more complex rotation matrix by multiplying the above basic rotation matrices. For example, we assume that a point p can be represented by the coordinates specified by p^0, p^1, p^2, and the relationship among these representations are

$$p^1 = R_{x,\phi} p^0, \tag{3.4}$$

$$p^2 = R_{y,\theta} p^1, \tag{3.5}$$

$$p^2 = R_{xy} p^0. \tag{3.6}$$

Comparing the equations (3.4)-(3.6), we can immediately infer that

$$\begin{aligned} R_{xy} &= R_{y,\theta} R_{x,\phi} \\ &= \begin{bmatrix} c_\theta & s_\phi s_\theta & -c_\phi s_\theta \\ 0 & c_\phi & s_\phi \\ s_\theta & -s_\phi c_\theta & c_\phi c_\theta \end{bmatrix}. \end{aligned} \tag{3.7}$$

Figure 3.2 illustrates the composition of the rotations about the x-axis and the y-axis respectively.

To describe any rotation in a three-dimensional space, let us consider the triple rotations in which the first rotation is an angle ϕ about the i-axis, the second rotation is an angle θ about the

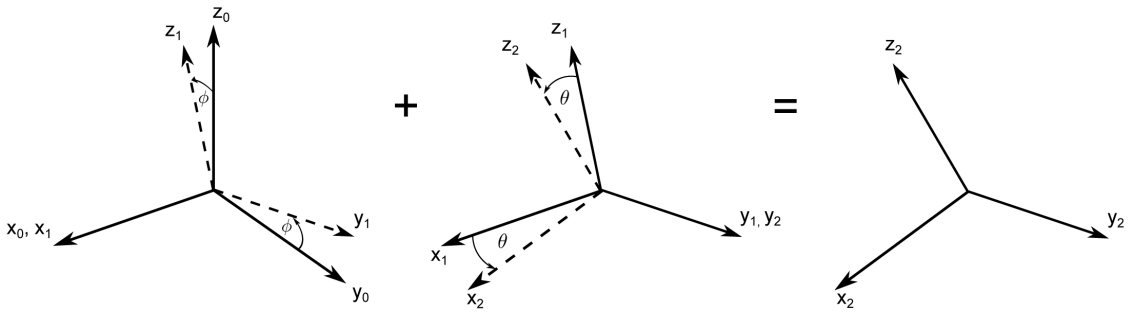

Figure 3.2: Composition of the coordinate rotations.

j-axis, and the third rotation is an angle ψ about the k-axis. For convenience, these angles are arranged in a three-dimensional vector, called the *Euler angle* vector and defined by

$$\alpha := [\phi \;\; \theta \;\; \psi]^T. \tag{3.8}$$

The function that maps the Euler angles to its corresponding rotation matrix R_{ijk} is defined by

$$R_{ijk}(\phi, \theta, \psi) := R_k(\psi) R_j(\theta) R_i(\phi). \tag{3.9}$$

Obviously, there exist twelve possibilities of the permutation used to form the rotation matrices, which can be used to describe any rotation in the three dimensional space. In the general case, let $p^{\mathrm{E}} \in \mathbb{R}^3$ be a vector in the Earth-fixed coordinate frame and $p^{\mathrm{B}} \in \mathbb{R}^3$ be the same vector that is expressed in the Body-fixed coordinate frame. One of the functions that maps the Euler angle vector to the rotation matrix is obtained as follows

$$\begin{aligned} R_{xyz}(\phi, \theta, \psi) &= R_z(\psi) R_y(\theta) R_x(\phi) \\ &= \begin{bmatrix} c_\theta c_\psi & c_\phi s_\psi + s_\phi s_\theta c_\psi & s_\phi s_\psi - c_\phi s_\theta c_\psi \\ -c_\theta s_\psi & c_\phi c_\psi - s_\phi s_\theta s_\psi & s_\phi c_\psi + c_\phi s_\theta s_\psi \\ s_\theta & -s_\phi c_\theta & c_\phi c_\theta \end{bmatrix}, \end{aligned} \tag{3.10}$$

and the relationship between the vector p^{E} and the vector p^{B} is computed by

$$p^{\mathrm{B}} = R_{xyz}(\phi, \theta, \psi) p^{\mathrm{E}}. \tag{3.11}$$

Discussed thus far, we have considered only the coordinate transformation in terms of the positions as a function of the Euler angle vector. Since the Euler angles are changed while the object is rotating. In order to determine the value of the Euler angles, we will then consider the time-derivative of the Euler angles.

3.1.2 Angular velocities in the rotating coordinate

The time-derivative of the Euler angles, called the *Euler angle rates*, are the angular velocities of the objects relative to the rotating coordinate. To compute the Euler angle rates, we have

to express them as the functions of the angular velocities of the object relative to itself. For convenience, we define the three dimensional angular velocities relative to the Body-fixed coordinate frame as follows

$$\omega^{\mathrm{B}} := [p \;\; q \;\; r]^T . \tag{3.12}$$

The superscript 'B' denotes that the angular velocities are expressed in the Body-fixed coordinate frame. Furthermore, we also define the following *Euler angle rate matrix*

$$E^{\mathrm{B}}_{ijk}(\phi, \theta, \psi) := \left[R_k(\psi)R_j(\theta)\hat{e}_i, \;\; R_k(\psi)\hat{e}_j, \;\; \hat{e}_k\right], \tag{3.13}$$

where $\hat{e}_i, \hat{e}_j$, and $\hat{e}_k$ are the unit directional vectors in the $i,\ j$, and k directions respectively. The Euler angle rate matrix is used to transform the Euler angle rates to the angular velocities of the objects relative to the Body-fixed coordinate frame. More details about the angular velocities of the rotating coordinate are provided in [58], Section 4.2-4.4. If the rotation matrix used to transform the coordinate is defined as (3.10), then we have

$$\omega^{\mathrm{B}} = E^{\mathrm{B}}_{xyz}(\alpha)\dot{\alpha}, \tag{3.14}$$

where

$$E^{\mathrm{B}}_{xyz}(\alpha) = \begin{bmatrix} c_\theta c_\psi & s_\psi & 0 \\ -c_\theta s_\psi & c_\psi & 0 \\ s_\theta & 0 & 1 \end{bmatrix}. \tag{3.15}$$

As a result, we obtain the Euler angle rate vector as a function of the Euler angle vector and the angular velocities of the object relative to the Body-fixed coordinate frame as follows

$$\begin{bmatrix} \dot{\phi} \\ \dot{\theta} \\ \dot{\psi} \end{bmatrix} = \begin{bmatrix} c_\psi/c_\theta & -s_\psi/c_\theta & 0 \\ s_\psi & c_\psi & 0 \\ -c_\psi t_\theta & s_\psi t_\theta & 1 \end{bmatrix} \begin{bmatrix} p \\ q \\ r \end{bmatrix} \tag{3.16}$$

To this end, we obtain the attitude representation that can fully describe the kinematics of the objects in the three dimensional space. In the next section, we will apply this attitude representation to the quad-rotor helicopter for obtaining its dynamic model.

3.2 Nonlinear dynamic modeling

This section presents the nonlinear dynamic modeling of the quadrotor. As named, the quadrotor is composed of four rotors. Each rotor comprises an electric DC motor and a rotor blade. Figure 3.3 illustrates the quadrotor configuration. The forward motion of the quadrotor is accomplished by increasing speed of the rear rotor (#3) while simultaneously reducing speed of the forward rotor (#1) at the same amount. The aft, left, and right motions work similarly. The rotation around the yaw angle is accomplished by accelerating or decelerating the two clockwise

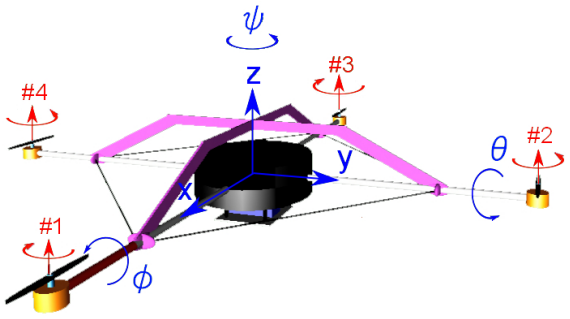

Figure 3.3: Quadrotor configuration.

turning rotors (#1, #3) while anti-accelerating or anti-decelerating the counter-clockwise turning rotors (#2, #4).

The equations describing the motions of the quadrotor are related to the basic rotation of a rigid body having six degrees of freedom. They can be separated into the following kinematics and dynamics.

3.2.1 Kinematics

The kinematic equations are related to the motion of the quadrotor without consideration of the forces and torques driving its motion. In the three dimensional space, let the position of the quadrotor is defined by $r := [r_x \;\; r_y \;\; r_z]^T$, the velocity of the quadrotor that is the time-derivative of the position is defined by $v := [v_x \;\; v_y \;\; v_z]^T$, the angular velocity of the quadrotor relative to itself is defined by $\omega := [p \;\; q \;\; r]^T$, and the Euler's angle is defined by $\alpha := [\phi \;\; \theta \;\; \psi]^T$. Furthermore, let the superscript 'B' and 'E' are used to denote that the variables are defined relatively to the Body-fixed coordinate frame and the Earth-fixed coordinate frame respectively. From the previous section, we readily obtain the following kinematic equations describing the motion of the quadrotor,

$$\begin{bmatrix} r_x^{\mathrm{E}} \\ r_y^{\mathrm{E}} \\ r_z^{\mathrm{E}} \end{bmatrix} = \begin{bmatrix} c_\theta c_\psi & -c_\theta s_\psi & s_\theta \\ c_\phi s_\psi + s_\phi s_\theta c_\psi & c_\phi c_\psi - s_\phi s_\theta s_\psi & -s_\phi c_\theta \\ s_\phi s_\psi - c_\phi s_\theta c_\psi & s_\phi c_\psi + c_\phi s_\theta s_\psi & c_\phi c_\theta \end{bmatrix} \begin{bmatrix} r_x^{\mathrm{B}} \\ r_y^{\mathrm{B}} \\ r_z^{\mathrm{B}} \end{bmatrix}, \tag{3.17}$$

and

$$\begin{bmatrix} \dot{\phi} \\ \dot{\theta} \\ \dot{\psi} \end{bmatrix} = \begin{bmatrix} c_\psi / c_\theta & -s_\psi / c_\theta & 0 \\ s_\psi & c_\psi & 0 \\ -c_\psi t_\theta & s_\psi t_\theta & 1 \end{bmatrix} \begin{bmatrix} p \\ q \\ r \end{bmatrix}. \tag{3.18}$$

3.2.2 Dynamics

The dynamic equations are concerned with the motion of the quadrotor influenced by the external forces and torques. By applying the Newton's laws at the center of the mass, we obtain the

following dynamic equations

$$m\ddot{r}^{\mathrm{E}} = \sum F_{\text{ext}}^{\mathrm{E}}, \tag{3.19}$$

$$J\dot{\omega}^{\mathrm{B}} = -\omega^{\mathrm{B}} \times J\omega^{\mathrm{B}} + \sum T_{\text{ext}}^{\mathrm{B}}, \tag{3.20}$$

where m is the total mass of the quadrotor, $\sum F_{\text{ext}}^{\mathrm{E}}$ is the summation of the external forces represented in the Earth-fixed coordinate frame, $\sum T_{\text{ext}}^{\mathrm{B}}$ is the summation of the external torques represented in the Body-fixed coordinate frame, and J is the inertia matrix given by

$$J = \begin{bmatrix} I_x & 0 & 0 \\ 0 & I_y & 0 \\ 0 & 0 & I_z \end{bmatrix}. \tag{3.21}$$

The exogenous forces and torques acting on the quadrotor consist of the gravity, thrusts, drags, gyroscopic effects, and aerodynamic effects. Of course, the gravity is considered as a constant. The thrusts, which are the inputs of this system, are produced by the rotor blades. The drags and gyroscopic effects occur when the quadrotor is moving and rotating. However, the amount of these two terms are very small. Therefore, to simplify our model, they are ignored. In practical consideration, the aerodynamic effects, such as airflow disruption, are hardly possible to anticipate their models. In this thesis, we treat them as the process noises which will be discussed later in Chapter 6.

Let F_i be the force produced by the i^{th} rotor blade, the summation of the external forces represented in the Earth-fixed coordinate frame is obtained as follows

$$\begin{aligned} \sum F_{\text{ext}}^{\mathrm{E}} &= R_{xyz}(\phi,\theta,\psi)^T \begin{bmatrix} 0 \\ 0 \\ \sum_{i=1}^{4} F_i \end{bmatrix} - \begin{bmatrix} 0 \\ 0 \\ mg \end{bmatrix} \\ &= \begin{bmatrix} s_\theta \sum_{i=1}^{4} F_i \\ -s_\phi c_\theta \sum_{i=1}^{4} F_i \\ c_\phi c_\theta \sum_{i=1}^{4} F_i - mg \end{bmatrix}. \end{aligned} \tag{3.22}$$

On the other hand, the summation of the external torques represented in the Body-fixed coordinate frame is obtained as follows

$$\sum T_{\text{ext}}^{\mathrm{B}} = \begin{bmatrix} \ell(F_2 - F_4) \\ \ell(F_3 - F_1) \\ d(F_1 + F_3 - F_2 - F_4) \end{bmatrix}, \tag{3.23}$$

where l is the lever and d is the scaling factor between the lift force and drag force produced by each rotor blade. Now, let the state vector and the control input vector of the quadrotor dynamic model are defined by

$$x = \left[v_x^{\mathrm{E}} \;\; v_y^{\mathrm{E}} \;\; v_z^{\mathrm{E}} \;\; r_x^{\mathrm{E}} \;\; r_y^{\mathrm{E}} \;\; r_z^{\mathrm{E}} \;\; p \;\; q \;\; r \;\; \phi \;\; \theta \;\; \psi\right]^T, \tag{3.24}$$

$$u = \left[F_1 \;\; F_2 \;\; F_3 \;\; F_4\right]^T, \tag{3.25}$$

respectively, the nonlinear dynamic model of the quadrotor is obtained as follows

$$\dot{x} = f(x,u) = \begin{bmatrix} s_\theta(\sum_{i=1}^4 F_i)/m \\ -s_\phi c_\theta(\sum_{i=1}^4 F_i)/m \\ c_\phi c_\theta(\sum_{i=1}^4 F_i)/m - g \\ v_x^{\mathrm{E}} \\ v_y^{\mathrm{E}} \\ v_z^{\mathrm{E}} \\ \ell(F_2 - F_4)/I_x - qr(I_z - I_y)/I_x \\ \ell(F_3 - F_1)/I_y - pr(I_x - I_z)/I_y \\ d(F_1 + F_3 - F_2 - F_4)/I_z - pq(I_y - I_x)/I_z \\ pc_\psi/c_\theta - qs_\psi/c_\theta \\ ps_\psi + qc_\psi \\ (qs_\psi - pc_\psi)t_\theta + r \end{bmatrix}. \tag{3.26}$$

3.3 LPV dynamic modeling

In order to apply the LPV control strategies, the nonlinear model of the quadrotor derived in the previous section is required to be transformed to the LPV model. The structure of the LPV model we are interested is discussed in Section 2.1. To obtain the polytopic structure from the nonlinear model of the quadrotor, the nonlinear model is linearized in the following

$$f(x,u) \approx f(x^*,u^*) + \left.\frac{\partial f(x,u)}{\partial x}\right|_{(x^*,u^*)} (x - x^*) + \left.\frac{\partial f(x,u)}{\partial u}\right|_{(x^*,u^*)} (u - u^*). \tag{3.27}$$

The Jacobian matrices are computed as follows

$$\frac{\partial f(x,u)}{\partial x} = \begin{bmatrix} 0_{3\times3} & 0_{3\times3} & 0_{3\times3} & \bar{A}_1 \\ I_{3\times3} & 0_{3\times3} & 0_{3\times3} & 0_{3\times3} \\ 0_{3\times3} & 0_{3\times3} & \bar{A}_2 & 0_{3\times3} \\ 0_{3\times3} & 0_{3\times3} & \bar{A}_3 & \bar{A}_4 \end{bmatrix}, \tag{3.28}$$

$$\frac{\partial f(x,u)}{\partial u} = \begin{bmatrix} s_\theta/m & s_\theta/m & s_\theta/m & s_\theta/m \\ -s_\phi c_\theta/m & -s_\phi c_\theta/m & -s_\phi c_\theta/m & -s_\phi c_\theta/m \\ c_\phi c_\theta/m & c_\phi c_\theta/m & c_\phi c_\theta/m & c_\phi c_\theta/m \\ 0_{3\times1} & 0_{3\times1} & 0_{3\times1} & 0_{3\times1} \\ 0 & \ell/I_x & 0 & -\ell/I_x \\ -\ell/I_y & 0 & \ell/I_y & 0 \\ d/I_z & -d/I_z & d/I_z & -d/I_z \\ 0_{3\times1} & 0_{3\times1} & 0_{3\times1} & 0_{3\times1} \end{bmatrix}, \tag{3.29}$$

where

$$\bar{A}_1 = \begin{bmatrix} 0 & c_\theta(\sum_{i=1}^4 F_i)/m & 0 \\ -c_\phi c_\theta(\sum_{i=1}^4 F_i)/m & s_\phi s_\theta(\sum_{i=1}^4 F_i)/m & 0 \\ -s_\phi c_\theta(\sum_{i=1}^4 F_i)/m & -c_\phi s_\theta(\sum_{i=1}^4 F_i)/m & 0 \end{bmatrix},$$

$$\bar{A}_2 = \begin{bmatrix} 0 & r(I_y - I_z)/I_x & q(I_y - I_z)/I_x \\ r(I_z - I_x)/I_y & 0 & p(I_z - I_x)I_y \\ 0 & 0 & 0 \end{bmatrix},$$

$$\bar{A}_3 = \begin{bmatrix} c_\psi/c_\theta & -s_\psi/c_\theta & 0 \\ s_\psi & c_\psi & 0 \\ -c_\psi t_\theta & s_\psi t_\theta & 1 \end{bmatrix},$$

$$\bar{A}_4 = \begin{bmatrix} 0 & (pc_\psi - qs_\psi)t_\theta/c_\theta & -(ps_\psi + qc_\psi)/c_\theta \\ 0 & 0 & pc_\psi - qs_\psi \\ 0 & (qs_\psi - pc_\psi)/c_\theta^2 & (ps_\psi + qc_\psi)t_\theta \end{bmatrix}.$$

Then, they are evaluated at

$$x^* = \begin{bmatrix} 0 & 0 & 0 & r_x^{\mathrm{E}} & r_y^{\mathrm{E}} & r_z^{\mathrm{E}} & 0 & 0 & 0 & 0 & 0 & \psi \end{bmatrix}^T, \tag{3.30}$$

$$u^* = \begin{bmatrix} mg/4 & mg/4 & mg/4 & mg/4 \end{bmatrix}^T. \tag{3.31}$$

Consequently, we have the following LPV model of the quadrotor

$$\dot{x} = A(\psi)x + B(u - u^*), \tag{3.32}$$

where

$$A(\psi) = \begin{bmatrix} 0 & 0 & 0 & 0 & 0 & 0 & 0 & 0 & 0 & 0 & g & 0 \\ 0 & 0 & 0 & 0 & 0 & 0 & 0 & 0 & 0 & -g & 0 & 0 \\ 0 & 0 & 0 & 0 & 0 & 0 & 0 & 0 & 0 & 0 & 0 & 0 \\ 1 & 0 & 0 & 0 & 0 & 0 & 0 & 0 & 0 & 0 & 0 & 0 \\ 0 & 1 & 0 & 0 & 0 & 0 & 0 & 0 & 0 & 0 & 0 & 0 \\ 0 & 0 & 1 & 0 & 0 & 0 & 0 & 0 & 0 & 0 & 0 & 0 \\ 0 & 0 & 0 & 0 & 0 & 0 & 0 & 0 & 0 & 0 & 0 & 0 \\ 0 & 0 & 0 & 0 & 0 & 0 & 0 & 0 & 0 & 0 & 0 & 0 \\ 0 & 0 & 0 & 0 & 0 & 0 & 0 & 0 & 0 & 0 & 0 & 0 \\ 0 & 0 & 0 & 0 & 0 & 0 & c_\psi & -s_\psi & 0 & 0 & 0 & 0 \\ 0 & 0 & 0 & 0 & 0 & 0 & s_\psi & c_\psi & 0 & 0 & 0 & 0 \\ 0 & 0 & 0 & 0 & 0 & 0 & 0 & 0 & 1 & 0 & 0 & 0 \end{bmatrix}, \quad (3.33)$$

$$B = \begin{bmatrix} 0 & 0 & 0 & 0 \\ 0 & 0 & 0 & 0 \\ 1/m & 1/m & 1/m & 1/m \\ 0 & 0 & 0 & 0 \\ 0 & 0 & 0 & 0 \\ 0 & 0 & 0 & 0 \\ 0 & \ell/I_x & 0 & -\ell/I_x \\ -\ell/I_y & 0 & \ell/I_y & 0 \\ d/I_z & -d/I_z & d/I_z & -d/I_z \\ 0 & 0 & 0 & 0 \\ 0 & 0 & 0 & 0 \\ 0 & 0 & 0 & 0 \end{bmatrix}. \quad (3.34)$$

Finally, the matrix $A(\psi)$ is transformed to the polytopic structure. That is

$$A(\rho) = \sum_{i=1}^{4} \rho_i(\psi) A_i, \quad (3.35)$$

where each element in A_i is equal to the element in $A(\psi)$ except the nonlinear part that is equal to $a_1,\ a_2,\ a_3$, and a_4,

$$a_1 = \begin{bmatrix} -1 & -1 \\ 1 & -1 \end{bmatrix}, \quad a_2 = \begin{bmatrix} 1 & -1 \\ 1 & 1 \end{bmatrix}, \quad a_3 = \begin{bmatrix} -1 & 1 \\ -1 & -1 \end{bmatrix}, \quad a_4 = \begin{bmatrix} 1 & 1 \\ -1 & 1 \end{bmatrix},$$

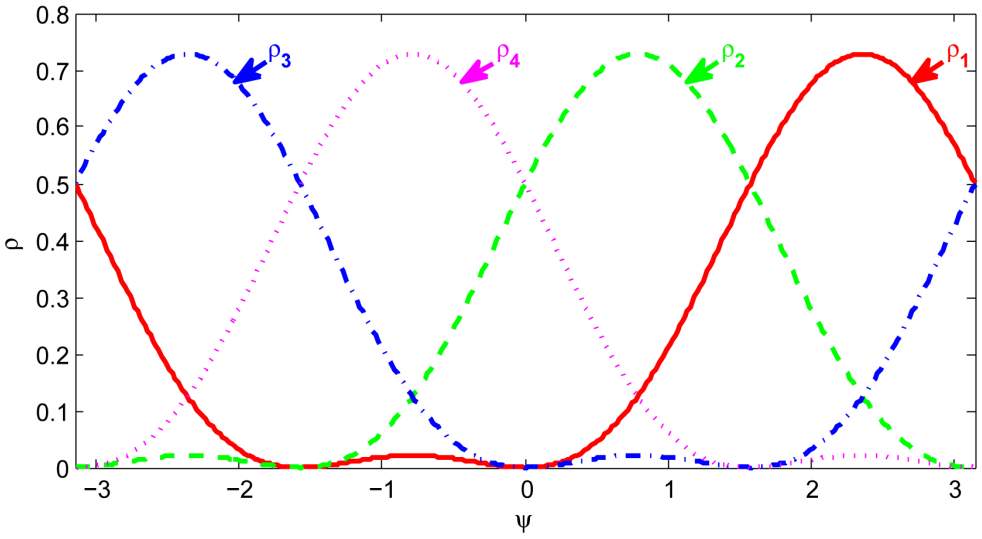

Figure 3.4: Parameter ρ_i as the function of ψ.

for $A_1,\ A_2,\ A_3$, and A_4 respectively. Here, the new parameters corresponding to the bases A_i for all $i \in I[1,4]$ are computed as the following

$$\rho_1 = \left(\frac{1+s_\psi}{2}\right)\left(\frac{1-c_\psi}{2}\right), \tag{3.36}$$

$$\rho_2 = \left(\frac{1+s_\psi}{2}\right)\left(\frac{1+c_\psi}{2}\right), \tag{3.37}$$

$$\rho_3 = \left(\frac{1-s_\psi}{2}\right)\left(\frac{1-c_\psi}{2}\right), \tag{3.38}$$

$$\rho_4 = \left(\frac{1-s_\psi}{2}\right)\left(\frac{1+c_\psi}{2}\right). \tag{3.39}$$

Figure 3.4 illustrates the parameter ρ_i as the function of ψ.

In this chapter, we have derived the dynamical model of the quad-rotor helicopter. Both the nonlinear model and its approximated LPV model have been considered. Next, in chapter 4, to obtain the LPV state feedback control of the quadrotor, the LQR control of LPV systems will be considered.

CHAPTER IV

CONTROL OF LINEAR PARAMETER-VARYING SYSTEMS

This chapter presents the control of polytopic LPV systems of the form

$$\dot{x}(t) = A(\rho(t))x(t) + B(\rho(t))u(t). \tag{4.1}$$

We assume that the state space matrices $A(\rho(t))$ and $B(\rho(t))$ are the bounded continuous functions depending affinely on $\rho(t)$, i.e., $\rho(t) = [\rho_1(t) \dots \rho_N(t)]^T$ and

$$A(\rho(t)) = \sum_{i=1}^{N} \rho_i(t) A_i \,, \tag{4.2}$$

$$B(\rho(t)) = \sum_{i=1}^{N} \rho_i(t) B_i \,. \tag{4.3}$$

We further assume that the real parameter vector $\rho(t)$ is online measured and varied in a certain polytope, i.e., $\rho(t) \in \Lambda_N$ such that

$$\Lambda_N := \left\{ \lambda \in \mathbb{R}^N : \sum_{i=1}^{N} \lambda_i = 1,\ \lambda_i \geq 0 \right\}. \tag{4.4}$$

For the sake of simplicity, the time specific t will be omitted. However, it is important to keep in mind that the parameter still depends on time. In order to obtain a good state feedback controller, this chapter provides the following. In Section 4.1, the stabilization problem of the LPV systems (4.1) is first considered. The common quadratic Lyapunov function and the parameter-dependent quadratic Lyapunov function are applied so that the quadratic Lyapunov stability conditions are obtained. Then, in Section 4.2, all the results are extended to the LQR problem. These lead to the linear parameter-varying quadratic regulator, which will be called LPVQR. The LPVQR computed via the parameter-dependent quadratic Lyapunov function requires the knowledge about the bound on the rate of the parameter. This is rarely available in practice. Therefore, in this section we also propose the use of the composite quadratic Lyapunov function to avoid this problem.

4.1 Quadratic stabilization

The quadratic stabilization of LPV systems concerns with finding the state feedback controller that makes the closed-loop systems satisfy the quadratic Lyapunov stability condition mentioned in Chapter 2.

4.1.1 LPV quadratic stabilization via common quadratic Lyapunov function

The quadratic stabilization of the LPV system (4.1) considers the control law given by

$$u = -K(\rho)x, \tag{4.5}$$

where $K(\rho) = \sum_{i=1}^{N} \rho_i K_i$. Substituting (4.5) into (4.1), the closed-loop system can be written as

$$\dot{x} = \left(A(\rho) - B(\rho)K(\rho)\right) x. \tag{4.6}$$

The condition for the closed-loop system (4.6) to be quadratically stable is the existence of a quadratic Lyapunov function such that $V(0) = 0$, $V(x) > 0$ and $\dot{V}(x) < 0$ for all $x \neq 0$. The adoptation of the common quadratic Lyapunov function defined by

$$V(x) = x^T P x, \tag{4.7}$$

where $P = P^T > 0$, results in the following time derivative of the Lyapunov function

$$\dot{V}(x) = x^T \Big(P\left(A(\rho) - B(\rho)K(\rho)\right) + \left(A(\rho) - B(\rho)K(\rho)\right)^T P \Big) x. \tag{4.8}$$

The neccessary and sufficient condition for quadratic stabilization of the LPV system (4.1) via the common quadratic Lyapunov function is then obtained as the following lemma.

Lemma 4.1 (Quadratic stabilization of LPV systems via the common quadratic Lyapunov function)**.** *The LPV system (4.1) is quadratically stabilizable via the common quadratic Lyapunov function if and only if there exist a positive definite matrix Y and an arbitrary real matrix-valued function $L(\rho)$ such that*

$$A(\rho)Y + YA(\rho)^T - B(\rho)L(\rho) - L(\rho)^T B(\rho)^T < 0. \tag{4.9}$$

Consequently, the LPV stabilizing gain is given by

$$K(\rho) = L(\rho)Y^{-1}. \tag{4.10}$$

Proof. See Appendix A.2.1. □

To solve the LMI feasibility problem with the infinite dimensional LMI constraint in Lemma 4.1, a sufficient condition with the finite constraints is given as the following theorem.

Theorem 4.1 (Sufficient condition for quadratic stabilization of LPV systems via the common quadratic Lyapunov function)**.** *If there exist a positive definite matrix Y and a set of real matrices $\{L_1, \ldots, L_N\}$ such that*

$$A_i Y + Y A_i^T - B_i L_i - L_i^T B_i^T < 0, \qquad \forall i \in I[1, N], \tag{4.11}$$

$$A_i Y + A_j Y + Y A_i^T + Y A_j^T - B_i L_j - B_j L_i - L_i^T B_j^T - L_j^T B_i^T < 0, \qquad \forall i \in I[1, N-1], \ \forall j \in I[i+1, N], \tag{4.12}$$

then the LPV system (4.1) is quadratically stabilizable and the LPV stabilizing gain is given by

$$K(\rho) = \sum_{i=1}^{N} \rho_i(t) K_i, \tag{4.13}$$

where $K_i = L_i Y^{-1}$ for all $i \in I[1, N]$.

Proof. See Appendix A.2.2. □

The use of the common P for quadratic Lyapunov functions often gives the conservative result or even fails to stabilize the system. Next, to obtain a less conservative result, the use of the parameter-dependent quadratic Lyapunov function will be considered.

4.1.2 LPV quadratic stabilization via parameter-dependent quadratic Lyapunov function

The parameter-dependent quadratic stabilization of LPV systems also considers the control law given by (4.5), but the Lyapunov function is defined by

$$V(x) = x^T P(\rho) x, \tag{4.14}$$

where $P(\rho) = P(\rho)^T > 0$. We assume that the parameter dependency of the matrix $P(\rho)$ has the same structure as the feedback gain matrix $K(\rho)$, i.e.,

$$P(\rho) = \sum_{i=1}^{N} \rho_i P_i. \tag{4.15}$$

The time derivative of the parameter-dependent quadratic Lyapunov function is computed as follows

$$\dot{V}(x) = x^T \left(\dot{P}(\rho) + P(\rho)(A(\rho) - B(\rho)K(\rho)) + (A(\rho) - B(\rho)K(\rho))^T P(\rho) \right) x, \tag{4.16}$$

and the neccessary and sufficient condition for parameter-dependent quadratic stabilization of the LPV system (4.1) via the parameter-dependent quadratic Lyapunov function is obtained as the following lemma.

Lemma 4.2 (Parameter-dependent quadratic stabilization of LPV systems via the parameter-dependent quadratic Lyapunov function)**.** *The LPV system (4.1) is parameter-dependent quadratically stabilizable via the parameter-dependent quadratic Lyapunov function if and only if there exist a positive definite matrix-valued function $Y(\rho)$ and an arbitrary real matrix-valued function $L(\rho)$ such that*

$$A(\rho)Y(\rho) + Y(\rho)A(\rho)^T - B(\rho)L(\rho) - L(\rho)^T B(\rho)^T - Y(\dot{\rho}) < 0. \tag{4.17}$$

Consequently, the LPV stabilizing gain is given by

$$K(\rho) = L(\rho)Y(\rho)^{-1}. \tag{4.18}$$

Proof. See Appendix A.2.3. □

To obtain a sufficient condition with finite constraints for solving the LMI feasibility problem in Lemma 4.2, there are necessary assumptions to be defined. First, we assume that the rate of the parameter varies in a certain convex polyhedral set. Clearly,

$$\dot{\rho}(t) = \sum_{k=1}^{M} \sigma_k(t)\nu_k \in \operatorname{co}\{\nu_1, \ldots, \nu_M\}, \tag{4.19}$$

where $\nu_k \in \mathbb{R}^N$ and $\sigma(t) = [\sigma_1 \dots \sigma_M]^T \in \Lambda_M$ such that

$$\Lambda_M := \left\{ \lambda \in \mathbb{R}^M : \sum_{k=1}^{M} \lambda_k = 1,\ \lambda_k \geq 0 \right\}. \tag{4.20}$$

To determine the set $\{\nu_1, \dots, \nu_M\}$, since $\sum_{i=1}^{N} \rho_i(t) = 1$, it is important to restrict the magnitude of $\dot{\rho}(t)$ by imposing that $||\nu||_1 = 0$ and $||\nu||_\infty \leq \nu_0$. Moreover, we define the linear matrix function as

$$U(x) := \sum_i x_i U_i, \tag{4.21}$$

for any finite dimension vector x. To this end, we have the following sufficient condition.

Theorem 4.2 (Sufficient condition for parameter-dependent quadratic stabilization of LPV systems via the parameter-dependent quadratic Lyapunov function)**.** *If there exist a set of positive definite matrices* $\{Y_1, \dots, Y_N\}$ *and a set of real matrices* $\{L_1, \dots, L_N\}$ *such that*

$$A_i Y_i + Y_i A_i^T - B_i L_i - L_i^T B_i^T - Y(\nu_k) < 0, \quad \forall i \in I[1, N], \quad \forall k \in I[1, M], \tag{4.22}$$

$$A_i Y_j + A_j Y_i + Y_i A_j^T + Y_j A_i^T - B_i L_j - B_j L_i - L_i^T B_j^T - L_j^T B_i^T - 2Y(\nu_k) < 0, \quad \forall i \in I[1, N-1], \ \forall j \in I[i+1, N], \ \forall k \in I[1, M], \tag{4.23}$$

then the LPV system (4.1) is parameter-dependent quadratically stabilizable and the LPV stabilizing gain is given by

$$K(\rho) = \sum_{i=1}^{N} \rho_i(t) K_i, \tag{4.24}$$

where $K_i = L_i Y(\rho)^{-1}$ *for all* $i \in I[1, N]$ *and* $Y(\rho) = \sum_{i=1}^{N} \rho_i(t) Y_i$.

Proof. See Appendix A.2.4. □

So far we have considered only the problem of stabilization. To obtain the controller that can guarantee the cost function while the worst case on this cost function is minimized, next we will apply the LQR mentioned in Chapter 2 to the LPV systems.

4.2 Linear Parameter-Varying Quadratic Regulator (LPVQR)

The LQR control of LPV systems, denoted by LPVQR, concerns with finding the state feedback controller that minimizes the upper bound on the cost function defined by

$$J = \int_0^\infty \left(x(t)^T Q x(t) + u(t)^T R u(t) \right) dt \tag{4.25}$$

The LPVQR is straightforward by applying the LQR control of LTI systems to the LPV systems. Here we consider both the use of the common quadratic Lyapunov function and the parameter-dependent quadratic Lyapunov function. The sufficient conditions are obtained in the same way as the stability analysis. Furthermore, we also propose the LPVQR that use the composite quadratic Lyapunov function (2.19) to avoid the problem of unknowing the bound on the rate of the parameter.

4.2.1 LPVQR via common quadratic Lyapunov function

Consider the LPV system (4.1) under the LPV control law,

$$u = -K(\rho)x, \tag{4.26}$$

where $K(\rho) = \sum_{i=1}^{N} \rho_i K_i$. By using the common quadratic Lyapunov function defined by

$$V(x) = x^T P x, \tag{4.27}$$

an upper bound on the cost function (4.25) can be computed by the following theorem.

Theorem 4.3 (Sufficient condition for LPVQR via the common quadratic Lyapunov function)**.** *Assume the existence of a positive definite matrix Y and a set of real matrices $\{L_1, \ldots, L_N\}$ satisfying*

$$\begin{aligned}
&\max_{Y,\, L_1,\ldots,L_N} \operatorname{tr}(Y) \\
&\text{s.t.} \begin{bmatrix} -(A_iY - B_iL_i) - (A_iY - B_iL_i)^T & Y & L_i^T \\ Y & Q^{-1} & 0 \\ L_i & 0 & R^{-1} \end{bmatrix} > 0, \quad \forall i \in I[1,N], \qquad (4.28) \\
&\begin{bmatrix} -(A_iY + A_jY - B_iL_j - B_jL_i) \\ -(A_iY + A_jY - B_iL_j - B_jL_i)^T & 2Y & L_i^T + L_j^T \\ 2Y & 2Q^{-1} & 0 \\ L_i + L_j & 0 & 2R^{-1} \end{bmatrix} > 0, \quad \begin{matrix} \forall i \in I[1,N-1], \\ \forall j \in I[i+1,N], \end{matrix} \qquad (4.29)
\end{aligned}$$

then the LPV system (4.1) under the control law (4.26) such that $K_i = L_iY^{-1}$ for all $i \in I[1,N]$ satisfies

$$J(x(0), u(\cdot)) < \min_{Y,\, L_1,\ldots,L_N} x(0)^T P x(0),$$

where $P = Y^{-1}$.

Proof. See Appendix A.2.5. □

It is remarkable that if the matrix B is constant, i.e. $B(\rho) = B$, then the LMI constraints in Theorem 4.3 can be reduced as stated in the following corollary.

Corollary 4.1 (Sufficient condition for LPVQR via the common quadratic Lyapunov function, $B(\rho) = B$)**.** *Assume the existence of a positive definite matrix Y and a set of matrices $\{L_1, \ldots, L_N\}$ satisfying*

$$\begin{aligned}
&\max_{Y,\, L_1,\ldots,L_N} \operatorname{tr}(Y) \\
&\text{s.t.} \begin{bmatrix} -(A_iY - BL_i) - (A_iY - BL_i)^T & Y & L_i^T \\ Y & Q^{-1} & 0 \\ L_i & 0 & R^{-1} \end{bmatrix} > 0, \quad \forall i \in I[1,N], \qquad (4.30)
\end{aligned}$$

then the LPV system (4.1) in which $B(\rho) = B$ under the control law (4.26) such that $K_i = L_i Y^{-1}$ for all $i \in I[1, N]$ satisfies

$$J(x(0), u(\cdot)) < \min_{Y,\, L_1,\ldots,L_N} x(0)^T P x(0),$$

where $P = Y^{-1}$.

Proof. See Appendix A.2.6. □

The use of the common P for Lyapunov functions always leads to the conservative result. To reduce the conservativeness, we will next consider the use of the parameter-dependent quadratic Lyapunov function for the LPVQR.

4.2.2 LPVQR via parameter-dependent quadratic Lyapunov function

The LPV system (4.1) under the control law (4.26) is again considered. By using the parameter-dependent quadratic Lyapunov function defined by $V(x) = x^T P(\rho) x$, an upper bound on the cost function (4.25) can be computed by the following theorem.

Theorem 4.4 (Sufficient condition for LPVQR via the parameter-dependent quadratic Lyapunov function)**.** *Assume the existence of a set of positive definite matrices $\{Y_1, \ldots, Y_N\}$ and a set of real matrices $\{L_1, \ldots, L_N\}$ satisfying*

$$\max_{\substack{Y_1,\ldots,Y_N \\ L_1,\ldots,L_N}} \sum \mathrm{tr}(Y_i)$$

$$\text{s.t.} \begin{bmatrix} Y(\nu_k) - (A_i Y_i - B_i L_i) - (A_i Y_i - B_i L_i)^T & Y_i & L_i^T \\ Y_i & Q^{-1} & 0 \\ L_i & 0 & R^{-1} \end{bmatrix} > 0, \quad \begin{matrix} \forall i \in I[1, N], \\ \forall k \in I[1, M], \end{matrix} \tag{4.31}$$

$$\begin{bmatrix} 2Y(\nu_k) - (A_i Y_j + A_j Y_i - B_i L_j - B_j L_i) \\ -(A_i Y_j + A_j Y_i - B_i L_j - B_j L_i)^T & Y_i + Y_j & L_i^T + L_j^T \\ Y_i + Y_j & 2Q^{-1} & 0 \\ L_i + L_j & 0 & 2R^{-1} \end{bmatrix} > 0, \quad \begin{matrix} \forall i \in I[1, N-1], \\ \forall j \in I[i+1, N], \\ \forall k \in I[1, M], \end{matrix} \tag{4.32}$$

then the LPV system (4.1) under the control law (4.26) such that $K_i = L_i \left(\sum_{j=1}^N \rho_j(t) Y_j \right)^{-1}$ for all $i \in I[1, N]$ satisfies

$$J(x(0), u(\cdot)) < \min_{\substack{Y_1,\ldots,Y_N \\ L_1,\ldots,L_N}} x(0)^T P(\rho(0)) x(0),$$

where $P(\rho(0)) = \left(\sum_{i=1}^N \rho_i(0) Y_i \right)^{-1}$.

Proof. See Appendix A.2.7. □

With a good choice of the bound on the rate of the parameter, the parameter-dependent quadratic Lyapunov function significantly outperforms the common quadratic Lyapunov function in terms of the conservatism. This will be seen in the illustrating example in Section 4.2.4. However in practice, the bound on the rate of the parameter is often unknown. Moreover in our LPV model of quadrotor, the use of the parameter-dependent quadratic Lyapunov function is still being suffered from the conservativeness and failed to stabilize. This will be discussed later in Chapter 6. Therefore, we propose to use the composite quadratic Lyapunov function for the LPVQR, because this kind of Lyapunov function does not attend to the rate of the parameter and also work well with our system.

4.2.3 LPVQR via composite quadratic Lyapunov function

Consider the composite quadratic Lyapunov function defined by

$$V_c(x) := \min_{\rho} x^T P(\rho) x. \tag{4.33}$$

From the fact that if ρ^* is the optimal ρ such that $x^T P(\rho)x$ is minimized then

$$\frac{\partial V_c}{\partial x} = 2P(\rho^*(x))x, \tag{4.34}$$

we obtain the following time derivative of the composite quadratic Lyapunov function

$$\dot{V}_c(x) = x^T \left(P(\rho^*)(A(\rho^*) + B(\rho^*)K(\rho^*)) + (A(\rho^*) + B(\rho^*)K(\rho^*))^T P(\rho^*) \right) x. \tag{4.35}$$

As a result, an upper bound on the cost function (4.25) can be computed by the following theorem.

Theorem 4.5 (Sufficient condition for LPVQR via the composite quadratic Lyapunov function)**.** *Assume the existence of a positive definite matrix-valued function $Y(\rho)$ and an arbitrary real matrix-valued function $L(\rho)$ satisfying*

$$\begin{aligned} &\max_{Y(\rho),\, L(\rho)} \operatorname{tr}(Y(\rho)) \\ &\text{s.t.} \begin{bmatrix} -(A(\rho)Y(\rho) - B(\rho)L(\rho)) - (A(\rho)Y(\rho) - B(\rho)L(\rho))^T & Y(\rho) & L(\rho) \\ Y(\rho) & Q^{-1} & 0 \\ L(\rho)^T & 0 & R^{-1} \end{bmatrix} > 0, \end{aligned} \tag{4.36}$$

then the LPV system (4.1) under the control law (4.26) such that $K_i = L_i \left(\sum_{j=1}^{N} \rho_j(t) Y_j \right)^{-1}$ for all $i \in I[1, N]$ satisfies

$$J(x(0), u(\cdot)) < \min_{Y(\rho),\, L(\rho)} x(0)^T P(\rho(0)) x(0),$$

where $P(\rho(0)) = Y(\rho(0))^{-1}$.

Proof. See Appendix A.2.8. □

However, this infinite dimensional optimization problem has to be solved along the trajectory of the parameter. To solve this problem in a systematic way, we apply the tensor product transformation by griding the system and solve for a set of fixed-parameter LMI optimization problems instead. Finally, we obtain the approximated solution that is expressed by the parameter of the system with a finite set of the basis of solution.

4.2.4 Illustrating example

Example 4.1. *Consider the following simple model of an inverted pendulum [59]*

$$\dot{x}_1 = x_2, \tag{4.37}$$

$$\dot{x}_2 = -0.1x_2 + \sin(x_1) + u. \tag{4.38}$$

This nonlinear dynamical system can be transformed to an LPV system as follows

$$\dot{x} = A(\rho)x + B(\rho)u, \tag{4.39}$$

where

$$A(\rho) = \rho_1 A_1 + \rho_2 A_2, \quad \begin{cases} A_1 = \begin{bmatrix} 0 & 1 \\ 1 & -0.1 \end{bmatrix}, \ \rho_1 = \dfrac{\sin(x_1)}{x_1} \\ A_2 = \begin{bmatrix} 0 & 1 \\ 0 & -0.1 \end{bmatrix}, \ \rho_2 = \dfrac{x_1 - \sin(x_1)}{x_1} \end{cases},$$

$$B(\rho) = \begin{bmatrix} 0 \\ 1 \end{bmatrix}.$$

Note that $\rho_i \geq 0$ for all i and $\rho_1 + \rho_2 = 1$ for all $t \geq 0$. Figure 4.1 illustrates the parameter ρ_i as a function of x_1 and the partial derivative of ρ_i with respect to x_1. Let $Q = \mathrm{diag}(4, 4)$ and $R = 1$, the LPVQR with various types of the quadratic Lyapunov function give the following results:

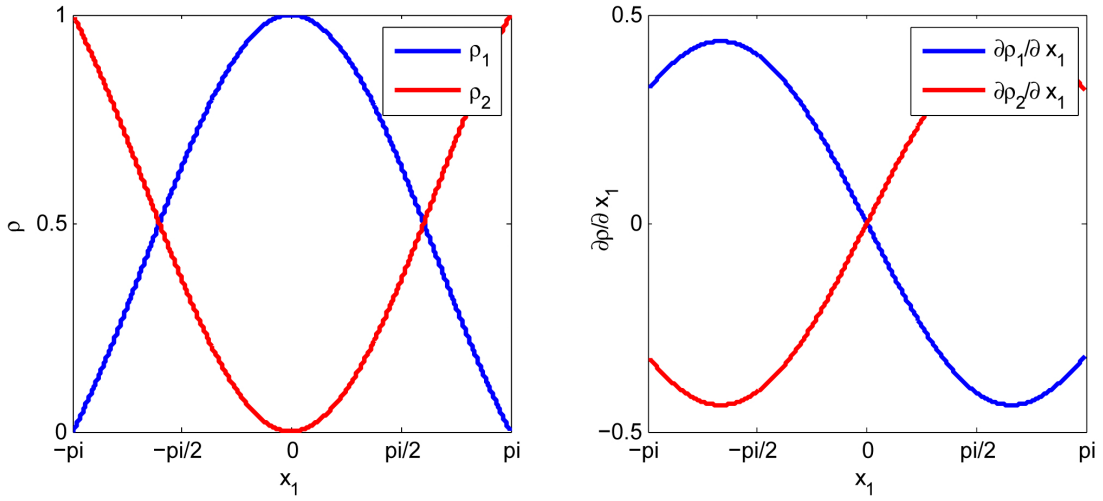

Figure 4.1: The parameter ρ (left) and the partial derivative of ρ with respect to x_1 (right).

	Guaranteed cost	Actual cost	Remark
Common quadratic Lyapunov function	77.9747	58.5117	–
	77.9747	58.2753	$B(\rho) = B$
Parameter dependent quadratic Lyapunov function	72.3877	58.0670	$\lvert\dot{x}_1\rvert \leq \pi$
	55.7618	55.6300	$\lvert\dot{x}_1\rvert \leq 2$
Composite quadratic Lyapunov function	55.8658	55.7392	–
Piecewise quadratic Lyapunov function [59]	58.75	–	–

Table 4.1: Performance assessment of the LPVQR control with various types of Lyapunov function

Table 4.1 shows the performance evaluation of each Lyapunov function. The use of the piecewise quadratic Lyapunov function, accompanying with the original work of this example, is also compared. The table shows that the Lyapunov function with variable parameter, including the composite quadratic Lyapunov function, gives the better performance than the common quadratic Lyapunov function and the piecewise quadratic Lyapunov function. However, the use of Theorem 4.4 requires the appropriate value of the bound on the rate of the parameter. Figure 4.2 illustrates the comparison between the use of Theorem 4.3 and Corollary 4.1. The results are quite similar. However, Corollary 4.1 gives a slightly better performance in terms of the actual cost, while the implementation is easier because of the use of fewer LMI conditions. Figure 4.3 illustrates the comparison between the use of Theorem 4.4 with two values of the bound on the rate of the parameter, $\pm\pi$ and ± 2. It is obvious that the bound closer to the actual value of $\dot{x}_1$ gives the better performance. Figure 4.4 illustrates the guaranteed cost that is computed by Theorem 4.4 as a function of the bound on the rate of x_1. The guaranteed cost grows up to a limited value. However, this value is less than the guaranteed cost computed by the use of the common quadratic Lyapunov function. Figure 4.5 illustrates the comparison between the use of Theorem 4.4 with $|\dot{x}_1| \leq 2$ and Theorem 4.5. Both give quite similar results. The composite quadratic Lyapunov function gives a bit worse result owing to the effect of approximation.

In this chapter, the quadratic stabilization and the quadratic regulator control of LPV systems have been studied. Three types of the Lyapunov function, the common quadratic Lyapunov function, the parameter-dependent quadratic Lyapunov function, and the composite quadratic Lyapunov function, have been considered. The parameter-dependent quadratic Lyapunov function gives the best result while the common quadratic Lyapunov function gives the worst result. However, the parameter-dependent quadratic Lyapunov function requires the appropriate value of the pre-defined bound on the rate of the parameter which is often unknown in practice. Therefore, the use of the composite quadratic Lyapunov function for LPVQR is proposed. To use the composite quadratic Lyapunov function, the LMI optimization problem needs to be solved along the trajectory of the parameter. The tensor product transformation is applied to reduce the infinite dimensional LMI optimization problem into a set of finite dimensional LMI optimization problems.

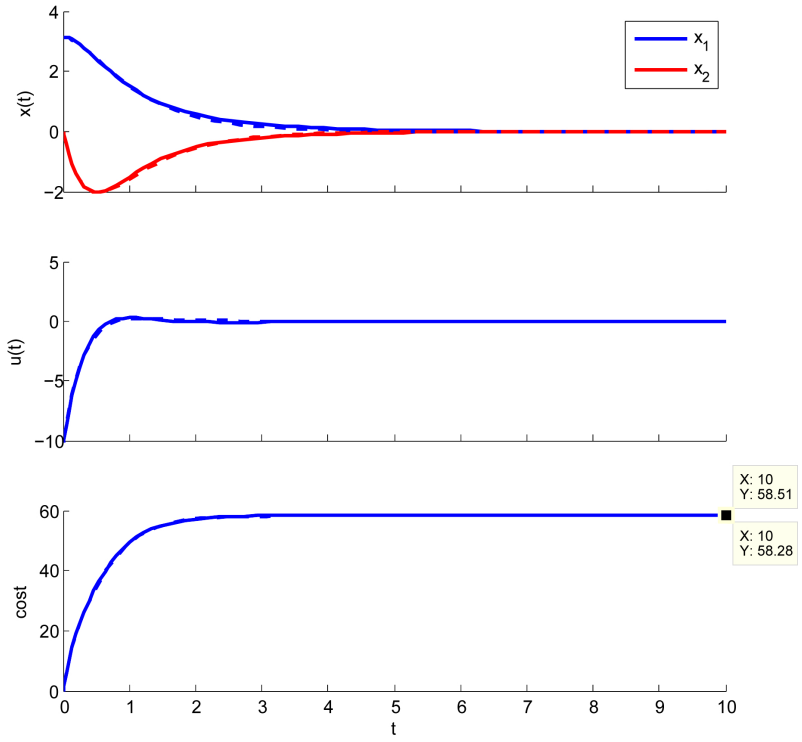

Figure 4.2: Comparison of control responses, control inputs, and costs between the use of Theorem 4.3 (solid lines) and Corollary 4.1 (dash lines).

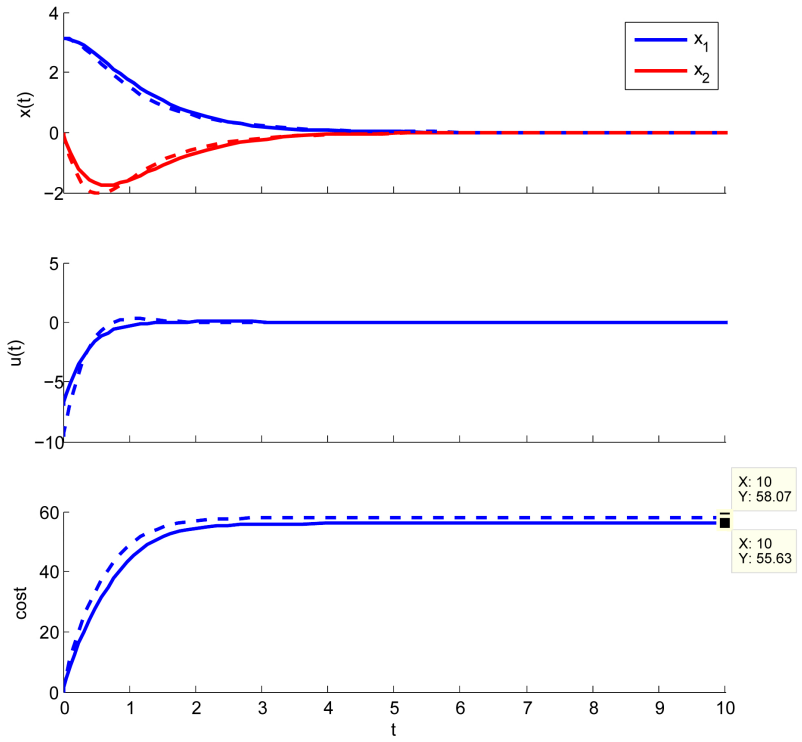

Figure 4.3: Comparison of control responses, control inputs, and costs between the use of Theorem 4.4 with $|\dot{x}_1| \leq 2$ (solid lines) and Theorem 4.4 with $|\dot{x}_1| \leq \pi$ (dash lines).

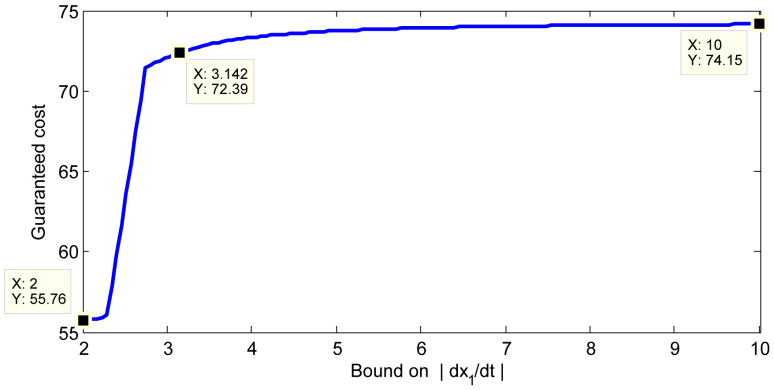

Figure 4.4: Guaranteed cost of the controller computed by Theorem 4.4 as the function of the bound on the rate of x_1.

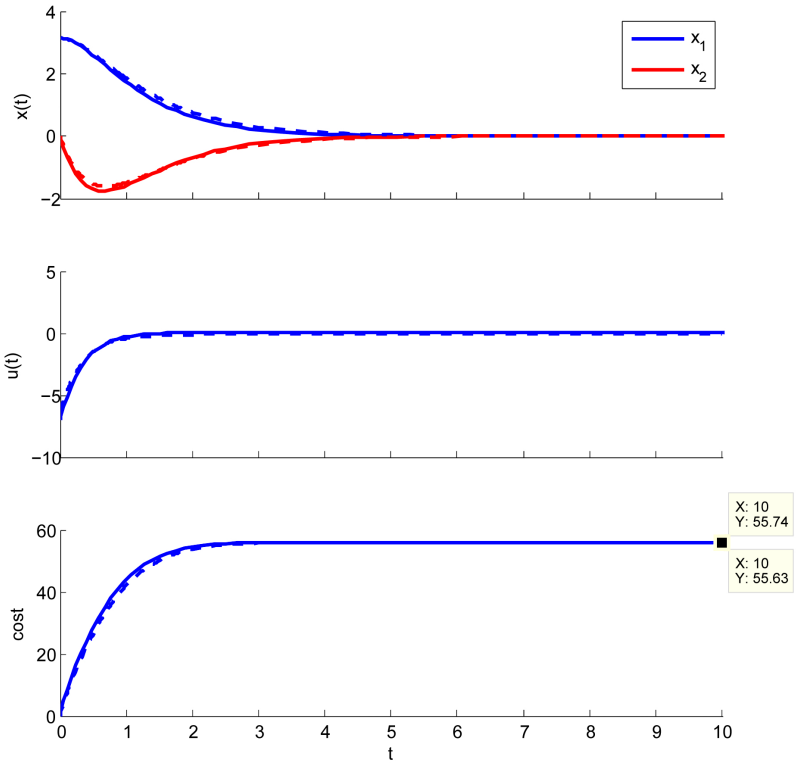

Figure 4.5: Comparison of control responses, control inputs, and costs between the use of Theorem 4.4 with $|\dot{x}_1| \leq 2$ (solid lines) and Theorem 4.5 (dash lines).

CHAPTER V

CONTROL OF SATURATED LINEAR PARAMETER-VARYING SYSTEMS

This chapter considers the LQR control of saturated LPV systems. First in Section 5.1, we focus on the LQR control of the saturated LTI systems. The controller obtained in this section is named saturated LQR (SLQR). Unlike the conventional LQR, the SLQR can guarantee both stability and performance of the saturated LTI systems. Nevertheless, the appearing performance of the SLQR is dropped from one obtained from the LQR. To improve the performance of the SLQR, in Section 5.2, the idea of using the high-gain controller, stated in [60], is applied to the SLQR. This results in the high-gain SLQR. Finally in Section 5.3, both the SLQR and the high-gain SLQR are incorporated with the LQR control of the saturated LPV systems, the saturated LPVQR (SLPVQR) and the high-gain SLPVQR are then obtained, respectively.

5.1 Saturated linear quadratic regulator

This section considers LTI systems with the bounded control inputs of the form

$$\dot{x} = Ax + Bu, \tag{5.1}$$

$$u = -\mathrm{sat}_\sigma(Kx), \tag{5.2}$$

where

$$\mathrm{sat}_\sigma(Kx) = \begin{bmatrix} \mathrm{sgn}(k_1 x)\min(|k_1 x|, \sigma) \\ \vdots \\ \mathrm{sgn}(k_m x)\min(|k_m x|, \sigma) \end{bmatrix}, \qquad \begin{array}{ll} k_i: & i^{\text{th}} \text{ row of } K \\ \sigma: & \text{bounding level} \end{array}. \tag{5.3}$$

To understand the effect of saturation on the dynamical systems, we consider the following LTI system

$$\begin{bmatrix} \dot{x}_1 \\ \dot{x}_2 \end{bmatrix} = \begin{bmatrix} 0 & 1 \\ 0 & 0 \end{bmatrix} \begin{bmatrix} x_1 \\ x_2 \end{bmatrix} + \begin{bmatrix} 0 \\ 1 \end{bmatrix} u. \tag{5.4}$$

Under the cost function defined by

$$\int_0^\infty \left(x^T Q x + u^T R u\right) dt, \tag{5.5}$$

where $Q = \mathrm{diag}(1, 1)$ and $R = 0.001$, the LQR state feedback control law is computed as follows

$$u = -Kx, \quad K = \begin{bmatrix} 31.6241 & 32.6078 \end{bmatrix}. \tag{5.6}$$

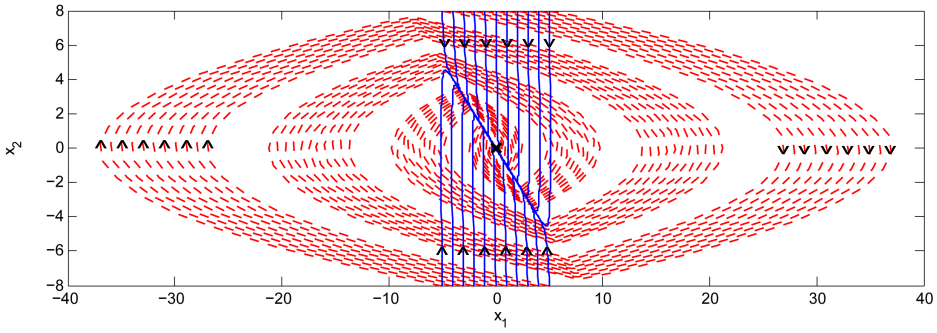

Figure 5.1: State trajectories of the LQR control; the control input is unbounded (solid lines) and bounded by $|u| \leq 1$ (dashed lines).

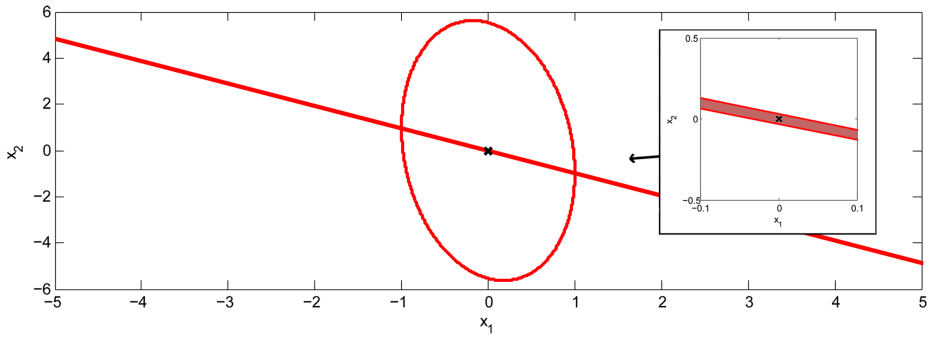

Figure 5.2: Ellipsoidal domain of attraction and unsaturated region computed by the LQR.

Figure 5.1 illustrates the state trajectories of the closed-loop system. This figure shows that the saturation entails degradation of the closed-loop performance. Figure 5.2 illustrates an ellipsoidal domain of attraction defined by $\{x : \ x^T P x \leq 1\}$. It also illustrates the unsaturated region which is bounded by the two straight lines. Obviously, the performance degradation occurs because the real input cannot reach to the desired input. This will happen if the state of the system is outside the unsaturated region. To guarantee stability and performance of this system, next, the ellipsoid is stipulated to be inside the unsaturated region. The LMI condition stated in Lemma 2.2 is applied to the conventional LQR. This leads to the following theorem.

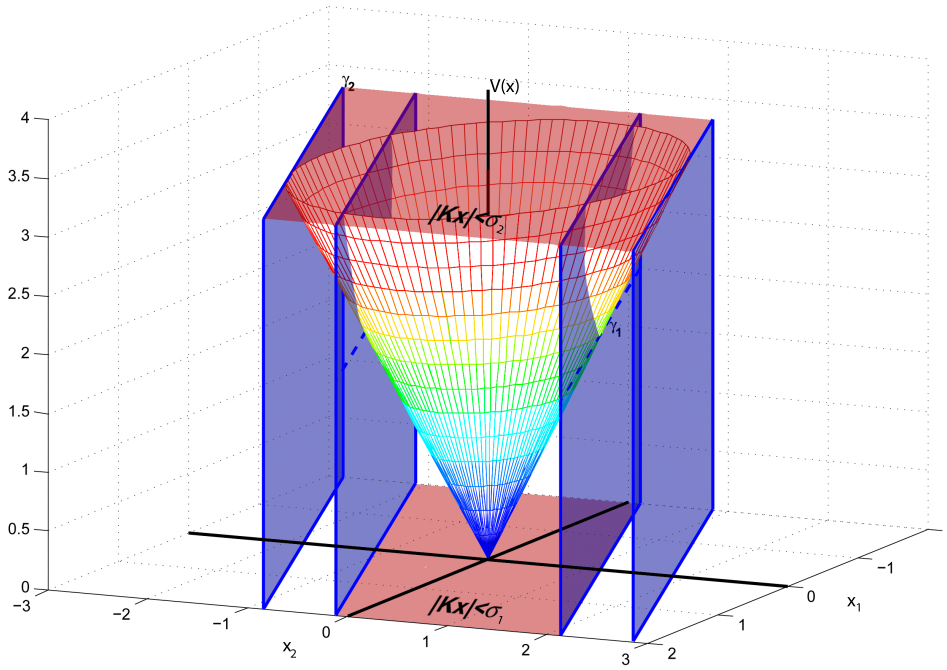

Figure 5.3: Geometrical representation of the use of Theorem 5.1.

Theorem 5.1 (Linear quadratic regulator for saturated LTI systems)**.** *Assume the existence of a positive definite matrix Y and an arbitrary real matrix L satisfying*

$$\max_{Y,\,L} \ \mathrm{tr}(Y)$$

$$\text{s.t.} \quad \begin{bmatrix} -(AY-BL)-(AY-BL)^T & Y & L^T \\ Y & Q^{-1} & 0 \\ L & 0 & R^{-1} \end{bmatrix} > 0, \tag{5.7}$$

$$\begin{bmatrix} \sigma^2/\gamma & \ell_i \\ \ell_i^T & Y \end{bmatrix} > 0, \quad \forall i \in I[1,m], \quad \ell_i : \ i^{th} \text{ row of } L, \tag{5.8}$$

then the LTI systems (5.1) with the bounded control inputs (5.2) in which $K = LY^{-1}$ satisfies

$$J(x(0),u(\cdot)) < \min_{Y,\,L} x(0)^T P x(0),$$

where $P = Y^{-1}$ for all $x(0) \in \{x : \ x^T P x \le \gamma\}$.

Proof. See Appendix A.3.1 □

The state feedback gain K obtained from Theorem 5.1 is called the SLQR. Figure 5.3 illustrates the geometrical representation of the use of Theorem 5.1. Here, we assume that the system has single input. Furthermore, we assume that $\sigma_1^2/\gamma_1 = \sigma_2^2/\gamma_2$. This results in the same matrix P. The figure shows that the value of σ determines the bounding level of the unsaturated region. This value is limited by the physical property of the actuator. It also shows that the value of γ determines

the bound on the guaranteed performance corresponding to the bounding level σ. The value of γ can be increased arbitrarily to obtain the larger size of the ellipsoid. However, this trades with the increased upper bound on the cost function.

Applying Theorem 5.1, in which $\sigma = 1$ and $\gamma = 1$, to the system (5.4) with the cost function (5.5) gives the following SLQR state feedback control law

$$u = -Kx, \quad K = \begin{bmatrix} 0.4378 & 1.1094 \end{bmatrix}. \tag{5.9}$$

Figure 5.4 illustrates the state trajectories and the ellipsoidal domains of attraction computed by the LQR and the SLQR. Obviously, the ellipsoid computed by the LQR cannot guarantee performance or even stability of the system. On the other hand, the ellipsoid computed by the SLQR is invariant. This implies the capability of guaranteeing stability of the system. It is noticeable that this ellipsoid is also inside the unsaturated region, which is bounded by the two blue straight lines. Figure 5.5 illustrates the ellipsoidal domains of attraction computed by the SLQR with various values of σ. Here, the value of γ is fixed to 1. This figure shows that the unsaturated region is enlarged as the value of σ is increased. The shape of the ellipsoid, fitted to the unsaturated region, gradually tends to the shape of the ellipsoid that is computed by the LQR. However, its shape is no larger than the shape of the ellipsoid computed by the LQR, though the value of σ is further increased. Figure 5.6 also illustrates the ellipsoidal domains of attraction computed by the SLQR. Here, the value of σ is fixed to 1 and the value of γ is varied. This figure shows that the larger ellipsoid can be obtained by increasing the upper bound on the guaranteed cost.

The controller obtained from Theorem 5.1 is sometimes called the low-gain controller. Figure 5.7 illustrates the comparison of the control responses, the control inputs, and the costs obtained by applying the LQR control and the SLQR control, of which the value of γ is varied. This figure shows that though the SLQR with $\gamma = 60$ can guarantee both stability and performance of the system, i.e., $x(0) = [0 \;\; 2]^T \in \mathcal{E}(P, \gamma)$, its performance is much worse than one obtained from the LQR. Therefore, next, we will consider how to improve the performance of the SLQR.

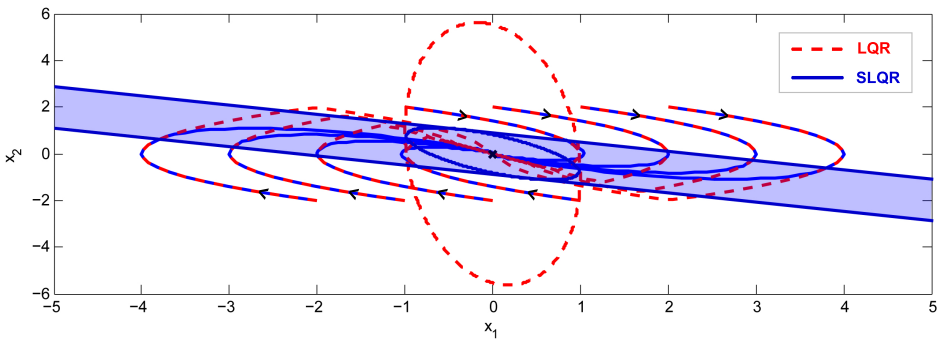

Figure 5.4: State trajectories and their corresponding ellipsoidal domains of attraction computed by the LQR and the SLQR.

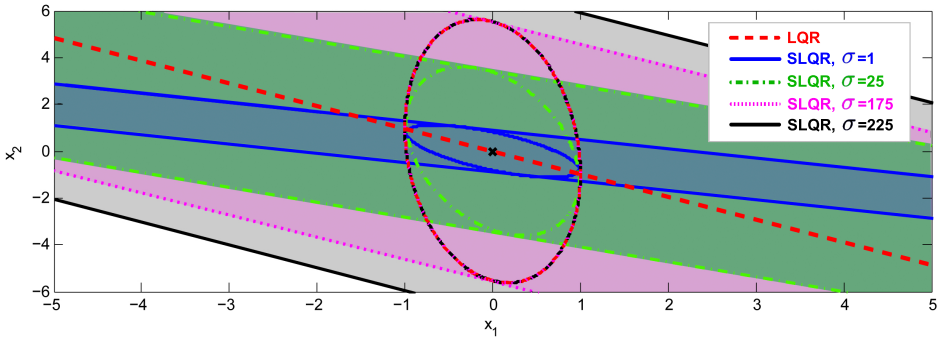

Figure 5.5: Ellipsoidal domains of attraction and unsaturated regions computed by the LQR and the SLQR with various values of σ.

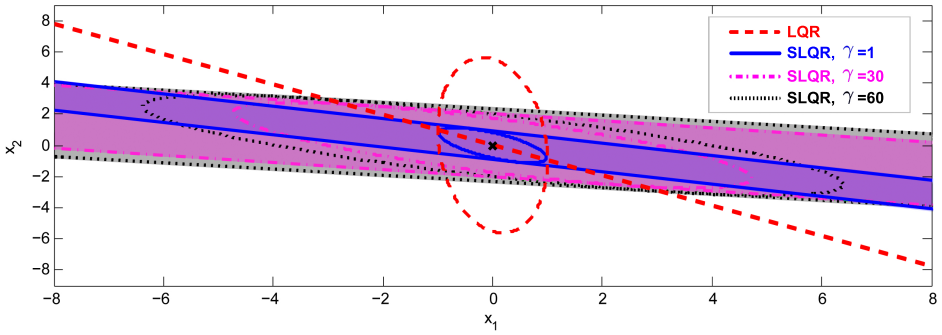

Figure 5.6: Ellipsoidal domains of attraction and unsaturated regions computed by the LQR and the SLQR with various values of γ.

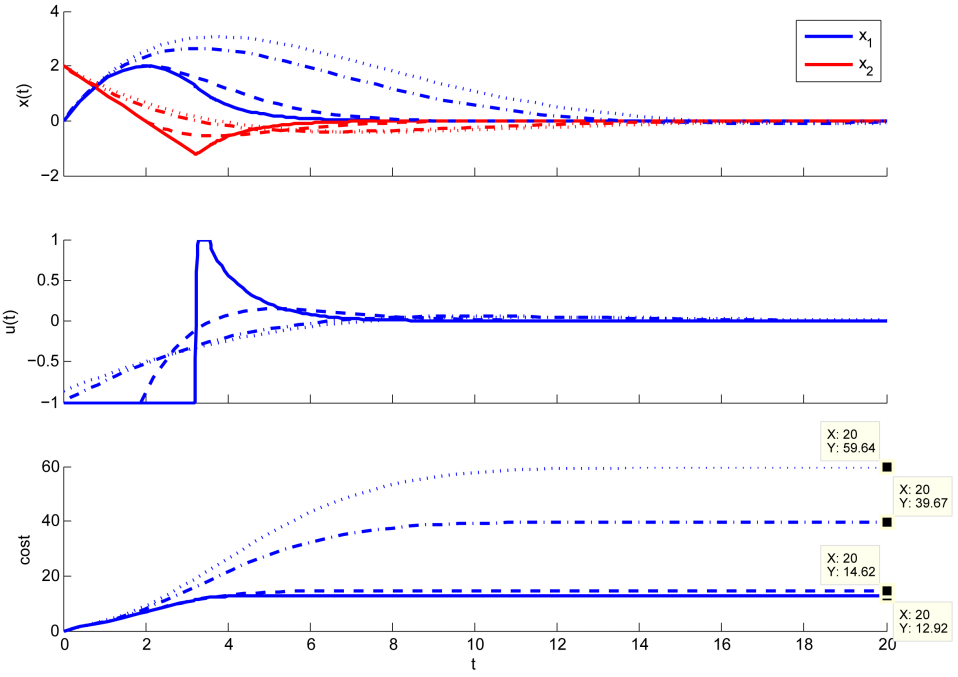

Figure 5.7: Control responses, control inputs, and costs by using the LQR control (solid lines) and the SLQR control with $\sigma = 1$ and $\gamma = 1$ (dashed lines), 30 (dot-dashed lines), and 60 (dotted lines).

5.2 Improvement using high-gain feedback

In the previous section, we have considered the ellipsoidal domain of attraction guaranteeing the upper bound on the cost function. The ellipsoid is forced to be inside the unsaturated region. This restriction leads to the lower gain and the lower performance. As suggested in [60], in this section, a more relaxed condition is considered to improve the performance of the SLQR. With an auxiliary state feedback gain, the ellipsoidal domain of attraction is provably need not to be inside the unsaturated region. For a vector $v \in \mathbb{V}$, such that

$$\mathbb{V} := \{v \in \mathbb{R}^m : \ v_i = 1 \text{ or } 0\}, \tag{5.10}$$

and two matrices K and $F \in \mathbb{R}^{m\times n}$, we define the following matrix function

$$S(v, K, F) = \begin{bmatrix} v_1 k_1 + (1 - v_1) f_1 \\ \vdots \\ v_m k_m + (1 - v_m) f_m \end{bmatrix}. \tag{5.11}$$

There are 2^m possibilities of v used to form a new matrix $S(v, K, F)$ from the rows of K and F, i.e., if $v_i = 1$, then the i^{th} row of $S(v, K, F)$ is k_i, otherwise the i^{th} row of $S(v, K, F)$ is f_i. With this definition, the improved SLQR is obtained as the following theorem.

Theorem 5.2 (Improved linear quadratic regulator for saturated LTI systems)**.** *Assume the existence of a positive definite matrix Y and arbitrary real matrices L and M satisfying*

$$\begin{aligned} &\max_{Y,\, L,\, M} \ \operatorname{tr}(Y) \\ &\text{s.t.} \begin{bmatrix} -(AY - BS(v, L, M)) - (AY - BS(v, L, M))^T & Y & S(v, L, M)^T \\ Y & Q^{-1} & 0 \\ S(v, L, M) & 0 & R^{-1} \end{bmatrix} > 0, \quad \forall v \in \mathbb{V}, \end{aligned} \tag{5.12}$$

$$\begin{bmatrix} \sigma^2/\gamma & \mathcal{M}_i \\ \mathcal{M}_i^T & Y \end{bmatrix} > 0, \quad \forall i \in I[1, m], \quad \mathcal{M}_i : \ i^{th} \textit{ row of } M, \tag{5.13}$$

then the LTI systems (5.1) with bounded control inputs (5.2) in which $K = LY^{-1}$ satisfies

$$J(x(0), u(\cdot)) < \min_{Y,\, L,\, M} x(0)^T P x(0),$$

where $P = Y^{-1}$ for all $x(0) \in \{x : \ x^T P x \le \gamma\}$.

Proof. See Appendix A.3.2 □

The state feedback gain K obtained from Theorem 5.2 is called the high-gain SLQR. Applying Theorem 5.2, in which $\sigma = 1$ and $\gamma = 1$, to the system (5.4) with the cost function (5.5) gives the following high-gain SLQR state feedback control law

$$u = -Kx, \quad K = \begin{bmatrix} 117.0280 & 152.2037 \end{bmatrix}. \tag{5.14}$$

Figure 5.8 illustrates the state trajectories and the ellipsoidal domain of attraction computed by the high-gain SLQR. They are also compared with the results from the LQR and the SLQR. In this figure, the two coinciding dash-dotted straight lines signify for the unsaturated region, which is very strait. This shows that the ellipsoid computed by the high-gain SLQR can guarantee the closed-loop stability, though it is not inside the unsaturated region. Figure 5.9 illustrates the comparison of the control responses, the control inputs, and the costs obtained by applying the LQR control, the SLQR control, and the high-gain SLQR control, of which the values of σ and γ are set to 1 and 60 respectively. Obviously, the cost obtained from the high-gain SLQR is significantly improved. This cost is very close to the cost obtained from the LQR.

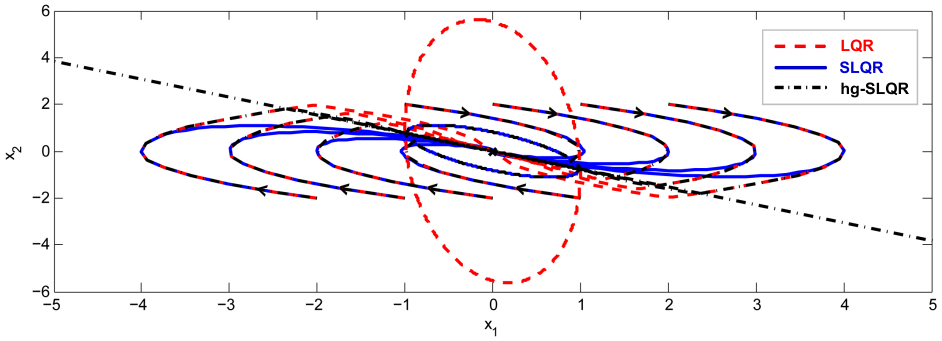

Figure 5.8: State trajectories and their corresponding ellipsoidal domains of attraction computed by the LQR, the SLQR, and the high-gain SLQR.

	Guaranteed costs	**Actual costs**	**Remarks**
LQR	0.1304	12.9183	Fail to guarantee stability.
SLQR	5.9236	14.6245	$\gamma = 1$, Fail to guarantee stability.
	39.6801	39.6767	$\gamma = 30$, Fail to guarantee stability.
	59.6855	59.6823	$\gamma = 60$, Guarantee stability and performance.
High-gain SLQR	5.9238	12.9800	$\gamma = 1$, Fail to guarantee stability.
	39.6809	13.7781	$\gamma = 30$, Fail to guarantee stability.
	59.6850	14.1560	$\gamma = 60$, Guarantee stability and performance.

Table 5.1: Performance assessment of the LQR, the SLQR, and the high-gain SLQR control of the saturated linear system.

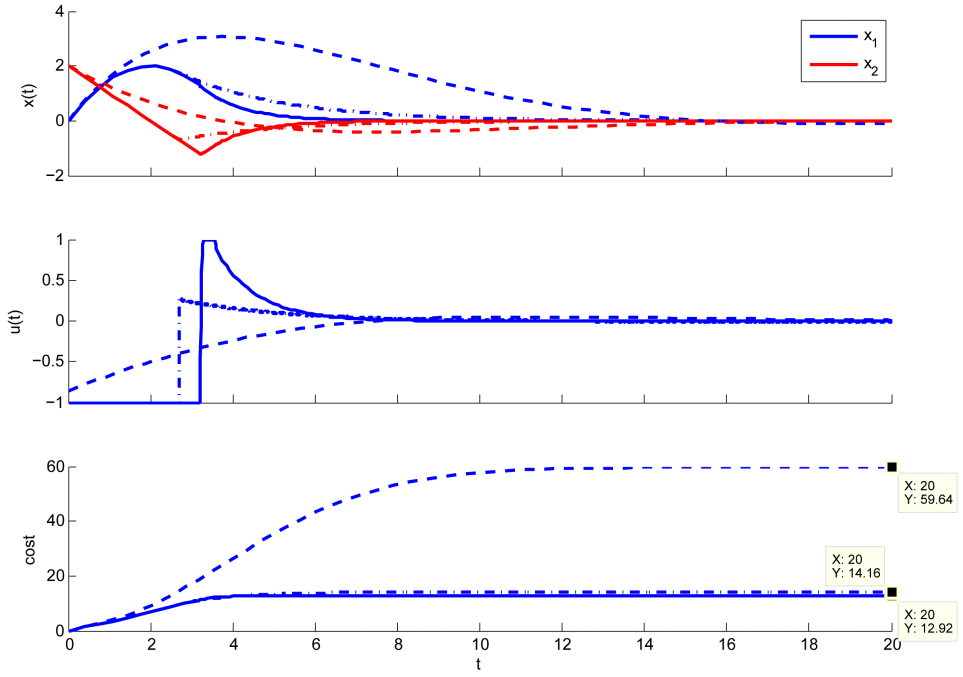

Figure 5.9: Control responses, control inputs, and costs by using the LQR control (solid lines), the SLQR control (dashed lines), and the high-gain SLQR control (dash-dotted lines) with $\sigma = 1$ and $\gamma = 60$.

All the results from the LQR, the SLQR, and the high-gain SLQR control of the LTI system (5.4) with the bounded control input, such that $|u| \leq 1$, can be concluded as showed in Table 5.1. The use of the LQR is failed certainly. For the use of the SLQR and the high-gain SLQR, the ellipsoids guaranteeing the stability of the system are quite similar. Therefore, the guaranteed costs are obtained similarly for each value of γ. When γ is set to 1 or 30, both the SLQR and the high-gain SLQR are failed to guarantee the stability. This is because the initial state, which is set to $[0 \;\; 2]^T$, is outside the guaranteeing ellipsoids. However, if γ is set to 60, the ellipsoids are large enough to guarantee the stability of the system. The guaranteed performance is then followed. In this case, the simulation shows that the actual cost obtained from the high-gain SLQR is much better than one obtained from the SLQR.

5.3 Extension to LPV systems

In chapter 4, we have derived the LQR control of the LPV systems. The use of the common quadratic Lyapunov function, the parameter-dependent quadratic Lyapunov function, and the composite quadratic Lyapunov function are considered. The first two Lyapunov functions are failed in the designing of the controller, used to control the LPV model of the quadrotor. This will be discussed in the next chapter. The use of the composite quadratic Lyapunov function seems to work well with our system. However, when the saturation is taken into account, the controllability of

the LPVQR decreases rapidly until the quadrotor is failed to stabilize. Therefore, in this section, we will extend the results from the SLQR control and the high-gain SLQR control to the LPVQR control, that uses only the composite quadratic Lyapunov function.

We recall here the LPV systems defined in (4.1)

$$\dot{x}(t) = A(\rho(t))x(t) + B(\rho(t))u(t). \tag{5.15}$$

Under the bounded control inputs of the form

$$u = -sat_{\sigma}(K(\rho)x), \tag{5.16}$$

$$K(\rho) = \sum_{i=1}^{N} \rho_i K_i, \tag{5.17}$$

the SLPVQR and the high-gain SLPVQR are obtained as the following theorems.

Theorem 5.3 (Sufficient condition for SLPVQR via the composite quadratic Lyapunov function)**.** *Assume the existence of a positive definite matrix-valued function $Y(\rho)$ and an arbitrary real matrix-valued function $L(\rho)$ satisfying*

$$\max_{Y(\rho),\, L(\rho)} \operatorname{tr}(Y(\rho))$$

$$\text{s.t.} \begin{bmatrix} -(A(\rho)Y(\rho) - B(\rho)L(\rho)) - (A(\rho)Y(\rho) - B(\rho)L(\rho))^T & Y(\rho) & L(\rho) \\ Y(\rho) & Q^{-1} & 0 \\ L(\rho)^T & 0 & R^{-1} \end{bmatrix} > 0, \tag{5.18}$$

$$\begin{bmatrix} \sigma^2/\gamma & \ell_i(\rho) \\ \ell_i(\rho)^T & Y(\rho) \end{bmatrix} > 0, \quad \forall i \in I\,[1, m]\,, \quad \ell_i(\rho)\text{: } i^{th} \text{ row of } L(\rho), \tag{5.19}$$

then the LPV system (5.15) with the bounded control inputs (5.16)–(5.17) such that

$$K_i = L_i \left(\sum_{j=1}^{N} \rho_j(t) Y_j \right)^{-1}, \quad \forall i \in I[1, N],$$

satisfies

$$J(x(0), u(\cdot)) < \min_{Y(\rho),\, L(\rho)} x(0)^T P(\rho(0)) x(0),$$

where $P(\rho(0)) = Y(\rho(0))^{-1}$, for all $x(0) \in \{x : \, x^T P(\rho) x \leq \gamma\}$.

Proof. See Appendix A.3.3. □

Theorem 5.4 (Sufficient condition for high-gain SLPVQR via the composite quadratic Lyapunov function)**.** *Assume the existence of a positive definite matrix-valued function $Y(\rho)$ and arbitrary real matrix-valued functions $L(\rho),\ M(\rho)$ satisfying*

$$\max_{Y(\rho),\ L(\rho),\ M(\rho)} \operatorname{tr}(Y(\rho))$$

$$\text{s.t.} \quad \begin{bmatrix} -(A(\rho)Y(\rho) - B(\rho)S(v, L(\rho), M(\rho))) & Y(\rho) & S(v, L(\rho), M(\rho)) \\ -(A(\rho)Y(\rho) - B(\rho)S(v, L(\rho), M(\rho)))^T & & \\ Y(\rho) & Q^{-1} & 0 \\ S(v, L(\rho), M(\rho))^T & 0 & R^{-1} \end{bmatrix} > 0, \quad \forall v \in \mathbb{V}, \tag{5.20}$$

$$\begin{bmatrix} \sigma^2/\gamma & \mathcal{M}_i(\rho) \\ \mathcal{M}_i(\rho)^T & Y(\rho) \end{bmatrix} > 0, \quad \forall i \in I\,[1, m]\,, \quad \mathcal{M}_i(\rho) :\ i^{th}\ \textit{row of}\ M(\rho), \tag{5.21}$$

then the LPV system (5.15) with the bounded control inputs (5.16)–(5.17) such that

$$K_i = L_i \left(\sum_{j=1}^{N} \rho_j(t) Y_j \right)^{-1}, \quad \forall i \in I[1, N],$$

satisfies

$$J(x(0), u(\cdot)) < \min_{Y(\rho),\ L(\rho),\ M(\rho)} x(0)^T P(\rho(0)) x(0),$$

where $P(\rho(0)) = Y(\rho(0))^{-1}$, for all $x(0) \in \{x :\ x^T P(\rho) x \le \gamma\}$.

Proof. The proof is followed in the proof of Theorem 5.2 and Theorem 5.3. □

In this chapter, the LQR control of the saturated LPV systems has been considered. Firstly, the LQR control of the saturated LTI systems was derived. Two approaches, the low-gain and the high gain, were considered. These result in the SLQR and the high-gain SLQR, respectively. The SLQR and the high-gain SLQR were then extended to the saturated LPV systems. Consequently, the SLPVQR and the high-gain SLPVQR were obtained. Evidently, the SLPVQR and the high-gain SLPVQR have the abilities of guaranteeing the stability and the performance of the closed-loop LPV systems in a local domain. In the next chapter, we will apply them to control the LPV model of the quadrotor, having been derived in Chapter 3.

CHAPTER VI

OUTPUT FEEDBACK CONTROL OF QUAD-ROTOR HELICOPTER WITH INPUT SATURATION

In this chapter, the LPVQR control of the quadrotor is considered. To verify the control strategies derived in Chapter 4 and Chapter 5, the simulation based on the MATLAB simulink is given. In Section 6.1, the simulation setup is presented. Then, the results from the simulation are discussed in Section 6.2. Here, we consider both the unsaturated and the saturated LPVQR control of the quadrotor. Moreover, the output feedback control problem, of which the system is incorporated with the process noise and the measurement noise, is also considered.

6.1 Simulation setup

The simulation given in this thesis is based on the MATLAB simulink. The simulink block called the VR Sink is used to build the 3D visualization of the quadrotor for demonstrating the results. The VR Sink links the signals from other simulink blocks to the WRL file. This is the file associated with the Virtual Reality Markup Language (VRML) [61]. The VR Sink then displays and interacts the 3D graphic user interface (GUI) as shown in Figure 6.1. Figure 6.2 illustrates the WRL editor, which is provided by the MATLAB. This editor is used to create the 3D objects and generate the input ports of the VR Sink for specifying the properties of these 3D objects. Figure 6.3 illustrates the simulink block diagram comprising the quadrotor dynamic s-function, the LPV controller, the EKF, and the VR Sink. The EKF algorithm was provided in Chapter 2 and the nonlinear dynamic model of the quadrotor was derived in Chapter 3. Here, the parameters of the quadrotor are assumed as shown in Table 6.1. Of course, the LPVQR, the SLPVQR, and the high-gain SLPVQR, derived in Chapter 4 and Chapter 5, are applied to the LPV controller block. To verify the control strategies and study the characteristic of the controllers, in the next section, the simulation results with various parameter setting will be given and discussed.

Parameters	**Values**	**Units**	**Parameters**	**Values**	**Units**
m	2	kg	g	9.807	m/s^2
I_x	1.25	kg·m^2	ℓ	0.3	m
I_y	1.25	kg·m^2	d	0.0750	–
I_z	2.5	kg·m^2			

Table 6.1: Parameters of the dynamic model of the quadrotor.

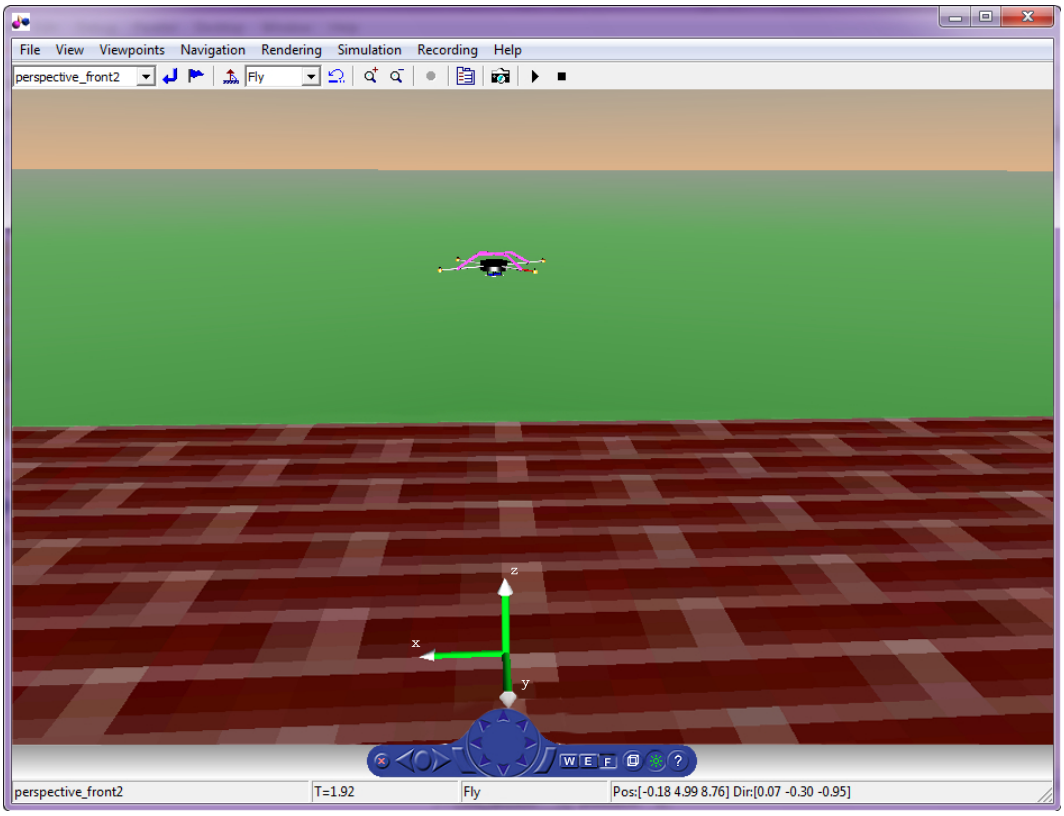

Figure 6.1: 3D visualization of the quad-rotor helicopter.

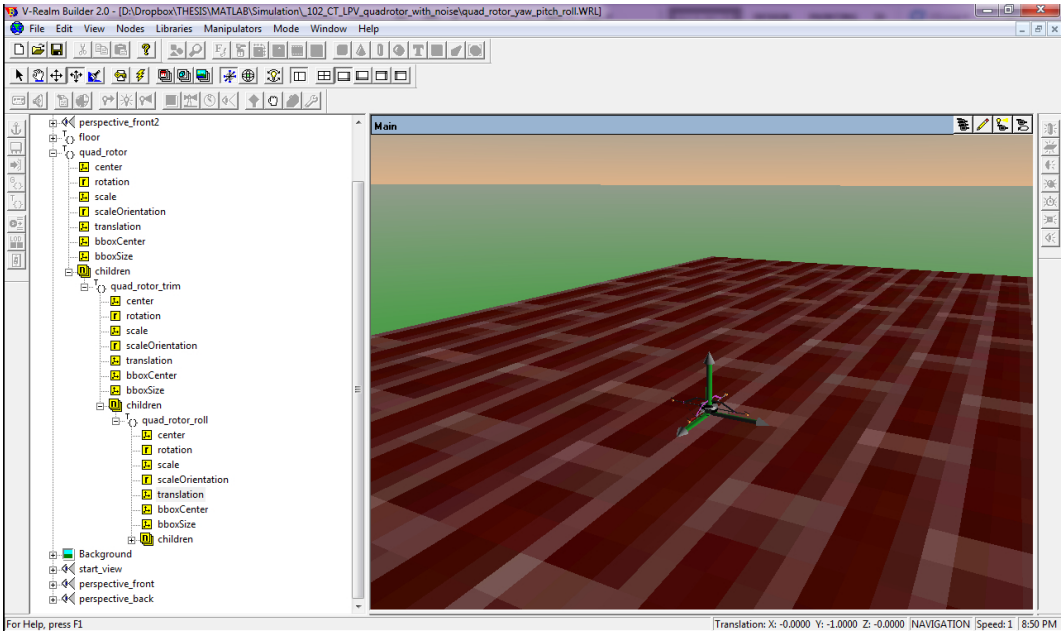

Figure 6.2: WRL editor.

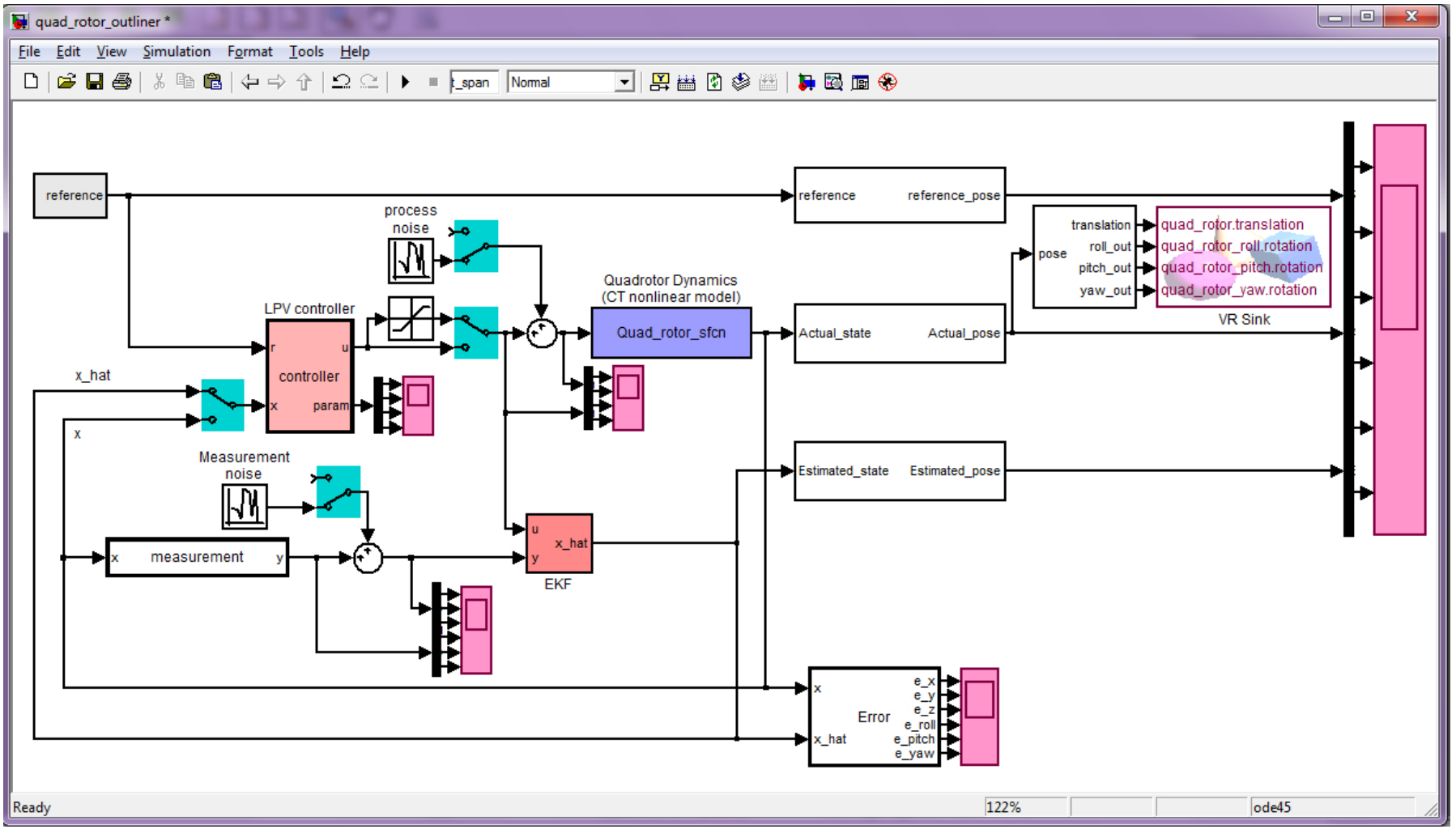

Figure 6.3: Simulink block diagram.

6.2 Results

In this section, the simulation results are given. The full state feedback control of the quadrotor, of which the control inputs are unbounded, is first considered. The LPVQR control is then applied. Next, the saturation of the control inputs is taken into account. The SLPVQR control and the high-gain SLPVQR control are then applied. Finally, we focus on the simulation of the real situation. We specify that only the partial information of the system state can be observed. Moreover, the control process and the measurement data are influenced by the noise. Then, we apply the EKF to do the state estimation in order that our control strategies can be applied to the output feedback control problem.

6.2.1 Full state feedback with unbounded control inputs

By applying Theorem 4.1 and Theorem 4.2 to the LPV model of the quadrotor (3.32), the LMI constraints produce no solution. This is because the LPV model of the quadrotor is very conservative. Specifically, to represent the whole range of the only parameter ψ, the polytopic structure of the LPV model requires at least four bases. As a result, Theorem 4.3 and Theorem 4.4 are failed to be applied to the LPV model of the quadrotor. However, when we apply Theorem 4.5 with

$$Q = \mathrm{diag}(1, 1, 100, 1, 1, 50, 50, 50, 50, 1, 1, 100), \tag{6.1}$$

$$R = \mathrm{diag}(0.001, 0.001, 0.001, 0.001), \tag{6.2}$$

the LPVQR via the composite quadratic Lyapunov function produces the following LPVQR state feedback gains

$$K_1 = \begin{bmatrix} -47.7494 & 47.7494 & 158.4679 & -22.3607 & 22.3607 & 111.8035 \\ -47.7494 & -47.7494 & 158.4679 & -22.3607 & -22.3607 & 111.8035 \\ 47.7494 & -47.7494 & 158.4679 & 22.3607 & -22.3607 & 111.8035 \\ 47.7494 & 47.7494 & 158.4679 & 22.3607 & 22.3607 & 111.8035 \end{bmatrix}$$

$$\begin{bmatrix} -0.0000 & -163.1777 & 123.0254 & -390.4586 & -390.4586 & 158.1147 \\ 163.1777 & -0.0000 & -123.0254 & 390.4586 & -390.4586 & -158.1147 \\ -0.0000 & 163.1777 & 123.0254 & 390.4586 & 390.4586 & 158.1147 \\ -163.1777 & -0.0000 & -123.0254 & -390.4586 & 390.4586 & -158.1147 \end{bmatrix} \tag{6.3}$$

$$K_2 = \begin{bmatrix} 47.7494 & 47.7494 & 158.4679 & 22.3607 & 22.3607 & 111.8035 \\ -47.7494 & 47.7494 & 158.4679 & -22.3607 & 22.3607 & 111.8035 \\ -47.7494 & -47.7494 & 158.4679 & -22.3607 & -22.3607 & 111.8035 \\ 47.7494 & -47.7494 & 158.4679 & 22.3607 & -22.3607 & 111.8035 \end{bmatrix}$$

$$\begin{bmatrix} -0.0000 & -163.1777 & 123.0254 & -390.4586 & 390.4586 & 158.1147 \\ 163.1777 & -0.0000 & -123.0254 & -390.4586 & -390.4586 & -158.1147 \\ -0.0000 & 163.1777 & 123.0254 & 390.4586 & -390.4586 & 158.1147 \\ -163.1777 & -0.0000 & -123.0254 & 390.4586 & 390.4586 & -158.1147 \end{bmatrix} \tag{6.4}$$

$$K_3 = \begin{bmatrix} -47.7494 & -47.7494 & 158.4679 & -22.3607 & -22.3607 & 111.8035 \\ 47.7494 & -47.7494 & 158.4679 & 22.3607 & -22.3607 & 111.8035 \\ 47.7494 & 47.7494 & 158.4679 & 22.3607 & 22.3607 & 111.8035 \\ -47.7494 & 47.7494 & 158.4679 & -22.3607 & 22.3607 & 111.8035 \end{bmatrix}$$

$$\begin{bmatrix} -0.0000 & -163.1777 & 123.0254 & 390.4586 & -390.4586 & 158.1147 \\ 163.1777 & -0.0000 & -123.0254 & 390.4586 & 390.4586 & -158.1147 \\ -0.0000 & 163.1777 & 123.0254 & -390.4586 & 390.4586 & 158.1147 \\ -163.1777 & -0.0000 & -123.0254 & -390.4586 & -390.4586 & -158.1147 \end{bmatrix} \quad (6.5)$$

$$K_4 = \begin{bmatrix} 47.7494 & -47.7494 & 158.4679 & 22.3607 & -22.3607 & 111.8035 \\ 47.7494 & 47.7494 & 158.4679 & 22.3607 & 22.3607 & 111.8035 \\ -47.7494 & 47.7494 & 158.4679 & -22.3607 & 22.3607 & 111.8035 \\ -47.7494 & -47.7494 & 158.4679 & -22.3607 & -22.3607 & 111.8035 \end{bmatrix}$$

$$\begin{bmatrix} -0.0000 & -163.1777 & 123.0254 & 390.4586 & 390.4586 & 158.1147 \\ 163.1777 & -0.0000 & -123.0254 & -390.4586 & 390.4586 & -158.1147 \\ -0.0000 & 163.1777 & 123.0254 & -390.4586 & -390.4586 & 158.1147 \\ -163.1777 & -0.0000 & -123.0254 & 390.4586 & -390.4586 & -158.1147 \end{bmatrix} \quad (6.6)$$

correspondingly to the parameters given by (3.36)-(3.39). It should be noted that the above state feedback gains can be reduced to the LPV state feedback gain depending on the yaw angle as follows

$$K(\psi) = \begin{bmatrix} 47.7494c_\psi & 47.7494s_\psi & 158.4679 & 22.3607c_\psi & 22.3607s_\psi & 111.8035 \\ -47.7494s_\psi & 47.7494c_\psi & 158.4679 & -22.3607s_\psi & 22.3607c_\psi & 111.8035 \\ -47.7494c_\psi & -47.7494s_\psi & 158.4679 & -22.3607c_\psi & -22.3607s_\psi & 111.8035 \\ 47.7494s_\psi & -47.7494c_\psi & 158.4679 & 22.3607s_\psi & -22.3607c_\psi & 111.8035 \end{bmatrix}$$

$$\begin{bmatrix} -0.0000 & -163.1777 & 123.0254 & -390.4586s_\psi & 390.4586c_\psi & 158.1147 \\ 163.1777 & -0.0000 & -123.0254 & -390.4586c_\psi & -390.4586s_\psi & -158.1147 \\ -0.0000 & 163.1777 & 123.0254 & 390.4586s_\psi & -390.4586c_\psi & 158.1147 \\ -163.1777 & -0.0000 & -123.0254 & 390.4586c_\psi & 390.4586s_\psi & -158.1147 \end{bmatrix} \quad (6.7)$$

Figure 6.4 illustrates the control responses. Here, only the position and the orientation of the quadrotor are considered. The red solid lines signify for the references and the blue dashed lines signify for the responses. Figure 6.5 illustrates the varying parameters of the system. In Figure 6.6, the forces required to drive the quadrotor are presented. We see that when the set point is changed, the controller requires the actuators to produce the impulse forces. This is impossible in the real system. Therefore, next, we will consider the situation when the saturation is taken into account.

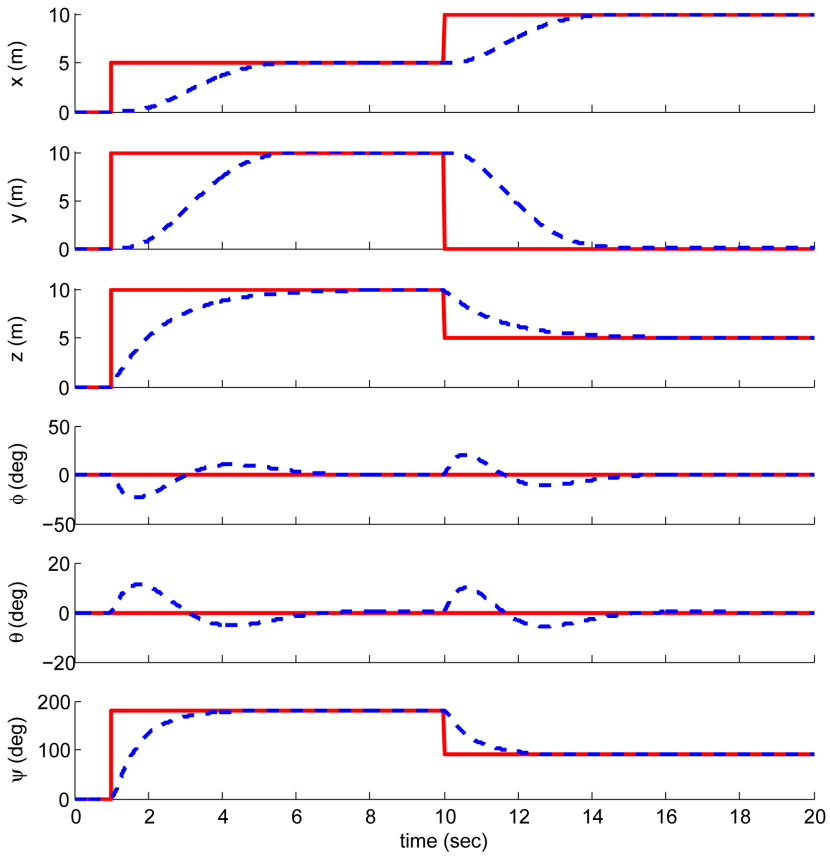

Figure 6.4: Control responses of the quadrotor with the unbounded control inputs by using the LPVQR control.

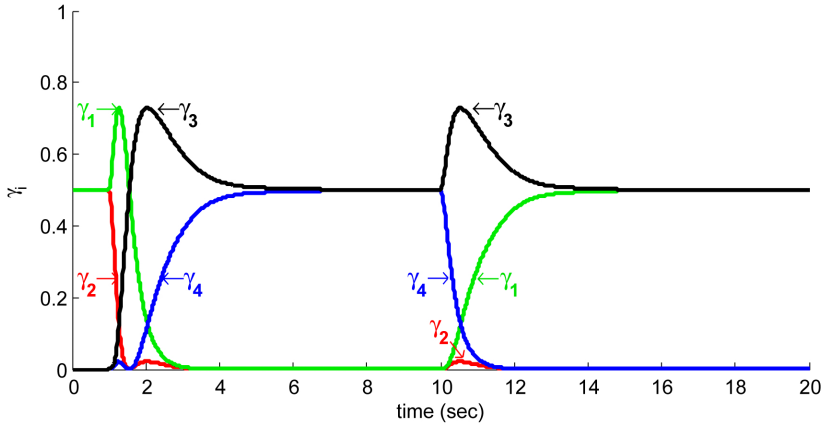

Figure 6.5: Varying parameters of the quadrotor.

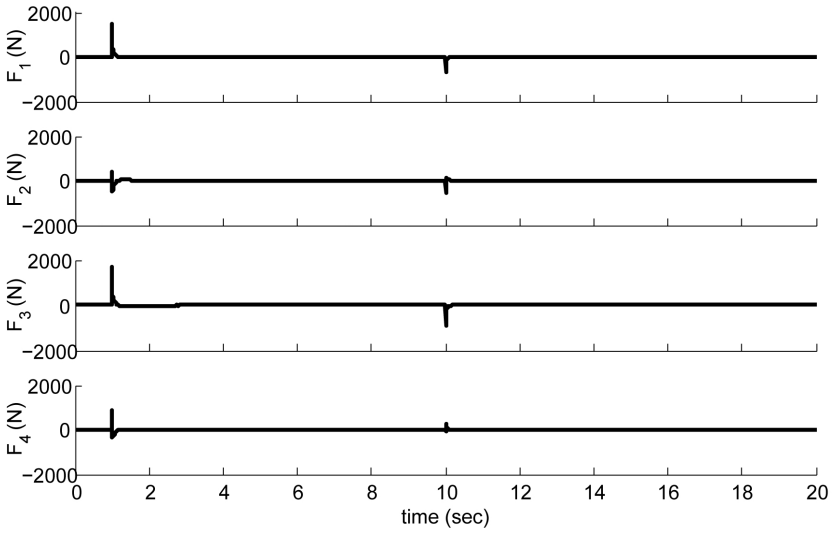

Figure 6.6: Unbounded control inputs of the quadrotor by using the LPVQR control.

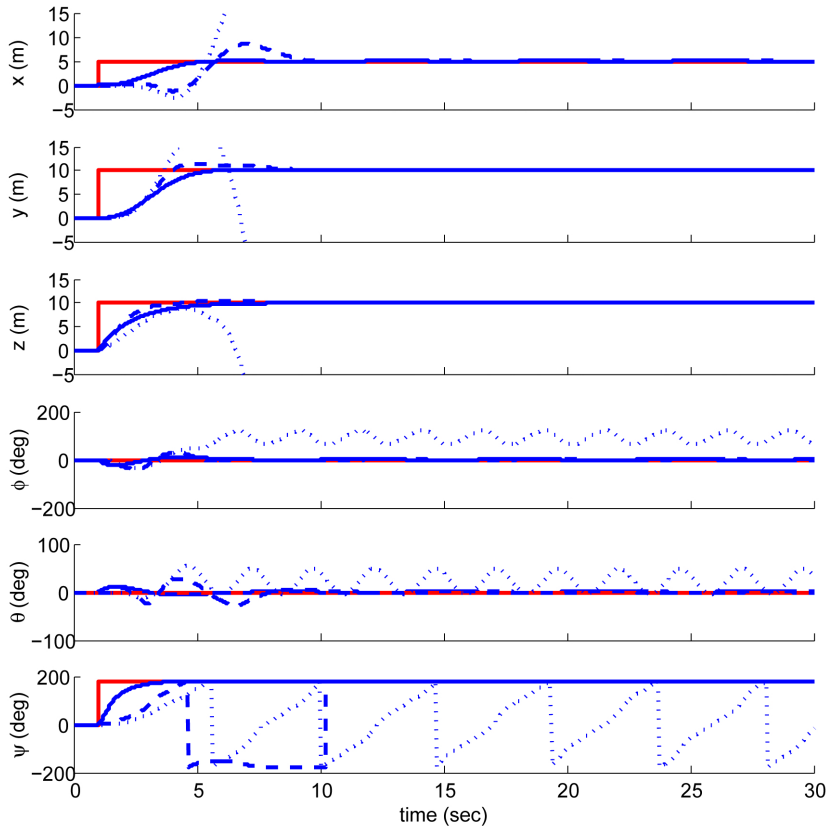

Figure 6.7: Control responses of the quadrotor with the unbounded (solid lines), the $2g$ bounded (dashed lines), and the $1g$ bounded (dotted lines) control inputs by using the LPVQR control.

6.2.2 Full state feedback with bounded control inputs

Now, we take the limit on the forces produced by the actuators. By using the state feedback gain computed by the LPVQR, the control responses of the quadrotor are obtained as shown in Figure 6.7. Obviously, the controllability of the quadrotor goes down as the capability of producing the forces is reduced. Moreover, when the force is limited by 1g for each rotor, the LPVQR is failed to control the quadrotor. Next, we will apply the SLPVQR control and the high-gain SLPVQR control, which were given respectively in Theorem 5.3 and Theorem 5.4. We note that both the SLPVQR and the high-gain SLPVQR are only applicable to the case that the saturation is symmetry. However, in the real system, the motors driving the rotor blades are always rotateable in one direction. This makes the saturation asymmetry. Fortunately, our LPV model of the quadrotor has the non-zero inputs when it is stationary. Clearly, the force produced by each rotor is equal to $mg/4$ when the quadrotor is floating stationary. Thus, we can apply the SLPVQR and the high-gain SLPVQR by defining the input range to be $[0, mg/2]$ for each rotor. Figure 6.8, Figure 6.9, and Figure 6.10 illustrate respectively the control responses, the control inputs, and the hovering paths by using the SLPVQR control. Here, the value of σ is set to $mg/4$ and the value of γ is varied. In

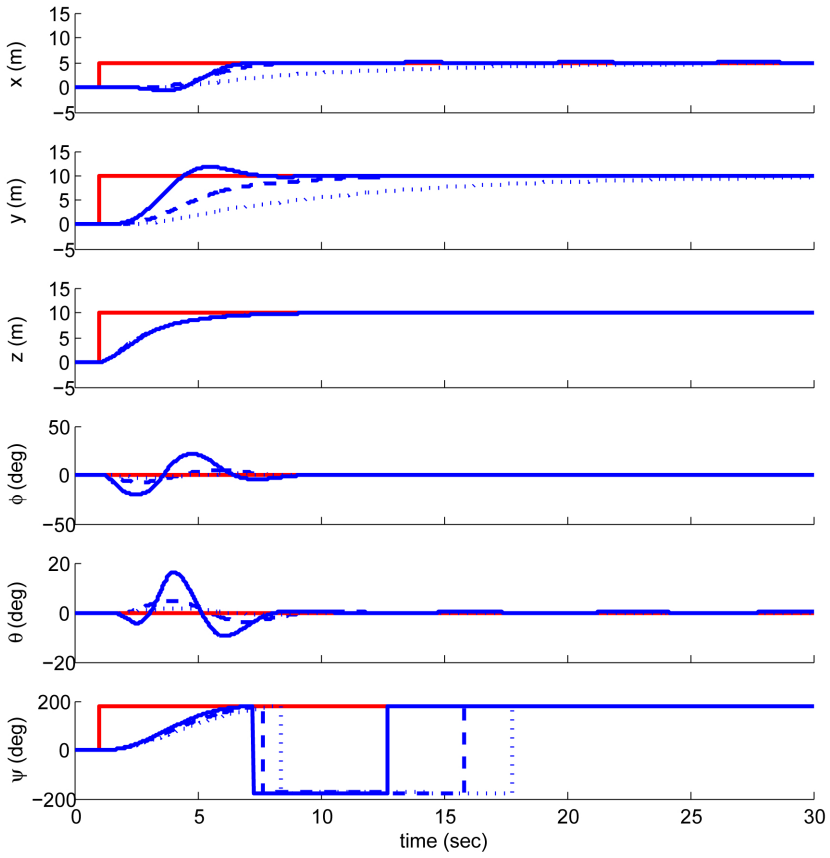

Figure 6.8: Control responses of the quadrotor with the $1g$ bounded control inputs by using the SLPVQR control with $\sigma = mg/4$ and $\gamma = 1$ (solid lines), 10 (dashed lines), and 20 (dotted lines).

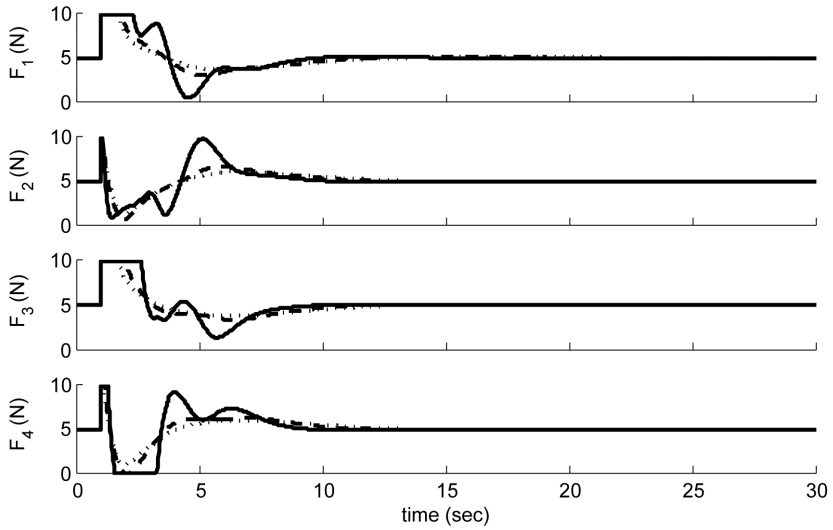

Figure 6.9: $1g$ bounded control inputs of the quadrotor by using the SLPVQR control with $\sigma = mg/4$ and $\gamma = 1$ (solid lines), 10 (dashed lines), and 20 (dotted lines).

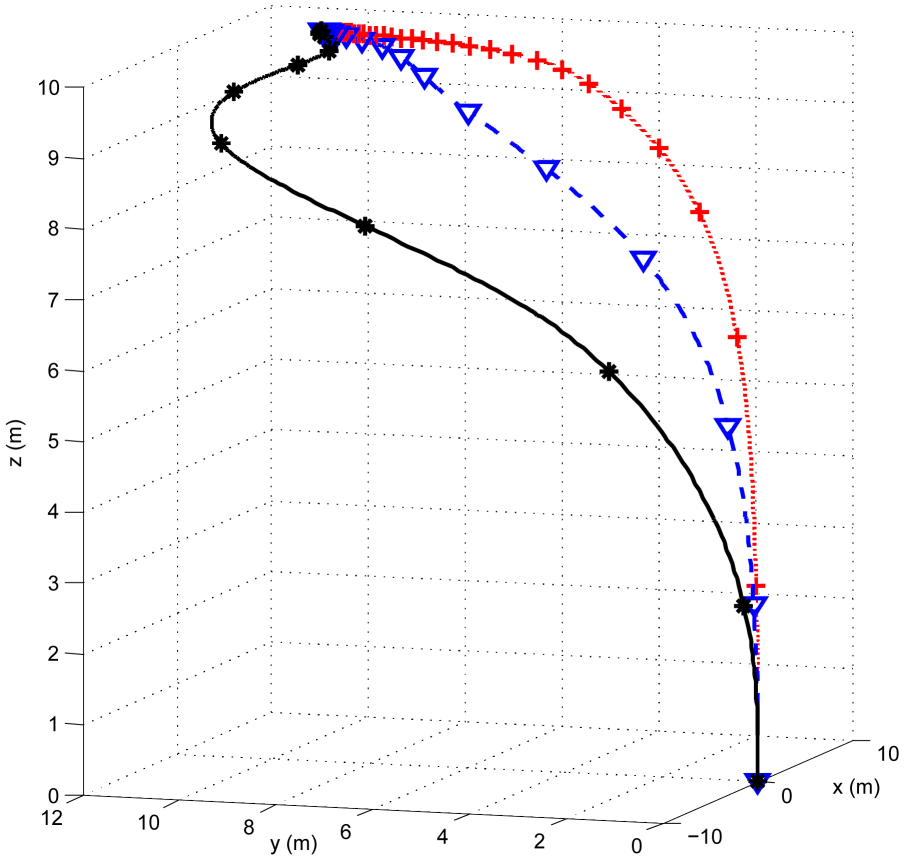

Figure 6.10: Hovering paths of the quadrotor with the $1g$ bounded control inputs by using the SLPVQR control with $\sigma = mg/4$ and $\gamma = 1$ (solid lines), 10 (dashed lines), and 20 (dotted lines).

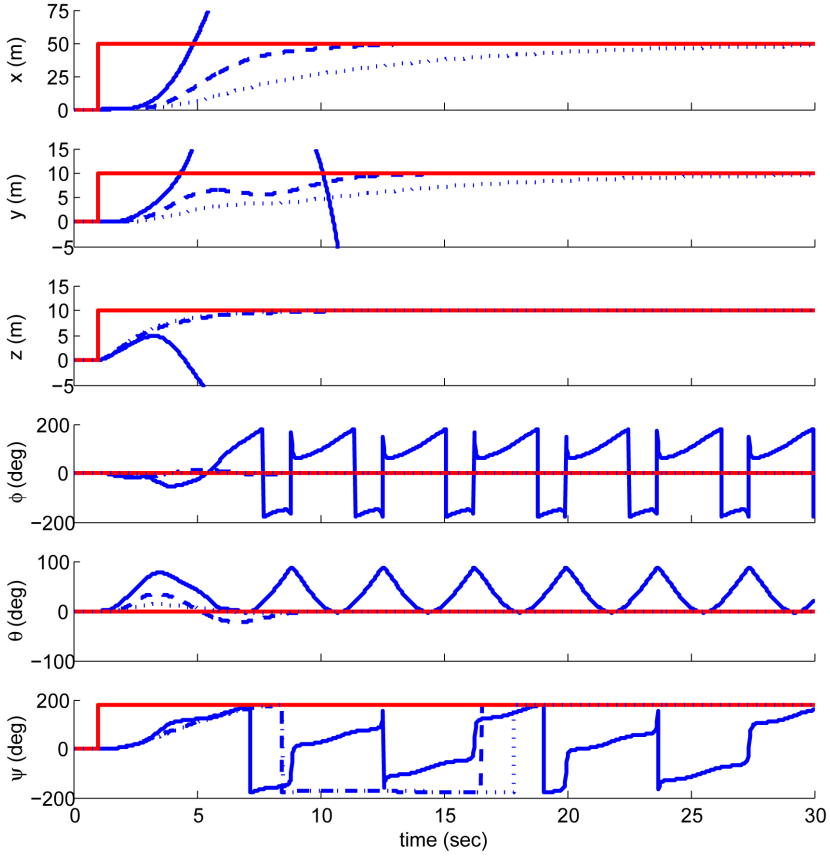

Figure 6.11: Control responses of the quadrotor with the $1g$ bounded control inputs by using the SLPVQR control with $\sigma = mg/4$ and $\gamma = 1$ (solid lines), 10 (dashed lines), and 20 (dotted lines); the distance in the x-axis is increased.

Figure 6.10, we use the markers to indicate for each one second time step. These figures show that the SLPVQR is satisfactory for using to control the quadrotor, of which the actuators are saturated. They also show that the more the value of γ is increased, the lower the performance is obtained. Although the lower value of γ is better, it should be assigned by a large enough number so that the system keep stable in the design domain. For the sake of clarification, in Figure 6.11, the distance in the x-axis is increased. The SLPVQR, of which the value of γ is set to 1, is then failed to control the quadrotor. This is because the value of γ is too small. From this figure, the selection policy of the value of γ becomes evidently dependent on the domain of the state space we are considering. Next, by applying the high-gain SLPVQR control, of which the values of σ and γ are set to $mg/4$ and 20 respectively, we have the control responses and their corresponding control inputs as illustrated in Figure 6.12 and Figure 6.13. They are also compared with the SLPVQR control with the same values of σ and γ. These figures show that the high-gain SLPVQR can significantly improve the control responses from the SLPVQR.

As yet, we have considered only the saturation problem. Next, the problem of the state estimation, which is also an important problem in the practice, will be considered.

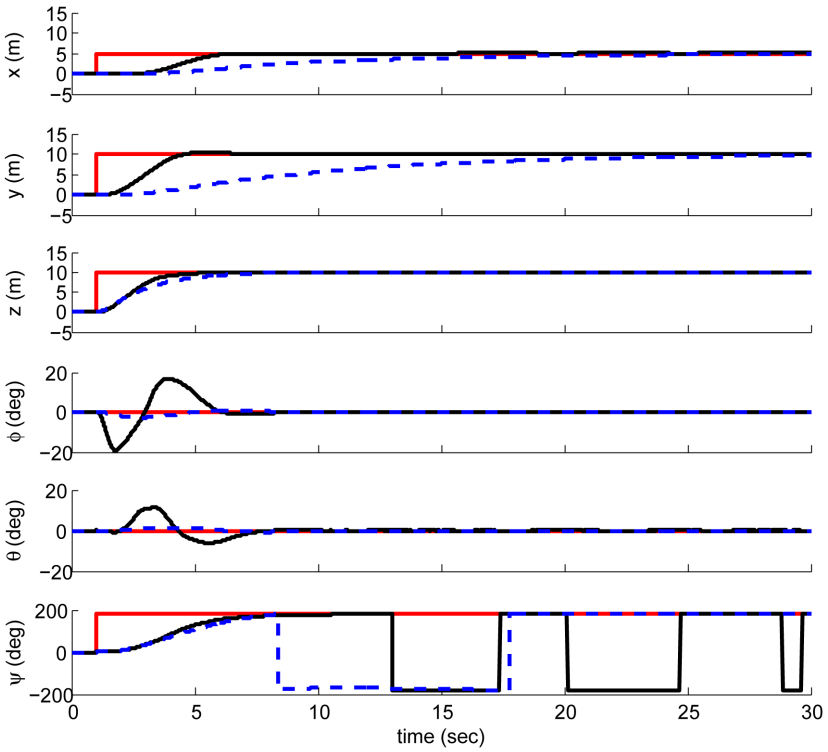

Figure 6.12: Comparison of the control responses obtained by using the high-gain SLPVQR (solid lines) and the SLPVQR (dashed lines) with $\sigma = mg/4$ and $\gamma = 20$.

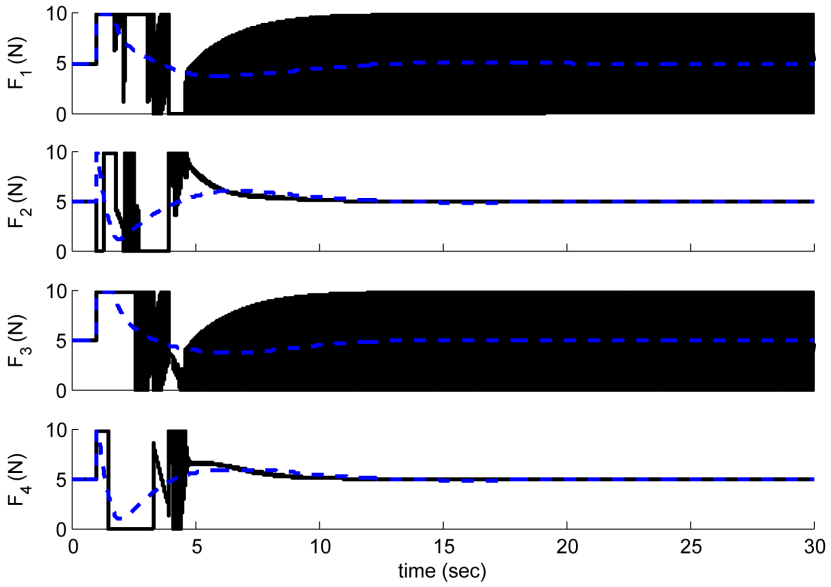

Figure 6.13: Comparison of the control inputs computed by the high-gain SLPVQR (solid lines) and the SLPVQR (dashed lines) with $\sigma = mg/4$ and $\gamma = 20$.

6.2.3 Output feedback control with input saturation

To do the output feedback control, in this thesis, the EKF is used to estimate the unknown states of the quadrotor. For simulating purpose, the nonlinear dynamic model of the quadrotor is assumed that the forces applied to the system are blended with the process noises $w_i(t)$, i.e.,

$$\dot{x} = f(x,u,w) = \begin{bmatrix} s_\theta(\sum_{i=1}^4 F_i + w_i)/m \\ -s_\phi c_\theta(\sum_{i=1}^4 F_i + w_i)/m \\ c_\phi c_\theta(\sum_{i=1}^4 F_i + w_i)/m - g \\ v_x^{\mathrm{E}} \\ v_y^{\mathrm{E}} \\ v_z^{\mathrm{E}} \\ \ell(F_2 + w_2 - F_4 - w_4)/I_x - qr(I_z - I_y)/I_x \\ \ell(F_3 + w_3 - F_1 - w_1)/I_y - pr(I_x - I_z)/I_y \\ d(F_1 + w_1 + F_3 + w_3 - F_2 - w_2 - F_4 - w_4)/I_z - pq(I_y - I_x)/I_z \\ pc_\psi/c_\theta - qs_\psi/c_\theta \\ ps_\psi + qc_\psi \\ (qs_\psi - pc_\psi)t_\theta + r \end{bmatrix}. \tag{6.8}$$

Furthermore, the measurement model is assumed that only the position and the orientation of the quadrotor are measurable. They are also blended with the measurement noises $v_i(t)$, i.e.,

$$y = h(x,v) = \begin{bmatrix} r_x^{\mathrm{E}} + v_1 \\ r_y^{\mathrm{E}} + v_2 \\ r_z^{\mathrm{E}} + v_3 \\ \phi + v_4 \\ \theta + v_5 \\ \psi + v_6 \end{bmatrix}. \tag{6.9}$$

Here, the discrete-time covariance matrices of the process noises and the measurement noises are assumed to be known. They are defined by

$$Q_d = 0.0001\mathbf{I}_{4\times 4}, \tag{6.10}$$

$$R_d = \begin{bmatrix} 0.01\mathbf{I}_{3\times 3} & \mathbf{0}_{3\times 3} \\ \mathbf{0}_{3\times 3} & (5\pi/180)^2\,\mathbf{I}_{3\times 3} \end{bmatrix}, \tag{6.11}$$

for the sampling time $T = 0.002$. To perform the EKF, we first compute the following Jacobian matrices

$$A(x,u,w) = \frac{\partial f}{\partial x} = \begin{bmatrix} \mathbf{0}_{3\times3} & \mathbf{0}_{3\times3} & \mathbf{0}_{3\times3} & \bar{A}_1 \\ \mathbf{I}_{3\times3} & \mathbf{0}_{3\times3} & \mathbf{0}_{3\times3} & \mathbf{0}_{3\times3} \\ \mathbf{0}_{3\times3} & \mathbf{0}_{3\times3} & \bar{A}_2 & \mathbf{0}_{3\times3} \\ \mathbf{0}_{3\times3} & \mathbf{0}_{3\times3} & \bar{A}_3 & \bar{A}_4 \end{bmatrix}, \tag{6.12}$$

$$L(x,u,w) = \frac{\partial f}{\partial w} = \begin{bmatrix} s_\theta/m & s_\theta/m & s_\theta/m & s_\theta/m \\ -s_\phi c_\theta/m & -s_\phi c_\theta/m & -s_\phi c_\theta/m & -s_\phi c_\theta/m \\ c_\phi c_\theta/m & c_\phi c_\theta/m & c_\phi c_\theta/m & c_\phi c_\theta/m \\ \mathbf{0}_{3\times1} & \mathbf{0}_{3\times1} & \mathbf{0}_{3\times1} & \mathbf{0}_{3\times1} \\ 0 & \ell/I_x & 0 & -\ell/I_x \\ -\ell/I_y & 0 & \ell/I_y & 0 \\ d/I_z & -d/I_z & d/I_z & -d/I_z \\ \mathbf{0}_{3\times1} & \mathbf{0}_{3\times1} & \mathbf{0}_{3\times1} & \mathbf{0}_{3\times1} \end{bmatrix}, \tag{6.13}$$

$$C = \frac{\partial h}{\partial x} = \begin{bmatrix} \mathbf{0}_{3\times3} & \mathbf{I}_{3\times3} & \mathbf{0}_{3\times3} & \mathbf{0}_{3\times3} \\ \mathbf{0}_{3\times3} & \mathbf{0}_{3\times3} & \mathbf{0}_{3\times3} & \mathbf{I}_{3\times3} \end{bmatrix}, \tag{6.14}$$

$$M = \frac{\partial h}{\partial v} = \mathbf{I}_{6\times6}, \tag{6.15}$$

where

$$\bar{A}_1 = \begin{bmatrix} 0 & c_\theta(\sum_{i=1}^4 F_i + w_i)/m & 0 \\ -c_\phi c_\theta(\sum_{i=1}^4 F_i + w_i)/m & s_\phi s_\theta(\sum_{i=1}^4 F_i + w_i)/m & 0 \\ -s_\phi c_\theta(\sum_{i=1}^4 F_i + w_i)/m & -c_\phi s_\theta(\sum_{i=1}^4 F_i + w_i)/m & 0 \end{bmatrix},$$

$$\bar{A}_2 = \begin{bmatrix} 0 & r(I_y - I_z)/I_x & q(I_y - I_z)/I_x \\ r(I_z - I_x)/I_y & 0 & p(I_z - I_x)I_y \\ 0 & 0 & 0 \end{bmatrix},$$

$$\bar{A}_3 = \begin{bmatrix} c_\psi/c_\theta & -s_\psi/c_\theta & 0 \\ s_\psi & c_\psi & 0 \\ -c_\psi t_\theta & s_\psi t_\theta & 1 \end{bmatrix},$$

$$\bar{A}_4 = \begin{bmatrix} 0 & (pc_\psi - qs_\psi)t_\theta/c_\theta & -(ps_\psi + qc_\psi)/c_\theta \\ 0 & 0 & pc_\psi - qs_\psi \\ 0 & (qs_\psi - pc_\psi)/c_\theta^2 & (ps_\psi + qc_\psi)t_\theta \end{bmatrix}.$$

We assume that the initial state is exactly known. This results in the following

$$\hat{x}(0) = x(0), \tag{6.16}$$

$$P(0) = \mathbf{0}_{12\times12}. \tag{6.17}$$

Executing the EKF algorithm to the high-gain SLPVQR control of the quadrotor gives the following results. Figure 6.14 illustrates the measurement data compared with the actual states. This figure shows that the high-gain SLPVQR is usable to control the quadrotor, though the only partial information from the noisy measurement is observed. Figure 6.15 illustrates the saturated control inputs with and without the process noises. This figure shows that the system is work well, though the unsaturated region is very small and the control inputs are noisy. In figure 6.16, the state estimation errors and their corresponding $\pm 3\sigma$ bounding levels are also given to proof the consistency of the EKF.

In this chapter, we have presented the way to simulate the quadrotor. The 3D visualization via the MATLAB simulink is used. Then, we apply the LPV control methods derived in Chapter 4 and Chapter 5 to the LPV model of the quadrotor. The simulation results show that our control strategies are satisfactory for using to do both the full state feedback control and the output feedback control of the quadrotor, the control inputs of which are bounded.

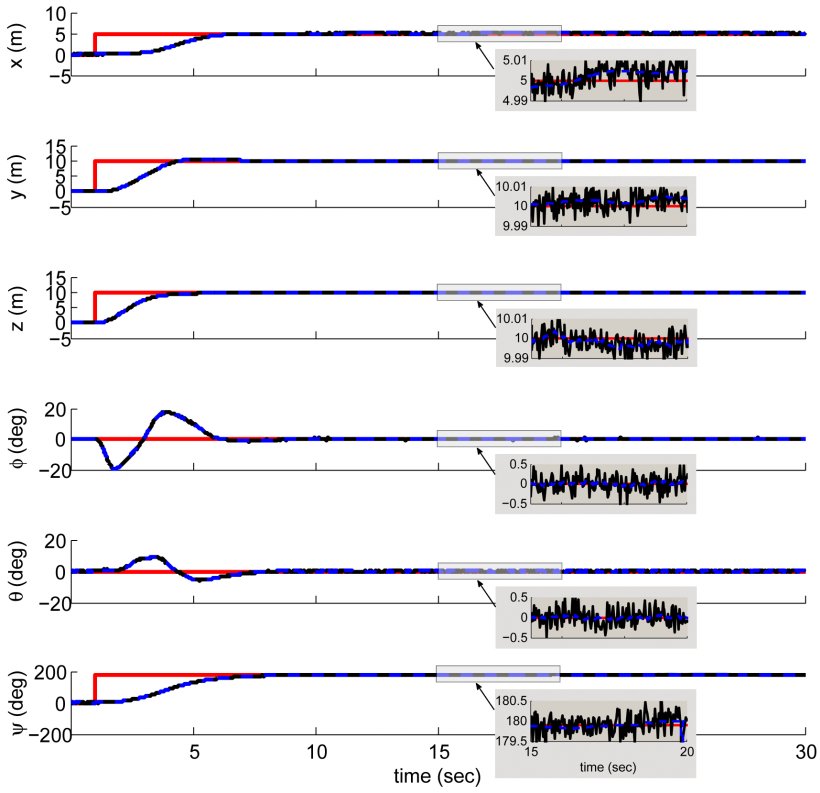

Figure 6.14: Control responses and measurement data.

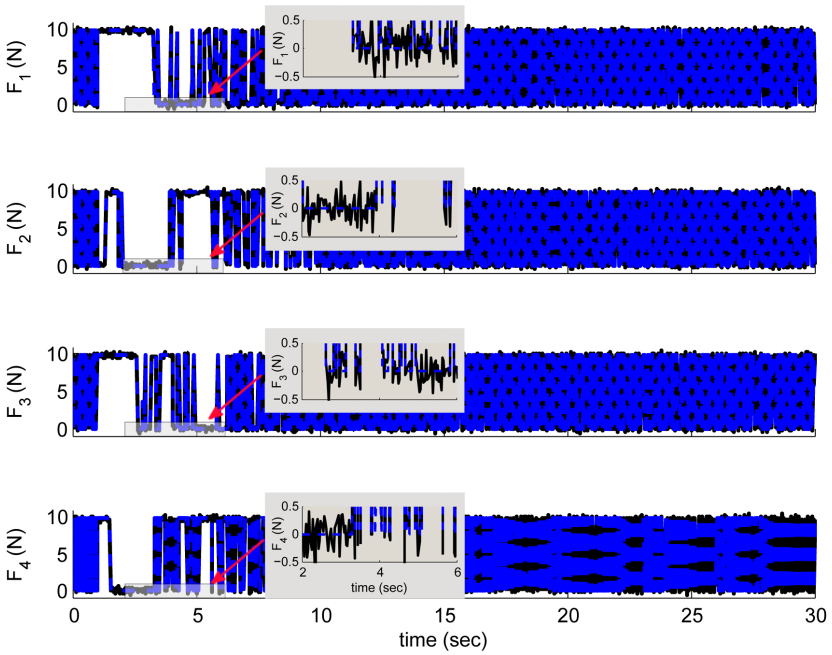

Figure 6.15: Saturated control inputs with and without process noises.

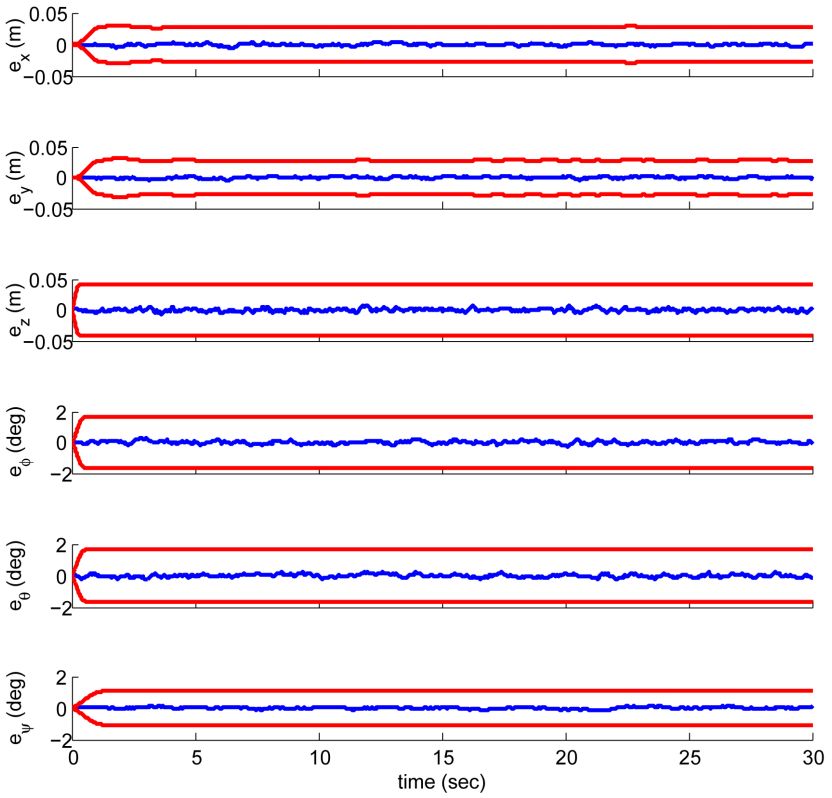

Figure 6.16: State estimation errors and $\pm 3\sigma$ bounding levels.

CHAPTER VII

CONCLUSIONS

7.1 Summary

This thesis has presented the output feedback control of the quad-rotor helicopter with input saturation constraints. The main idea underlying the controller design is the transformation of the nonlinear model to an approximated LPV model of the quadrotor. Then, the LPV control technique is applied. The advantage of the LPV control strategy is that we can apply almost the existed tools used in linear control analysis to control the nonlinear systems.

In this thesis, the nonlinear and the LPV dynamic modeling of the quadrotor were first considered in Chapter 3. To obtain the nonlinear dynamic model, we assumed that forces and torques acting on the quadrotor are induced by the thrust and the gravity. We noted that the drag force and the gyroscopic effect are ignored. Moreover, the aerodynamic effects are treated as the process noises. By linearizing the nonlinear dynamic model of the quadrotor around the zero roll and pitch angle, we obtained the LPV model of the quadrotor that depends on the yaw angle. The polytopic structure of the LPV model was then obtained by applying the tensor product model transformation.

Next, in Chapter 4, the LPV quadratic stabilization and the LPVQR control were derived. To obtain the LPV quadratic stabilization, two types of the Lyapunov function, the common quadratic Lyapunov function and the parameter-dependent quadratic Lyapunov function, were considered. Then, they were extended to the LPVQR control problem. The use of the parameter-dependent quadratic Lyapunov function gives the better result than the use of the common quadratic Lyapunov function in terms of the conservativeness. Nevertheless, the sufficient condition for solving the LPVQR via the parameter-dependent quadratic Lyapunov function requires the knowledge about the bound on the rate of parameters, which is often unknonwn in practice. Moreover, when we are dealing with the highly conservative LPV systems, e.g., the LPV model of the quadrotor of which the parameter dependence is polynomial, the use of the parameter-dependent quadratic Lyapunov function is still suffered from the conservativeness. This makes the quadrotor cannot be stabilized. Therefore, we also proposed the use of the composite quadratic Lyapunov fiunction. By using this kind of the Lyapunov function, the matrix derivative term in the time-derivative of the parameter-dependent quadratic Lyapunov function is eliminated. The simulation results also showed that the use of the composite quadratic Lyapunov function works well with our system.

In Chapter 5, the saturation of the control inputs was taken into consideration. We first derived the LQR control of the saturated LTI systems. Two approaches, the low-gian SLQR and

the high-gain SLQR, were obtained. For the low-gain SLQR, the ellipsoidal domain of attraction was forced to be inside the unsaturated region. In this case, the effect of the saturation is avoided by decreasing the controller gain in order that the control inputs are unsaturated. This leads to the lower closed-loop performance. On the other hand, for the high-gain SLQR, the ellipsoidal domain of attraction was proved that it need not to be inside the unsaturated region. In this case, the desired control inputs tolerate the occurrence of the saturation. The simulation results showed that the high-gain controller significantly improves the closed-loop performance. Subsequently, we extended the SLQR and the high-gain SLQR to the saturated LPV systems. The SLPVQR and the high-gain SLPVQR were then obtained respectively.

In Chapter 6, we applied the LPVQR, the SLPVQR, and the high-gain SLPVQR to control the quadrotor. At the beginning of this chapter, the simulation setup was discussed. The 3D visualization of the quadrotor via the MATLAB simulink was given to demonstrate the results. Then, by applying the LPVQR, the simulation results showed that the LPVQR via the composite quadratic Lyapunov function can control the LPV model of the quadrotor. Nevertheless, the forces required to be applied to the quadrotor are the impulse functions. In addition, when the force is bounded by $[0,\ 1g]$ for each rotor, the quadrotor is failed to be stabilized. This problem was subsequently fixed by applying the SLPVQR and the high-gain SLPVQR. As expected, the simulation results showed that the high-gain SLPVQR gives the better performance than the SLPVQR. Beside the LQR control of the quadrotor, we also applied the EKF to do the state estimation in order that our LPV control methods can cope with the output feedback control problem. The output feedback control of the quadrotor with the input saturation constraints was then accomplished.

7.2 Future work guideline

There is still a lot of room for additional development in the LPV control of the quadrotor. It is stated in the following topics.

1. *Robustness and model uncertainties*

   In this thesis, the model parameters of the quadrotor are assumed to be exactly known. However, in practice, these parameters are experimentally acquired. In addition, the quadrotor is not a rigid body. It is assembled from many components with many kinds of material. The looseness of joints and the elasticity of materials may make the system model changeable as the system is processing. Designing the controller regardless of model uncertainties may cause the undesired situation. To cope with this problem, we suggest applying the robust control of linear systems with model uncertainties, e.g., [26–31], which can be applied directly to the LPV model of the quadrotor.

2. *Off equilibrium improvement*

The approximated LPV model of the quadrotor was obtained by linearizing the nonlinear model around the zero roll and pitch angle. The simulation results showed that this model is properly used in a local domain around the equilibrium space. However, when the system is unawares stirred to a particular roll and pitch angle, the system becomes unstable. This problem should be fixed by extending the control space to include the overall range of the roll angle and the pitch angle. Unfortunately, the polytopic LPV model of the quadrotor describing the whole space of those angles is too complicated. It makes the real-time implementation impossible.

In recent years, many researchers concentrate on studying the piecewise linear control [59]. This control method divides the nonlinear system into many approximated linear systems. Then the modified linear control strategies are applied. The advantage of the PWL system over the LPV system is that it can be used to represent the more complex nonlinear system. Even if we have showed in Chapter 4 that the LPVQR control outperforms the PWL quadratic regulator control in terms of the performance, we recommend combining the PWL control to the LPV control for obtaining the better result.

3. *Discrete-time control*

   This thesis considers only the controller designed in the continuous-time domain. However, to implement the control algorithms in a digital controller, we need to analyse them in the discrete-time domain. This problem have been intensively studied in the publications.

4. *Trajectory planning and tracking problem*

   To obtain a fully autonomous controller, it is essential to do the trajectory planning. In addition, the controller must has the ability of tracking the generated path. For these reasons, both the trajectory planning problem and the tracking problem have to be encompassed and included into the control design procedure.

Beside the control of the quadrotor, finally, we hope that this thesis had better be useful in the control of other nonlinear systems.

REFERENCES

[1] Naidoo, Y., Stopforth, R., and Bright, G. Development of an UAV for search & rescue applications. Africon 2011 (September 2011) : 1–6.

[2] Kong, W.W., and Abidin, M.S.B. Design and control of a quad-rotor flying robot for aerial surveillance. Student Conference on Research and Development 2006 (June 2006) : 173–177.

[3] Kim, J., Kang, M.S., and Park, S. Accurate modeling and robust hovering control for a quad-rotor VTOL aircraft. Journal of Intelligent and Robotic Systems 57 (January 2010) : 9–26.

[4] Pounds, P., Mahony, R., Hynes, P., and Roberts, J. Design of a four-rotor aerial robot. Proceedings of the Australasian Conference on Robotics and Automation 2002 (November 2002) : 145–150.

[5] Naidoo, Y., Stopforth, R., and Bright, G. Quad-rotor unmanned aerial vehicle helicopter modelling & control. International Journal on Advance Robotic Systems 8 (2011) : 139–149.

[6] Rodić, A., and Mester, G. Modeling and simulation of quad-rotor dynamics and spatial navigation. IEEE International Symposium on Intelligent Systems and Informatics 2011 (September 2011) : 23–27.

[7] Bouabdallah, S., Noth, A., and Siegwart, R. PID vs LQ control techniques applied to an indoor micro quadrotor. Proceedings of the International Conference on Intelligent Robots and Systems 3 (September 2004) : 2451–2456.

[8] Mian, A.A., Ahmad, M.I., and Wang, D. Backstepping based nonlinear flight control strategy for 6 DOF aerial robot. International Conference on Smart Manufacturing Application 2008 (April 2008) : 146–151.

[9] Mistler, V., Benallegue, A., and M'Sirdi, N.K. Exact linearization and noninteracting control of a 4 rotors helicopter via dynamic feedback. Proceedings of the IEEE International Workshop on Robot and Human Interactive Communication (2001) : 586–593.

[10] Rangajeeva, S.L.M.D., and Whidborne, J.F. Linear parameter varying control of a quadrotor. IEEE International Conference on Idustrial and Information Systems 2011 (August 2011) : 483–488.

[11] Alexis, K., Nikolakopoulos, G., and Tzes, A. Constrained-control of a quadrotor helicopter for trajectory tracking under wind-gust disturbances. IEEE Mediterranean Electrotechnical Conference 2010 : 1411–1416.

[12] Shamma, J.S., and Athans, M. Guaranteed properties for nonlinear gain scheduled control systems. Proceedings of the IEEE Conference on Decision and Control 3 (December 1988) : 2202–2208.

[13] Källström, C.G., Åström, K.J., Thorell, N.E., Eriksson, J., and Sten, L. Adaptive autopilots for tankers. Automatica 15 (May 1979) : 241–254.

[14] Rugh, W.J., and Shamma, J.S. Research on gain scheduling. Automatica 36 (October 2000) : 1401–1425.

[15] Draper, C.S. Flight control. Journal of the Royal Aeronautical Society 59 (1959) : 451–477.

[16] Stein, G., Hartmann, G.L., and Hendrick, R.C. Adaptive control laws for F-8 flight test. IEEE Conference on Decision and Control including the 14th Symposium on Adaptive Processes 14 (December 1975) : 230.

[17] Stein, G. Adaptive flight control – a pragmatic view. In K.S.Narendra and R.V.Monopoli (ed.), Applications of Adaptive Control. New York : Academic Press, 1980.

[18] Shamma, J.S., and Athans, M. Analysis of gain scheduled control for linear parameter-varying plants. Symposium on Nonlinear Control Systems Design 1989 (June 1989).

[19] Shamma, J.S., and Xiong, D. Control of rate constrained linear parameter varying systems. Proceedings of the IEEE Conference on Decision and Control 3 (December 1995) : 2515–2520.

[20] Packard, A. Gain scheduling via linear fractional transformations. Systems & Control Letters 22 (February 1994) : 79–92.

[21] Apkarian, P., Gahinet, P., and Becker, G. Self-scheduled $\mathcal{H}_\infty$ control of linear parameter-varying systems: a design example. Automatica 31 (September 1995) : 1251–1261.

[22] Apkarian, P., and Adams, R.J. Advanced gain-scheduling techniques for uncertain systems. IEEE Transactions on Control Systems Technology 6 (1998) : 21–32.

[23] Kajiwara, H., Apkarian, P., and Gahinet, P. LPV techniques for control of an inverted pendulum. IEEE Control Systems 19 (February 1999) : 44–54.

[24] Wu, F. An unified framework for LPV system analysis and control synthesis. Proceedings of the IEEE Conference on Decision and Control 5 (December 2000) : 4578–4583.

[25] Wu, F. A generalized LPV system analysis and control synthesis framework. International Journal of Control 74 (November 2001) : 745–759.

[26] Chesi, G., Garulli, A., Tesi, A., and Vicino, A. Polynomially parameter-dependent Lyapunov functions for robust stability of polytopic systems: an LMI approach. IEEE Transactions on Autonomatic Control 50 (March 2005) : 365–370.

[27] Chesi, G., Garulli, A., Tesi, A., and Vicino, A. Robust stability of time-varying polytopic systems via parameter-dependent homogeneous Lyapunov functions. Automatica 43 (February 2007) : 309–316.

[28] Feron, E., Apkarian, P., and Gahinet, P. Analysis and synthesis of robust control systems via parameter-dependent Lyapunov functions. IEEE Transactions on Automatic Control 41 (July 1996) : 1041–1046.

[29] Kau, S.W. et al. A new LMI condition for robust stability of discrete-time uncertain systems. Systems & Control Letters 54 (2005) : 1195–1203.

[30] de Oliveira, P.J., Oliveira, R.C.L.F., Leite, V.J.S., Montagner, V.F., and Peres, P.L.D. LMI based robust stability conditions for linear uncertain systems: a numerical comparison. Proceedings of the IEEE Conference on Decision and Control 1 (December 2002) : 644–649.

[31] Oliveira, R.C.L.F., and Peres, P.L.D. LMI conditions for robust stability analysis based on polynomially parameter-dependent Lyapunov functions. Systems & Control Letters 55 (January 2006) : 52–61.

[32] Montagner, V.F., Oliveira, R.C.L.F., Leite, V.J.S., and Peres, P.L.D. LMI approach for $\mathcal{H}_\infty$ linear parameter-varying state feedback control. Proceedings of the IEE Conference on Control Theory and Applications 152 (March 2005) : 195–201.

[33] Geromel, J.C., and Colaneri, P. Robust stability of time varying polytopic systems. Systems & Control Letters 55 (January 2006) : 81–85.

[34] Butcher, M., and Karimi, A. Linear parameter-varying iterative learning control with application to a linear motor system. IEEE/ASME Transactions on Mechatronics 15 (June 2010) : 412–420.

[35] Henry, D., and Zolghadri, A. Robust fault diagnosis in uncertain linear parameter-varying systems. IEEE Internatioal Conference on Systems, Man, and Cybernatics 6 (October 2004) : 5165–5170.

[36] Lind, R. Linear parameter-varying modeling and control of structural dynamics with aerothermoelastic effects. Journal of Guidance, Control, and Dynamics 25 (August 2002) : 733–739.

[37] Cerone, V., Andreo, D., Larsson, M., and Regruto, D. Stabilization of a riderless bicycle. IEEE Control Systems 30 (October 2010) : 23–32.

[38] Xu, Z., Zhao, J., and Qian, J. Nonlinear MPC using an identified LPV model. Industrial & Engineering Chemistry Research 48 (February 2009) : 3043–3051.

[39] Tóth, R. Modeling and identification of linear parameter-varying systems. Germany : Springer-Verlag Berlin Heidelberg, 2010.

[40] Lathauwer, L.D., Moor, B.D., and Vandewalle, J. A multilinear singular value decomposition. SIAM Journal on Matrix Analysis and Applications 21 (2000) : 1253–1278.

[41] Baranyi, P. TP model transformation as a way to LMI based controller design. IEEE Transaction on Industrial Electronics 51 (April 2004) : 387–400.

[42] Baranyi, P., Várkonyi, P.L., Korondi, P., and Yam, Y. Different affine decomposition of the model of the prototypical aeroelastic wing section by TP model transformation. IEEE International Conference on Intelligent Engineering Systems 2005 (September 2005) : 93–98.

[43] Baranyi, P., Petres, Z., Várkonyi, P.L., Korondi, P., and Yam, Y. Determination of different polytopic models of the prototypical aeroelastic wing section by TP model transformation. Journal of Advanced Computational Intelligence 10 (2006) : 486–493.

[44] Baranyi, P. Output feedback control of two dimensional aeroelastic system. Journal of Guidance, Control, and Dynamics 29 (May 2006) : 762–767.

[45] Petres, Z., Baranyi, P., Várlaki, P., Gáspár, P., and Michelberger, P. Different polytopic decomposition of the model of heavy vehicles by TP model transformation. IEEE International Conference on Intelligent Engineering Systems 2007 (June 2005) : 265–270.

[46] Baranyi, P., Petres, Z., and Nagy, S. TP Tool : TP model transformation and HOSVD canonical form [Online]. 2007. Available from : http://tptool.sztaki.hu

[47] Lyapunov, A.M. The General Problem of the Stability of Motion. Doctoral dissertation, Department of Mathematics, Faculty of Applied Mathematics, University of Saint Petersburg, 1892.

[48] Hu, T., and Lin, Z. Composite quadratic Lyapunov functions for constrained control systems. IEEE Transactions on Automatic Control 48 (March 2003) : 440–450.

[49] Hu, T., and Lin, Z. Properties of the composite quadratic Lyapunov functions. IEEE Transactions on Automatic Control 49 (July 2004) : 1162–1167.

[50] Schur, I. New foundation for the theory of group characters. In Neue Begründung der Theorie der Gruppencharaktere, pp.406–432. Germany : Sitzungsberichte der Königlich Preußischen Akademie der Wissenschaften zu Berlin, 1905.

[51] Boyd, S., and Vandenberghe, L. Convex optimization. United States of America, New York : Cambridge University Press, 2004.

[52] Hu, T., and Lin, Z. Control systems with actuator saturation: Analysis and Design. Boston, MA : Birkhäuser, 2001.

[53] Jacobson, D.H., Martin, D.H., Pachter, M., and Geveci, T. Extensions of linear-quadratic control theory. Germany : Springer-Verlag Berlin Heidelberg, 1980.

[54] Kalman, R. A new approach to linear filtering and prediction problems. ASME Journal of Basic Engineering 82 (March 1960) : 35–45.

[55] Kalman, R, and Bucy, R. New results in linear filtering and prediction theory. ASME Journal of Basic Engineering 83 (March 1961) : 95–108.

[56] Schmidt, S.F. Applications of state space methods to navigation problems. In C.T.Leondes (ed.), Advance in control systems, pp.293–340. New York : Academic Press, 1966.

[57] Simon, D. Optimal state estimation: Kalman, $\mathcal{H}_\infty$, and nonlinear approaches. United States of America : John Wiley & Sons, 2006.

[58] Spong, M.W., Hutchison, S., and Vidyasagar, M. Robot modeling and control. United States of America : John Wiley & Sons, 2006.

[59] Johansson, M. Piecewise linear control systems: A computational approach. Germany : Springer-Verlag Berlin Heidelberg, 2003.

[60] Hu, T., Lin, Z., and Chen, B.M. An analysis and design method for linear systems subject to actuator saturation and disturbance. Automatica 38 (February 2002) : 351–359.

[61] Wolfgang, B., and Tanja, K. VRML: today and tomorrow. Computers & Graphics 20 (1996) : 427–434.

APPENDICES

APPENDIX A

PROOFS

A.1 Proof from Chapter2

A.1.1 Proof of Theorem 2.1

The proof starts with the quadratic Lyapunov function defined by

$$V(x) = x^T P x, \tag{A.1}$$

where P is a positive definite matrix. The time derivative of the quadratic Lyapunov function is computed as follows

$$\frac{d}{dt} x^T P x = (Ax + Bu)^T P x + x^T P (Ax + Bu). \tag{A.2}$$

It is supposed that the system (2.28) is stabilizable. Integrating (A.2) from $t = 0$ to ∞ gives

$$-x(0)^T P x(0) = \int_0^\infty \left(x^T (PA + A^T P) x + 2u^T B^T P x \right) dt. \tag{A.3}$$

We recall here the performance criterion defined in (2.30). For simplicity, the time specific t is omitted.

$$J(x(0), u(\cdot)) = \int_0^\infty \left(u^T R u + x^T Q x \right) dt. \tag{A.4}$$

Adding (A.3) to (A.4) gives

$$J(x(0), u(\cdot)) = \int_0^\infty \left(u^T R u + 2u^T B^T P x + x^T (A^T P + PA + Q) x \right) dt + x(0)^T P x(0), \tag{A.5}$$

which is equivalent to

$$\begin{aligned} J(x(0), u(\cdot)) = \int_0^\infty & \left[(u + R^{-1} B^T P x)^T R (u + R^{-1} B^T P x) \right. \\ & \left. + x^T (A^T P + PA - PBR^{-1} B^T P + Q) x \right] dt + x(0)^T P x(0). \end{aligned} \tag{A.6}$$

Now, we assume that the matrix P is chosen to satisfy the following algebraic Riccati inequality

$$A^T P + PA - PBR^{-1} B^T P + Q < 0. \tag{A.7}$$

Since R is a positive definite matrix, the optimal control $u(\cdot)$ is readily computed as follows

$$u = -Kx, \tag{A.8}$$

$$K = R^{-1} B^T P. \tag{A.9}$$

Consequently, we have the following upper bound on the cost function

$$J(x(0), u(\cdot)) < x(0)^T P x(0). \tag{A.10}$$

Now, to reformulate the nonlinear matrix inequality constraint (A.7) to the LMI constraint, it is first transformed to an equivalent matrix inequality of the form

$$-P(A - BK) - (A - BK)^T P - Q - K^T R K > 0. \tag{A.11}$$

Pre and post multiplying the inequality (A.11) by $Y = P^{-1}$ and defining $L = KP^{-1}$ give

$$-(AY - BL) - (AY - BL)^T - YQY - L^T R L > 0. \tag{A.12}$$

Then, by applying the Schur complement, an equivalent LMI constraint is obtained as follows

$$\begin{bmatrix} -(AY - BL) - (AY - BL)^T & Y & L^T \\ Y & Q^{-1} & 0 \\ L & 0 & R^{-1} \end{bmatrix} > 0. \tag{A.13}$$

To minimize the upper bound on the cost function, the criterion of minimizing the trace of the matrix P is chosen. Since $Y = P^{-1}$, the minimized upper bound on the cost function, for any initial condition $x(0)$, is then obtained by maximizing the trace of the matrix Y instead.

A.2 Proofs from Chapter 4

A.2.1 Proof of Lemma 4.1

Let $P = Y^{-1}$ and $K(\rho) = L(\rho)Y^{-1}$. Pre and post multiplying (4.9) by P, we have

$$P(A(\rho) - B(\rho)K(\rho)) + (A(\rho) - B(\rho)K(\rho))^T P < 0. \tag{A.14}$$

Thus the existence of a positive definite matrix Y and an arbitrary real matrix-valued function $L(\rho)$ satisfying (4.9) is equivalent to the existence of a positive definite matrix P satisfying the quadratic Lyapunov stability condition of the closed-loop system (4.6). The quadratic stabilizability of the LPV system (4.1) is then followed.

A.2.2 Proof of Theorem 4.1

We first multiply each inequality in (4.11) by the non-negative scalar ρ_i^2 and multiply each inequality in (4.12) by the non-negative scalar $\rho_i \rho_j$. Then, we sum them up. These yield

$$\sum_{i=1}^{N} \sum_{j=1}^{N} \rho_i \rho_j (A_i Y + Y A_i^T - B_i L_j - L_j^T B_i^T) < 0. \tag{A.15}$$

For each fixed i, summing up the result from $j = 1$ to N gives

$$\sum_{i=1}^{N} \rho_i (A_i Y + Y A_i^T - B_i L(\rho) - L(\rho)^T B_i^T) < 0. \tag{A.16}$$

Now, we sum up (A.16). This yield

$$A(\rho)Y + Y A(\rho)^T - B(\rho)L(\rho) - L(\rho)^T B(\rho)^T < 0, \tag{A.17}$$

which implies the quadratic stabilizability.

A.2.3 Proof of Lemma 4.2

Let $P(\rho) = Y(\rho)^{-1}$ and $K(\rho) = L(\rho)Y(\rho)^{-1}$. Pre and post multiplying (4.17) by $P(\rho)$, we have

$$P(\rho)(A(\rho) - B(\rho)K(\rho)) + (A(\rho) - B(\rho)K(\rho))^T P(\rho) - Y(\rho)^{-1}Y(\dot{\rho})Y(\rho)^{-1} < 0. \tag{A.18}$$

Since

$$\dot{P}(\rho) = P(\dot{\rho}) = -Y(\rho)^{-1}Y(\dot{\rho})Y(\rho)^{-1}, \tag{A.19}$$

the inequality (A.18) becomes

$$\dot{P}(\rho) + P(\rho)(A(\rho) - B(\rho)K(\rho)) + (A(\rho) - B(\rho)K(\rho))^T P(\rho) < 0. \tag{A.20}$$

Hence the existence of a positive definite matrix-valued function $Y(\rho)$ and an arbitrary real matrix-valued function $L(\rho)$ satisfying (4.17) is equivalent to the existence of a positive definite matrix-valued function $P(\rho)$ satisfying the parameter-dependent quadratic Lyapunov stability condition of the closed-loop system (4.6). The parameter-dependent quadratic stabilizability of the LPV system (4.1) is then followed.

A.2.4 Proof of Theorem 4.2

For each fixed i, multiplying each inequality in (4.22) by the non-negative scalar σ_k and summing up the results from $k = 1$ to M give

$$A_i Y_i + Y_i A_i^T - B_i L_i - L_i^T B_i^T - Y(\dot{\rho}(t)) < 0, \quad \forall i \in I[1, N]. \tag{A.21}$$

Also, for each fixed i and j, multiplying each inequality in (4.23) by the non-negative scalar σ_k and summing up the results from $k = 1$ to M give

$$\begin{aligned} A_i Y_j + A_j Y_i + Y_i A_j^T + Y_j A_i^T - B_i L_j - B_j L_i - L_i^T B_j^T - L_j^T B_i^T - 2Y(\dot{\rho}(t)) < 0, \quad & \forall i \in I[1, N-1], \\ & \forall j \in I[i+1, N]. \end{aligned} \tag{A.22}$$

We multiply each inequality in (A.21) by the non-negative scalar ρ_i^2 and multiply each inequality in (A.22) by the non-negative scalar $\rho_i \rho_j$. Then, we sum them up. These yield

$$\sum_{i=1}^{N} \sum_{j=1}^{N} \rho_i \rho_j (A_i Y_j + Y_j A_i^T - B_i L_j - L_j^T B_i^T - Y(\dot{\rho})) < 0. \tag{A.23}$$

For each fixed i, summing up the inequality (A.23) from $j = 1$ to N gives

$$\sum_{i=1}^{N} \rho_i (A_i Y(\rho) + Y(\rho) A_i^T - B_i L(\rho) - L(\rho)^T B_i^T - Y(\dot{\rho})) < 0. \tag{A.24}$$

Now, we sum up (A.24). This yields

$$A(\rho)Y(\rho) + Y(\rho)A(\rho)^T - B(\rho)L(\rho) - L(\rho)^T B(\rho)^T - Y(\dot{\rho}) < 0, \tag{A.25}$$

which implies the parameter-dependent quadratic stabilizability.

A.2.5 Proof of Theorem 4.3

In the analogous way of the proof of Theorem 4.1, the existence of a positive definite matrix Y and a set of matrices $\{L_1, \ldots, L_N\}$ satisfying (4.28)-(4.29) implies that

$$\begin{bmatrix} -\left(A(\rho)Y - B(\rho)L(\rho)\right) - \left(A(\rho)Y - B(\rho)L(\rho)\right)^T & Y & L(\rho)^T \\ Y & Q^{-1} & 0 \\ L(\rho) & 0 & R^{-1} \end{bmatrix} > 0. \tag{A.26}$$

We apply the Schur complement, then pre and post multiply the result by P. These yield

$$P\left(A(\rho) - B(\rho)K(\rho)\right) + \left(A(\rho) - B(\rho)K(\rho)\right)^T P < -Q - K(\rho)^T R K(\rho), \tag{A.27}$$

which is equivalent to the following algebraic Riccati inequality

$$A(\rho)^T P + PA(\rho) - PB(\rho)R^{-1}B(\rho)^T P + Q < 0. \tag{A.28}$$

The rest of this proof is now similar to the proof of Theorem 2.1.

A.2.6 Proof of Corollary 4.1

We multiply each inequality in (4.30) by the non-negative scalar ρ_i and sum up the results. These yield

$$\begin{bmatrix} -\left(A(\rho)Y - BL(\rho)\right) - \left(A(\rho)Y - BL(\rho)\right)^T & Y & L(\rho)^T \\ Y & Q^{-1} & 0 \\ L(\rho) & 0 & R^{-1} \end{bmatrix} > 0. \tag{A.29}$$

The rest of this proof is now similar to the proof of Theorem 4.3.

A.2.7 Proof of Theorem 4.4

In the analogous way of the proof of Theorem 4.2, the existence of a set of positive definite matrices $\{Y_1, \ldots, Y_N\}$ and a set of matrices $\{L_1, \ldots, L_N\}$ satisfying (4.31)-(4.32) implies that

$$\begin{bmatrix} Y(\dot{\theta}) - \left(A(\theta)Y(\theta) - B(\theta)L(\theta)\right) - \left(A(\theta)Y(\theta) - B(\theta)L(\theta)\right)^T & Y(\theta) & L(\theta) \\ Y(\theta) & Q^{-1} & 0 \\ L(\theta)^T & 0 & R^{-1} \end{bmatrix} > 0 \tag{A.30}$$

The parameter-dependent LMI (A.30) is equivalent to the following parameter-dependent algebraic Riccati inequality

$$\dot{P}(\rho) + A(\rho)^T P(\rho) + P(\rho)A(\rho) - P(\rho)B(\rho)R^{-1}B(\rho)^T P(\rho) + Q < 0. \tag{A.31}$$

This is derived similarly to the algebraic Riccati inequality in the proof of Theorem 2.1, but the Lyapunov function is the parameter-dependent quadratic Lyapunov function and the dynamic system is the LPV system instead. The rest of this proof is now similar to the proof of Theorem 2.1, other than the existence of the matrix derivative $\dot{P}(\rho)$.

A.2.8 Proof of Theorem 4.5

Because we are trying to minimize $x^T P(\rho)x$ along the trajectory of ρ, the solution of $P(\rho)$ is certainly satisfied the condition of the composite quadratic Lyapunov function and the algebraic Riccati inequality is readily obtained as follows

$$A(\rho)^T P(\rho) + P(\rho)A(\rho) - P(\rho)B(\rho)R^{-1}B(\rho)^T P(\rho) + Q < 0, \tag{A.32}$$

which is equivalent to (4.36). Therefore, the existence of a positive definite matrix-valued function $Y(\rho)$ and an arbitrary real matrix-valued function $L(\rho)$ satisfying (4.36) implies that

$$J(x(0), u(\cdot)) < x(0)^T P(\rho(0))x(0). \tag{A.33}$$

By the heuristic rule, the minimum of this bound is obtained by minimizing the trace of the matrix $P(\rho)$, or equivalently maximizing the trace of the matrix $Y(\rho)$, along the trajectory of the parameter.

A.3 Proofs from Chapter 5

A.3.1 Proof of Theorem 5.1

We define the analysis domain as follows

$$\mathcal{E}(P, \gamma) = \left\{x : \ x^T P x \leq \gamma\right\}. \tag{A.34}$$

With the Lyapunov function defined by $V(x) = x^T P x$, let $Y = P^{-1}$ and $L = KY$, we have the following LQR condition

$$\begin{bmatrix} -(AY - BL) - (AY - BL)^T & Y & L^T \\ Y & Q^{-1} & 0 \\ L & 0 & R^{-1} \end{bmatrix} > 0. \tag{A.35}$$

Since the system works aright inside the unsaturated region, to ensure that the analysis domain (A.34) can guarantee the LQR performance, it is enforced to be inside the unsaturated region. That

is $\mathcal{E}(P,\gamma) \subset \mathcal{L}(K,\sigma)$. From Lemma 2.2, we have the following LMI condition

$$\begin{bmatrix} \sigma^2 & k_i\,(P/\gamma)^{-1} \\ (P/\gamma)^{-1}\,k_i^T & (P/\gamma)^{-1} \end{bmatrix} \geq 0,\ \forall i \in I[1,m], \tag{A.36}$$

which is equivalent to

$$\begin{bmatrix} \sigma^2/\gamma & \ell_i \\ \ell_i & Y \end{bmatrix} \geq 0, \quad \ell_i:\ i^{\text{th}} \text{ row of } L, \quad \forall i \in I[1,m]. \tag{A.37}$$

Under these two conditions, (A.35) and (A.37), the cost function (5.5) readily satisfies

$$J(x(0),u(\cdot)) < x(0)^T P x(0), \quad \forall\, x(0) \in \mathcal{E}(P,\gamma). \tag{A.38}$$

By the heuristic rule, the minimum of this bound is obtained by minimizing the trace of the matrix P, or equivalently maximizing the trace of the matrix Y.

A.3.2 Proof of Theorem 5.2

The following quadratic Lyapunov function is considered

$$V(x) = x^T P x. \tag{A.39}$$

With the saturated LTI system (5.1), the time derivative of the Lyapunov function is computed as follows

$$\dot{V}(x) = x^T(PA + A^T P)x - \sum_{i=1}^{m} 2x^T P b_i \text{sat}_\sigma(k_i x), \quad b_i:\ i\text{th column of } B. \tag{A.40}$$

Let $P = Y^{-1}$ and $F = MY^{-1}$, the constraint (5.13) implies that $\mathcal{E}(P,\gamma) \subset \mathcal{L}(F,\sigma)$. This results in the following

$$-\sigma \leq f_i x \leq \sigma, \quad \forall x \in \mathcal{E}(P.\gamma),\ \forall i \in I[1,m].$$

Consequently, for each term of $2x^T P b_i \text{sat}_\sigma(k_i x)$, we have

1) If $x^T P b_i \geq 0$ and $k_i x \leq \sigma$, then $k_i x \leq \text{sat}_\sigma(k_i x)$ and $2x^T P b_i \text{sat}_\sigma(k_i x) \geq 2x^T P b_i k_i x$.

2) If $x^T P b_i \geq 0$ and $k_i x \geq \sigma$, since $f_i x \leq \sigma$, then $2x^T P b_i \text{sat}_\sigma(k_i x) = 2x^T P b_i \sigma \geq 2x^T P b_i f_i x$.

3) If $x^T P b_i \leq 0$ and $k_i x \geq -\sigma$, then $k_i x \geq \text{sat}_\sigma(k_i x)$ and $2x^T P b_i \text{sat}_\sigma(k_i x) \geq 2x^T P b_i k_i x$.

4) If $x^T P b_i \leq 0$ and $k_i x \leq -\sigma$, since $f_i x \geq -\sigma$, then $2x^T P b_i \text{sat}_\sigma(k_i x) = -2x^T P b_i \sigma \geq 2x^T P b_i f_i x$.

These can be deduced to a single inequality as follows

$$2x^T P b_i \text{sat}_\sigma(k_i x) \geq \min\left\{2x^T P b_i k_i x,\ 2x^T P b_i f_i x\right\}, \tag{A.41}$$

which is equivalent to

$$-2x^T P b_i \text{sat}_\sigma(k_i x) \leq -\min\left\{2x^T P b_i k_i x,\ 2x^T P b_i f_i x\right\}. \tag{A.42}$$

As a result, for all $x \in \mathcal{E}(P.\gamma)$, we have

$$\dot{V}(x) \leq x^T(PA + A^T P)x - \sum_{i=1}^{m} \min\left\{2x^T P b_i k_i x,\ 2x^T P b_i f_i x\right\}. \tag{A.43}$$

Next, with a vector $v \in \mathbb{V}$ defined in (5.10), if $2x^T P b_i k_i x < 2x^T P b_i f_i x$, we set $v_i = 1$, otherwise we set $v_i = 0$. The inequality (A.43) becomes

$$\begin{aligned} \dot{V}(x) &\leq x^T(PA + A^T P)x - 2x^T P \left(\sum_{i=1}^{m} b_i \left(v_i k_i + (1 - v_i) f_i\right)\right) x \\ &= x^T(PA + A^T P)x - 2x^T P B S(v, K, F)x. \end{aligned} \tag{A.44}$$

We now turn back to the LQR problem. From (A.44), we have

$$\begin{aligned} -x(0)^T P x(0) &= \int_0^\infty \left(x^T(PA + A^T P)x - 2x^T P B sat_\sigma(Kx)\right) dt \\ &\leq \int_0^\infty \left(x^T(PA + A^T P)x - 2x^T P B S(v, K, F)x\right) dt, \end{aligned} \tag{A.45}$$

for all $x \in \mathcal{E}(P, \gamma) \subset \mathcal{L}(F, \sigma)$. By incorporating (A.45) with the performance criterion of the form

$$J(x(0), u(\cdot)) = \int_0^\infty (u^T R u + x^T Q x) dt, \tag{A.46}$$

it follows that

$$\begin{aligned} J(x(0), u(\cdot)) &= \int_0^\infty \big(x^T(PA + A^T P + Q)x - 2x^T P B \text{sat}_\sigma(Kx) \\ &\qquad + \text{sat}_\sigma(Kx)^T R \text{sat}_\sigma(Kx)\big) dt + x(0)^T P x(0) \\ &\leq \int_0^\infty \big(x^T(PA + A^T P + Q)x - 2x^T P B S(v, K, F)x \\ &\qquad + x^T S(v, K, F)^T R S(v, K, F)x\big) dt + x(0)^T P x(0). \end{aligned} \tag{A.47}$$

This means that if $\mathcal{E}(P, \gamma) \subset \mathcal{L}(F, \sigma)$ and

$$A^T P + PA + Q - PBS(v, K, F) - S(v, K, F)^T B^T P + S(v, K, F)^T R S(v, K, F) < 0, \tag{A.48}$$

for all $v \in \mathbb{V}$, then we have an upper bound on the cost function as follows

$$J(x(0), u(\cdot)) < x(0)^T P x(0), \quad \forall x(0) \in \mathcal{E}(P, \gamma). \tag{A.49}$$

We note that the inequality (A.48) is equivalent to the following LMI condition

$$\begin{bmatrix} -(AY - BS(v,L,M)) - (AY - BS(v,L,M))^T & Y & S(v,L,M)^T \\ Y & Q^{-1} & 0 \\ S(v,L,M) & 0 & R^{-1} \end{bmatrix} > 0 \qquad \text{(A.50)}$$

where $Y = P^{-1},\ L = KP^{-1}$ and $M = FP^{-1}$. Finally, the trace of the matrix Y is maximized to obtain the minimum of the upper bound on the cost function.

A.3.3 Proof of Theorem 5.3

This proof is similar to the proof of Theorem 5.1, except that the analysis domain is defined by

$$\mathcal{E}(P(\rho), \gamma) := \left\{x :\ x^T P(\rho) x \leq \gamma\right\} \qquad \text{(A.51)}$$

and the unsaturated region is defined by

$$\mathcal{L}(K(\rho), \sigma) := \left\{x :\ |k_i(\rho)x| \leq \sigma,\ \forall i \in I[1,m]\right\}. \qquad \text{(A.52)}$$

To enforce the analysis domain (A.51) to be inside the unsaturated region (A.52), i.e., $\mathcal{E}(P(\rho), \gamma) \subset \mathcal{L}(K(\rho), \sigma)$, Lemma 2.2 is modified to the LPV condition. That is

$$\begin{bmatrix} \sigma^2/\gamma & \ell_i(\rho) \\ \ell_i(\rho)^T & Y(\rho) \end{bmatrix} > 0, \quad \forall i \in I[1,m]. \qquad \text{(A.53)}$$

The rest of this proof is now similar to the proof of Theorem 5.1.

Biography

Apichart Serirojanakul was born in Chonburi, Thailand. He graduated from Phanatpittayakarn School in 2005. Then, he began his studies at Kasetsart University and gained his Bachelor's Degree in Electrical Engineering. After graduated in 2009, Apichart enrolled the Master's Degree in Electrical Engineering at Chulalongkorn University and did research in Control Systems Research Laboratory under the supervision of Assistant Professor Manop Wongsaisuwan.

List of Publications

1. A. Serirojanakul, and M. Wongsaisuwan. Optimal Control of Quad-Rotor Helicopter Using State Feedback LPV Method. in *Proc. of ECTI-CON conference*. (2012).